Characterization of OATP1B3-1B7 (LST-3TM12) - a novel transporter of the OATP1B family

Inauguraldissertation

zur

Erlangung der Würde eines Doktors der Philosophie

vorgelegt der

Philosophisch-Naturwissenschaftlichen Fakultät

der Universität Basel

von

Vanessa Malagnino

aus Ettingen Baselland

2019

Genehmigt von der Philosophisch-Naturwissenschaftlichen Fakultät

auf Antrag von

Prof. Dr. Henriette E. Meyer zu Schwabedissen,

Prof. Dr. Manuel Haschke

Basel, den 25.06.2019

Prof. Dr. Martin Spiess

Dekan

Acknowledgements

Firstly, I would like to express my deepest gratitude to my supervisor Prof. Dr. Henriette E. Meyer zu Schwabedissen for giving me the opportunity to do my PhD thesis in the Institute of Biopharmacy. In particular, I have profited from the close mentoring by Prof. Dr. Henriette E. Meyer zu Schwabedissen that helped me in becoming the scientist I always dreamed to be.

I especially thank the committee members Prof. Dr. Manuel Haschke for being my co-referee and Prof. Dr. Alex Odermatt for chairing my defense.

I also want to thank the current and former members of the Institute of Biopharmacy for their ceaseless support and the countless funny moments we shared. I want to thank in particular Daniel Ehrsam, Janine Hussner, Isabel Seibert, Anima Schäfer, Petra Rohrwild, Celio Ferreira, Katharina Prestin, and Karin Brecht Brüngger.

Moreover, I would like to thank Alex Odermatt, Denise Kratschmar, and Julia Birk from the Institute of Molecular Systems and Toxicology for always giving me good counsel and encouraging me to keep on going.

I want to thank Urs Duthaler from the Institute Clinical Pharmacology and Toxicology for being the best project partner I ever had.

Special thanks goes to Blijke Kroezen and Anima Schäfer for proof reading my thesis and their helpful suggestions for improving it.

I also want to thank my family and friends for supporting me during this intense period of my life. I want to thank my mother in particular, as she is my greatest support. As for my friends, I consider each of them as family and I could not imagine a world without them. I namely thank Tamara Müller, Marisa La Vecchia, Jessica Bressler, Florine Schweizer, Selina Rhyner, Blijke Kroezen, Nadine Haas, and Yimu Wang for always being there for me.

Table of Contents

Abbreviations

By appearance

NCBI, National Center of Biotechnology information; FXR, farnesoid X receptor; DHEAS, dehydroepiandrosterone sulfate; E_2G, estradiol β-D-glucuronide; TCA, taurocholic acid; LCA, lithocholic acid; UGT, uridine 5'-diphospho-glucuronosyltransferase; SER, smooth endoplasmic reticulum; ADME, absorption distribution metabolism excretion; ABC, ATP binding cassette family; SLC, solute carrier superfamily; SLCO, family of organic anion transporting polypetides; OATP, organic anion transporting polypeptide; ACE, angiotensin converting enzyme; GWAS, genome wide association study; HMG-CoA, 3-hydroxy-3-methylglutaryl coenzyme reductase A; SNP, single nucleotide polymorphism; AUC, area under the curve; SHP1, small heterodimer partner 1.

Alphabetical

ABC, ATP binding cassette family; ACE, angiotensin converting enzyme; ADME, absorption distribution metabolism excretion; AUC, area under the curve; DHEAS, dehydroepiandrosterone sulfate; E_2G, estradiol β-D-glucuronide; FXR, farnesoid X receptor; GWAS, genome wide association study; HMG-CoA, 3-hydroxy-3-methylglutaryl coenzyme reductase A; LCA, lithocholic acid; NCBI, National Center of Biotechnology information; OATP, organic anion transporting polypeptide; SER, smooth endoplasmic reticulum; SHP1, small heterodimer partner 1; SLC, solute carrier superfamily; SLCO, family of organic anion transporting polypetides; SNP, single nucleotide polymorphism; TCA, taurocholic acid; UGT, uridine 5'-diphospho-glucuronosyltransferase.

Summary

The effectiveness of a drug is determined by its pharmacodynamic and pharmacokinetic properties. While pharmacodynamics describes the interaction between the target structure and the drug, pharmacokinetics is an umbrella term for all the processes influencing the entry of a drug into the organism and eventually its elimination from the organism (Langguth et al., 2004a; Wilson and Walker, 2010). An important mechanism that affects the pharmacokinetics of a drug is its transport across membranes by uptake and efflux transporters (Herdegen et al., 2010). Two uptake transporters that have been extensively studied for their impact on pharmacokinetics are OATP1B3 and OATP1B1 (Maeda, 2015). These two transporters are encoded on chromosome 12 by the genes *SLCO1B3* and *SLCO1B1*, respectively (Hagenbuch and Meier, 2003). Between these genes lies another gene locus annotated as *SLCO1B7*. This gene is deemed to be a pseudogene as no function has been reported for its translational product (Stieger and Hagenbuch, 2014). In 2005, an mRNA sequence named LST-3TM12 that is highly similar to *SLCO1B7* was submitted to the National Center of Biotechnology (NCBI) by Mizutamari, H. and Abe, T. (NCBI#, AY257470). The aim of this thesis was to assess the function and transcriptional regulation of this mRNA.

By aligning the transcripts of *SLCO1B3*, *SLCO1B7*, and LST-3TM12, we could show that the initial five exons of LST-3TM12 originate from *SLCO1B3* and the remaining part of LST-3TM12 is encoded by *SLCO1B7*. Due to this finding, LST-3TM12 is referred to as **OATP1B3-1B7** in this thesis. Because the OATP1B3-1B7 mRNA and OATP1B3 have the same 5'UTR it seemed likely that they share the same promoter, which was corroborated by our finding that silencing the exon 4 of *SLCO1B3* significantly inhibited OATP1B3-1B7 mRNA transcription. Given that the gene *SLCO1B*3 is controlled by, among others, farnesoid X receptor (FXR) (Jung et al., 2002), we tested and confirmed that FXR also regulates OATP1B3-1B7 transcription. Hence, OATP1B3-1B7 is part of the FXR regulated gene-network.

Our functional assessments of OATP1B3-1B7 revealed that OATP1B3-1B7 transports exogenous and endogenous compounds. Endogenous substances were dehydroepiandrosterone sulfate (DHEAS), estradiol β-D-glucuronide (E_2G), taurocholic acid (TCA), and lithocholic acid (LCA). Exogenous substances were the drugs ezetimibe and atorvastatin. Real-time PCR assessment of OATP1B3-1B7 mRNA showed that it is highly expressed in the liver and, to a lesser extent, in the small intestine. Consequently, the protein OATP1B3-1B7 is detectable in the liver and intestine. Strikingly, the cellular location of OATP1B3-1B7 is not sinusoidal, as is the case for OATP1B1 and OATP1B3, but it is located in the smooth endoplasmic reticulum (SER). Given that OATP1B3-1B7 has a broad substrate range and is expressed in tissues dedicated to metabolism, we hypothesized that OATP1B3-1B7 could have a function related to the high metabolic activity of these tissues (Thummel, 2007). One enzyme class that is highly expressed in such tissues are uridine 5'-diphospho-glucuronosyltransferases (UGTs) (Rouleau et al., 2016). UGTs are anchored in the SER membrane and have their active enzymatic site facing the SER lumen (Coleman, 2010). However, it is still not clearly understood how UGT substrates reach and leave the active enzymatic site (Petzinger and Geyer, 2006). As OATP1B3-1B7 is a SER transporter, we assessed whether it could provide access to or exit from the lumen and thus contribute to the metabolic activity of the UGTs. We have investigated this hypothesis with regard to ezetimibe, which is a substrate of OATP1B3-1B7 and is highly metabolized by UGTs (Ghosal et al., 2004). In this case, we were able to show that inhibition of OATP1B3-1B7 lowers the glucuronidation rate of ezetimibe. Hence, we propose that OATP1B3-1B7 is a drug transporter that is a gateway for the SER lumen.

1.0 Introduction

1.1 Pharmacology

The study of the interactions between a drug and an organism is a multidisciplinary science denoted by the term pharmacology. One focal area of pharmacological research is the characterization of the effect a drug has on an organism (Sandritter et al., 2017). These effects are called **pharmacodynamic** drug properties. In more detail, pharmacodynamic research investigates the biochemical interaction between the drug and its target structure that causes the therapeutic effect (Herdegen et al., 2010). Complementary to pharmacodynamic research is the **pharmacokinetic** characterization of a drug, which investigates all the processes the organism exerts on the drug (Langguth et al., 2004a).

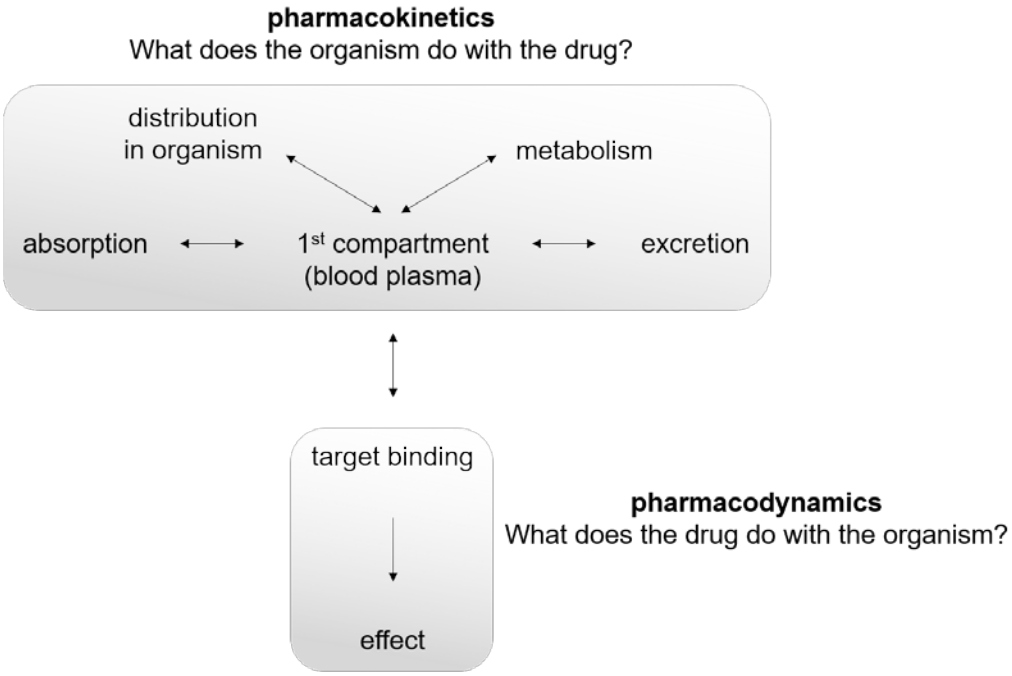

Figure 1. Overview of pharmacokinetic and pharmacodynamic processes. The flow chart represents the processes that a drug can undergo in the organism before being eliminated from the organism by excretion. Modified and adapted from Herdegen *et al.*, 2010 (Herdegen et al., 2010).

To give an overview of these two research areas, Herdegen *et al*. summarized them in a flow chart (see Figure 1) (Herdegen et al., 2010).

As can be derived from Figure 1, pharmacokinetics comprises several processes that influence the disposition of a drug in the organism. These processes are usually summarized by the

ADME concept, where A stands for absorption, D for distribution, M for metabolism, and E for excretion (Sandritter et al., 2017). As soon as an orally administered drug dissolves in the gastrointestinal tract (this process is also called liberation), the ADME processes start to take place. Initially, a fraction of the liberated drug is **a**bsorbed by the enterocytes in the gut, from where it can enter the blood stream, which **d**istributes the drug in the body. The first organ the drug is directed to is the liver. This organ contains a manifold of **m**etabolizing enzymes that alter the physicochemical properties of the drug to make it more likely to be **e**xcreted and hence eliminated from the organism. Although ADME is often explained in this order, it is important to note that all the ADME processes, except from elimination, are reversible and take place simultaneously (Herdegen et al., 2010). Eventually, pharmacokinetic processes influence the half-life, volume of distribution, and clearance of the drug and are thus crucial parameters for estimating the duration and extent of the drug action (Wilson and Walker, 2010).

Drug metabolism is frequently subdivided in four phases which are denoted as phase 0, phase I, phase II, and phase III (Doring and Petzinger, 2014; Langguth et al., 2004b). Phase I and II include biotransformation reactions that alter the chemical structure of the drug. In detail, phase I reactions comprise the addition of a functional group to the parent compound and phase II reactions comprise the conjugation of a endogenous molecule to the drug (Sandritter et al., 2017). Phase 0 and III differ from phase I and II as they do not describe a chemical reaction but the uptake (phase 0) and excretion (phase III) of a drug (Doring and Petzinger, 2014).

As anticipated by Figure 1, pharmacokinetic and pharmacodynamic processes are strongly interdependent, as the drug action can only take place when the drug reaches its target structure (Sandritter et al., 2017). Eventually, the effectiveness of a drug is determined by both its pharmacokinetic and pharmacodynamic properties (Wilson and Walker, 2010).

1.2 Diffusion

One physical process that fuels absorption, distribution, and excretion of a drug is the phenomenon of diffusion, which is the tendency of a system to equalize solute concentrations. Diffusion through semipermeable barriers (e.g., membranes) is described by Fick's diffusion law (Equation 1) (Langguth et al., 2004c): Where *(dM/dt)* is the mass flux, *D* the diffusion coefficient, *P* the distribution coefficient, *A* the diffusion area, *d* the thickness of the membrane, and c_2-c_1 the concentration gradient.

Equation 1

$$\left(\frac{dM}{dt}\right) = D\ P\ \frac{A}{d}\ (c_2 - c_1)$$

From this equation, it follows that high values for D, P, A, and ($c_2 - c_1$) favor mass flux, whereas a thick membrane (d) hinders diffusion. The distribution coefficient (*P*) reflects the likeliness of a drug to diffuse into the lipid containing membrane (lipid phase) and correlates with the lipophilicity of the drug. Therefore, drugs with high distribution coefficients diffuse more quickly into the lipid phase than drugs with low distribution coefficients (see Figure 2). As a rule of thumb, smaller, more apolar drugs have a high distribution coefficient, whereas charged, larger molecules are associated with smaller distribution coefficients (Langguth et al., 2004c). This relationship between the lipophilicity and the ability of a molecule to cross a membrane is also accounted for by the extended Rule of Five. It predicts that a drug with a log P value (measure of lipophilicity of a drug) between -0.4 to 5.6 is likely to adopt drug-like properties and hence is suitable for oral administration (Ghose et al., 1999; Lipinski et al., 2001). This empirical finding nicely demonstrates that neither a very polar drug, nor a highly lipophilic one has drug-like properties. On one hand, a highly hydrophilic drug would be confined to the water phases (e.g., blood, cytosol) and would therefore not reach the target cells. On the other hand, a highly lipophilic compound would be confined to the lipid phase (e.g., plasma membranes, lipid vesicles) (Langguth et al., 2004c).

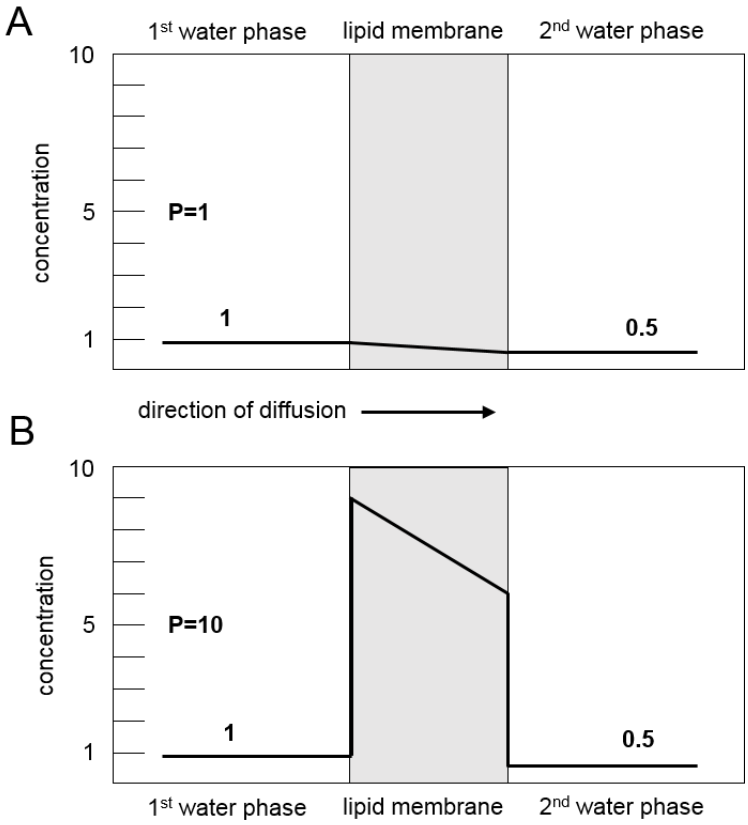

Figure 2. **Membrane passage of two drugs with different distribution coefficients.** In both cases drug concentrations are the same in the 1st and 2nd water phase. Both drugs diffuse into the lipid phase according to their distribution coefficients (P). (A) A P of 10 results in a higher concentration gradient than a P of 1 between the water and the lipid phase (B). Modified and adapted from Langguth *et al.*, 2004 (Langguth et al., 2004c).

1.3 Drug transporters

Diffusion only partially explains the journey of the drug through the organism as it is a non-directional process which aims to equalize the particle concentrations in all compartments. The directional transport of particles is facilitated by membrane spanning proteins (Herdegen et al., 2010). These proteins can act as facilitators of diffusion (pores) or actively transport drugs from one side of the membrane to the other (Herdegen et al., 2010). The latter are called transporters and can be functionally divided into influx (uptake) transporters and efflux transporters. Among them, the superfamily of the ATP binding cassette (ABC) family and transporters of the superfamily of the solute carrier (SLC) family transporters are of special interest in drug development and drug approval, as they recognize exogenous substances (e.g., drugs) as substrates (Liang et al., 2015). One subfamily of the SLCs, the organic anion transporting polypeptides of the subfamily 1B (SLCO1Bs), is of major concern in drug development as its

members interact with a manifold of drugs, thus testing new drug entities with these transporters has been recommended for pharmaceutical companies since 2010 (Giacomini et al., 2010).

In order to help the reader to understand the nomenclature of the SLCO1B subfamily, it is crucial to know that the gene names of the solute carriers are denoted with the prefix *SLCO* (e.g., *SLCO1B1*) and their corresponding proteins are identified with the prefix OATP, an acronym of organic anion transporting polypeptide (e.g., OATP1B1) (Hagenbuch and Meier, 2004).

1.4 SLCO1B transporters

Based on homology modeling, OATPs are assumed to have twelve transmembrane domains that are arranged as two bundles composed of six transmembrane domains (Schweizer et al., 2014). Moreover, they have a characteristic large fifth extracellular loop that contains conserved cysteine residues (Hagenbuch and Stieger, 2013). The OATPs facilitate the membrane passage of their substrates by a Na^+- and ATP-independent rocker switch type mechanism (Mahagita et al., 2007; Meier-Abt et al., 2005). As depicted in Figure 3, this mechanism is initiated by the two helix bundles exerting a rotary movement against each other that results in the revelation of a central substrate binding site towards one compartment, which allows for a substrate to bind to it. The substrate is then released at the opposed compartment (Schweizer et al., 2014). Given the fact that the central binding site can be sequentially accessed from both membrane sites, transport can be facilitated in both directions and is driven by the physicochemical gradient of one or more substrates (Schweizer et al., 2014). For some SLCOs it has been shown that transport is driven by counter ions such as bicarbonate or glutathione and that they have more than one substrate binding site (Hagenbuch and Stieger, 2013). As of yet, no counter ions for the OATP1B transporters have been identified (Mahagita et al., 2007). The OATP1B subfamily consists of two members, i.e., OATP1B1 and OATP1B3, which are highly similar (78% amino acid identity). It is assumed that they are gene duplicates, and that duplication occurred after divergence from rodents as rodents carry only one OATP1B transporter which

is Oatp1b2 (Hagenbuch and Gui, 2008; Meier-Abt et al., 2005). Both transporters are expressed in the sinusoidal (basolateral) membrane of hepatocytes and the expression of OATP1B1 is exclusive to the liver (Abe et al., 1999; Hsiang et al., 1999; Konig et al., 2000b). However, OATP1B3 is also expressed in other tissues, such as the placenta, colorectal tumors, and the pancreas (Briz et al., 2003; Lockhart et al., 2008; Meyer zu Schwabedissen et al., 2014). Members of the OATP1B subfamily recognize a broad range of both endogenous and exogenous substrates, of which several are substrates of both OATP1Bs and a few are only transported by only one of them (Hagenbuch and Gui, 2008; Kalliokoski and Niemi, 2009; Maeda, 2015). Examples of endogenous substrates are bile acids, bilirubin, thyroid hormones, inflammatory mediators, coproporphyrins, and steroid hormone metabolites (Bednarczyk and Boiselle, 2016; Hagenbuch and Gui, 2008; Kullak-Ublick et al., 2001). Furthermore, known exogenous substrates are found in the drug classes of statins, sartans, angiotensin converting enzyme (ACE) inhibitors, and glinides (Maeda, 2015). However, not every member of these drug classes is a substrate of OATP1Bs, and thus each needs to be evaluated independently in terms of its ability to undergo transportation.

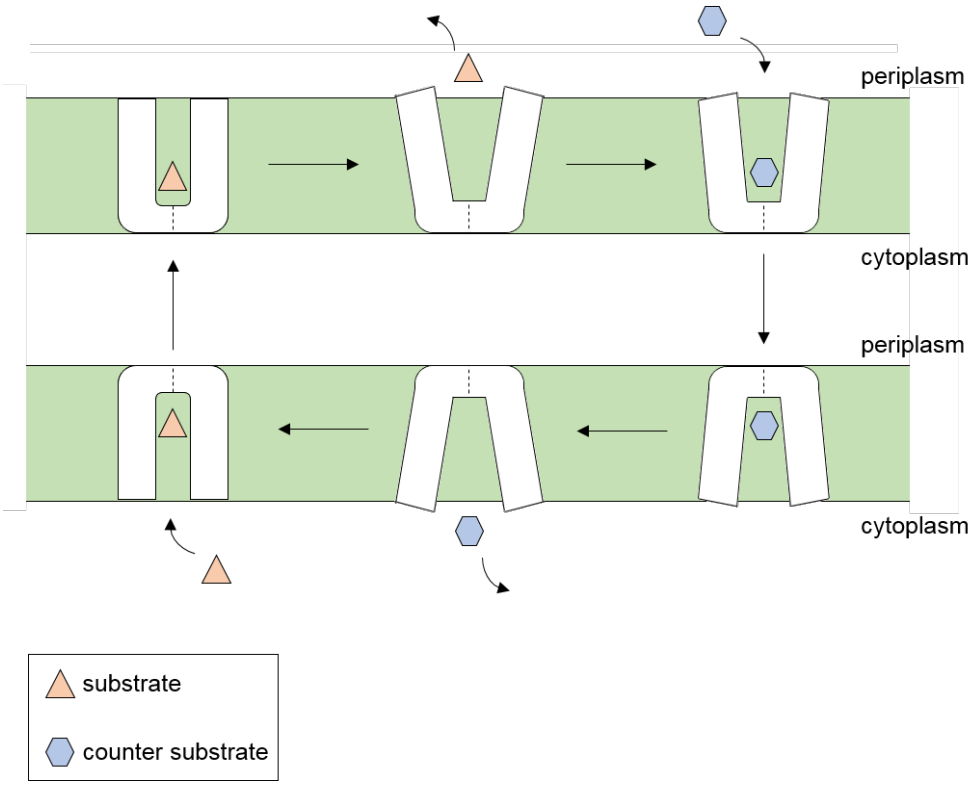

Figure 3. Rocker switch model of transmembrane transport. Transport through the membranes is facilitated by the conformational change of the two helix bundles. The central binding site of the transporter can be accessed from both sites, which allows for bi-directional transport. For the OATP1B transporter no counter substrate has been identified. Figure adapted and modified from Schweizer *et al*., 2014 (Schweizer et al., 2014).

1.5 OATP1Bs in bilirubin metabolism

Although several endogenous substrates of OATP1B1 and OATP1B3 were identified during their initial characterization (Abe et al., 1999; Abe et al., 2001; Hsiang et al., 1999; Konig et al., 2000a; Konig et al., 2000b), the physiological importance of these findings has only been rudimentarily assessed. The best-characterized endogenous role of OATP1Bs is their involvement in the bilirubin metabolism. Bilirubin is a heme metabolite that becomes neurotoxic if not eliminated from the organism (Watchko and Tiribelli, 2013). Functionally the involvement of OATP1Bs in the metabolism of bilirubin is explained by OATP1B1 and OATP1B3 mediating hepatocellular uptake of bilirubin and bilirubin glucuronide (Briz et al., 2003; Cui et al., 2001). In the hepatocytes bilirubin and its metabolites can then be further metabolized and/or secreted into the bile and thus be eliminated from the organism (Cui et al., 2001). This association of the OATP1Bs being involved in bilirubin metabolism was also confirmed by several genome wide association studies (GWAS) searching for genetic variants

associated with increased bilirubin levels (Bielinski et al., 2011; Johnson et al., 2009; Kang et al., 2010; Sanna et al., 2009). In summary, these studies have found that the deficiency of either OATP1B1 or OATP1B3 manifests itself in elevated bilirubin levels. Despite the elevated bilirubin levels, carriers of one non-functional OATP1B transporter are otherwise healthy. This finding is in accordance with the phenotype of a knock-out mouse model of Oatp1b2 (the mouse homologue of OATP1B1 and OATP1B3) created by Zaher *et al*.(Zaher et al., 2008). Similarly, to humans, the knock-out mice demonstrated elevated total bilirubin levels but were apart from that healthy (Zaher et al., 2008). Nonetheless, humans express two OATP1B transporters and thus the mice model might not be entirely representative for human physiology. In the rare case when both human OATP1Bs are non-functional, affected individuals will develop the benign Rotor-Syndrome (Online Mendelian Inheritance in Man #237450) (van de Steeg et al., 2012). The Rotor-Syndrome manifests itself in the form of conjugated hyperbilirubinemia, coproporphyrinuria, and near-absent hepatic uptake of anionic diagnostics (van de Steeg et al., 2012). Where the symptoms of coproporphyrinuria can be deduced to the coproporphyrin I and coproporphyrin III uptake function of the OATP1Bs (Bednarczyk and Boiselle, 2016). Additionally, the near-absent hepatic uptake of diagnostics is deemed to be due to the affinities of OATP1Bs for anionic diagnostics such as indocyanine green (only OATP1B3) and bromsulphtalein (Cui et al., 2001; de Graaf et al., 2011).

1.6 OATP1Bs in bile acid homeostasis

Another class of endogenous substrates that are most likely modulated by OATP1Bs are bile acids (Xiang et al., 2009; Yan et al., 2015). By investigating the bile acid levels of carriers of diminished activity polymorphisms of OATP1B1, Xiang *et al*. were able to show that these carriers displayed elevated bile acid plasma levels (Xiang et al., 2009). Furthermore, it has been speculated that placental bile acid transport is orchestrated by OATP1B3 as this transporter is down regulated in women suffering from intrahepatic cholestasis of pregnancy (Wang et al., 2012; Yan et al., 2015). In addition to these findings in humans, the murine knock out model

of Oatp1b2 demonstrated elevated levels of unconjugated bile acids in serum (Csanaky et al., 2011). The reason as to why elevated bile acid levels have not been associated with Rotor syndrome yet could be due to the fact that there is a high interindividual variance between bile acid levels and, consequently, groups have to be matched carefully in order to reveal any statistically relevant differences (Steiner et al., 2011).

One of the factors shown to regulate OATP1B transcription is the bile acid sensor FXR (*NR1H4*) (Jung et al., 2002; Meyer zu Schwabedissen et al., 2010). This receptor is activated upon binding to bile acids, the activated FXR forms a heterodimer with the 9-cis-retinoic acid receptor and this heterodimer binds to an inverted repeat response element, which fosters the initiation of gene transcription (Makishima et al., 1999). FXR is an important regulatory mechanism for intracellular bile acid levels (Matsubara et al., 2013). It orchestrates bile acid levels by initiating/inhibiting the transcription of bile acid transporters and bile acid synthesizing enzymes (Halilbasic et al., 2013). It is assumed that elevated expression of OATP1B during cholestasis could ensure moderate but continuous bile acid entry into hepatocytes in order to keep the FXR-machinery working (Meyer zu Schwabedissen et al., 2010).

Because OATP1Bs also transport thyroid hormones (Abe et al., 1999; Kullak-Ublick et al., 2001; van der Deure et al., 2008) and steroid hormones (Cui et al., 2001; Konig et al., 2000a; Konig et al., 2000b; Leuthold et al., 2009) it has also been hypothesized that the OATP1Bs could be important for the homeostasis of these hormones as well.

1.7 OATP1Bs in drug metabolism

The predominant reason for including the OATP1Bs in pre-clinical testing for drug interactions is that they transport a manifold of drugs including several statins (Giacomini et al., 2010). Statins are widely prescribed drugs that inhibit the 3-hydroxy-3-methylglutaryl coenzyme reductase A (HMG-CoA) (Joy and Hegele, 2009). By this mechanism of action, the

concentration of low density lipoprotein cholesterol levels is significantly lowered, which protects the patient from coronary events (Stewart, 2013). Although statins are well-tolerated drugs, they can in some rare cases cause statin-induced myopathy (Joy and Hegele, 2009). In a major study including 20,000 individuals, the single nucleotide polymorphism (SNP) rs4149056, which encodes for a diminished function variant of OATP1B1 (Tirona et al., 2001), was associated with an increased risk of statin-induced myopathy in high dose (80mg/day) simvastatin treatment (Link et al., 2008). Several other studies using other simvastatin doses and different definitions of statin-induced myopathy found similar associations (Brunham et al., 2012; Donnelly et al., 2011; Voora et al., 2009). However, the influence of rs4149056 on adverse events with other statins is controversial (Brunham et al., 2012; Puccetti et al., 2010; Voora et al., 2009). In more detail, there are two studies associating atorvastatin treatment in combination with rs4149056 with an increased odds ratio for statin-induced myopathy (Puccetti et al., 2010; Voora et al., 2009) and one study that did not observe a difference between exposed and control groups (Brunham et al., 2012). Moreover, for rosuvastatin (Puccetti et al., 2010) and pravastatin (Voora et al., 2009) treatment, it appears likely that there are no rs4149056-associated effects.

Pharmacokinetic studies on rs4149056 show that the area under the curve (AUC) of carriers has increased plasma concentrations of pravastatin, simvastatin, pitavastatin, atorvastatin, and rosuvastatin (Kalliokoski and Niemi, 2009). Presumably, the impaired function of OATP1B1 results in diminished uptake of statins into hepatocytes, which hampers drug clearance (Shitara, 2011). Thus, more of the drug is in circulation and is more likely to cause adverse events according to the pharmacological profile of the drug.

The rs4149056 of *SLCO1B1* is also associated with an increased AUC of repaglinide (Kalliokoski et al., 2008), nateglinide (Zhang et al., 2006) and torasemide (Werner et al., 2010); or with a higher plasma concentration of lopinavir (Hartkoorn et al., 2010).

Despite the fact that OATP1B3 contributes to simvastatin uptake into hepatocytes (Kunze et al., 2014) and that several reduced functional variants of OATP1B3 have been described (Picard et al., 2010; Schwarz et al., 2011), there are no GWASs associating *SLCO1B3* polymorphism with adverse events in simvastatin treatment. However, the polymorphism rs4149117 of *SLCO1B3* has been shown to influence the pharmacokinetics of mycophenolic acid and mycophenol glucuronide, which are metabolites of the immunosuppressant mycophenol mofetil (Miura et al., 2008; Picard et al., 2010).

Moreover, several drug-drug interactions between OATP1B1 inhibitors and substrates have been reported (Shitara, 2011). Co-administration of an OATP1B1 inhibitor (e.g., cyclosporine A, gemfibrozil, and rifampicin) and an OATP1B1 substrate (e.g., atorvastatin, cerivastatin, fluvastatin, pravastatin, repaglinide, bosentan) usually results in elevated AUCs of the substrate drugs, as the elimination of these drugs is slowed down due to diminished uptake into the liver (Shitara, 2011). However, each inhibitor-substrate combination needs to be addressed individually as it is assumed that the OATP1Bs have more than one substrate-binding site (Hagenbuch and Stieger, 2013) and thus prediction of unfavorable drug combinations is therefore intricate.

Inhibition of OATP1Bs can also result in a decreased therapeutic effect. This can occur when the drug is an OATP1B substrate and the target of the drug is located inside of the OATP1B-gated cell. These two criteria are fulfilled for statins as they target the hepatic HMG-CoA reductase, which is anchored in the endoplasmic reticulum (Roitelman et al., 1992). Indeed, there are a couple of studies indicating that the diminished functional polymorphism rs4149056 of OATP1B1 could be the cause for an attenuated therapeutic effect of statin treatment (Link et al., 2008; Meyer zu Schwabedissen et al., 2015).

Another example of this phenomenon is the interplay between OATP1B3 and its substrate glibenclamide (Meyer zu Schwabedissen et al., 2014). This antidiabetic drug inhibits the K_{ATP}

channel by binding to a cytosolic domain of the SUR1 subunit, which leads to depolarization of the plasma membrane and eventually stimulates insulin secretion (Boyd et al., 1990; Bryan and Aguilar-Bryan, 1999). Thus, impaired functional polymorphisms of OATP1B3 or inhibition of OATP1B3 could aggravate access to the SUR1 subunit, which would result in diminished effectiveness of glibenclamide (Meyer zu Schwabedissen et al., 2014).

1.8 The pseudogene SLCO1B7

Between the genes that encode for OATP1B1 and OATP1B3 lies an orphaned gene region annotated as *SLCO1B7*. There is little information available on this gene region; in Stieger and Hagenbuch's review, it is only mentioned that *SLCO1B7* is deemed to be a pseudogene as no function was reported for its translational product OATP1B7 (Stieger and Hagenbuch, 2014). Nevertheless, the publication of the mRNA sequences LST-3TM12 (NCBI#, AY257470) and LST-3b (NCBI#, AY442325) by Mizutamari, H. and Abe, T. in 2005 and 2006, respectively, suggested that *SLCO1B7* is transcribed. Both sequences contain a high sequence similarity to *SLCO1B7*. Additionally, one of the polymorphisms identified in a GWAS by Johnson *et al.* linked elevated bilirubin levels to the chromosomal area of *SLCO1B7* (Johnson et al., 2009). Moreover, in another GWAS of Legge *et al.* a polymorphism in the gene region of *SLCO1B7* correlates with the incidence of the adverse event of neutropenia during clozapine treatment (Legge et al., 2016). Accordingly, it seems that further research is necessary to elucidate the role of the gene region *SLCO1B7* and the mRNA sequences SLCO1B7, LST-3TM12 and LST-3b, which appear to be related to it.

2.0 Aim of the thesis

The aim of this thesis was the deorphanization of the gene locus *SLCO1B7* and the characterization of its translational products OATP1B7 and OATP1B3-1B7 (which is the translational product of the LST-3TM12 mRNA). Whereby, we investigated the role of

OATP1B3-1B7 in the context of drug metabolism and its physiological role in bile acid homeostasis.

3.0 Results

This doctoral thesis is based on three peer-reviewed publications and a short-study on atorvastatin accumulation:

1. LST-3TM12 is a member of the OATP1B family and a functional transporter. **Malagnino V**, Hussner J, Seibert I, Stolzenburg A, Sager CP, Meyer Zu Schwabedissen HE. Biochemical Pharmacology. 2018

2. OATP1B3-1B7 (LST-3TM12) is a drug transporter that affects endoplasmic reticulum access and the metabolism of ezetimibe.
Malagnino V, Duthaler U, Seibert I, Krähenbühl S, Meyer Zu Schwabedissen HE. Molecular Pharmacology. 2019

3. OATP1B3-1B7, a novel organic anion transporting polypeptide, is modulated by FXR ligands and transports bile acids.
Malagnino V, Hussner J, Issa A, Midzic A, and Meyer Zu Schwabedissen HE. Am J Physiol Gastrointestinal Liver Physiology. 2019

3.1 LST-3TM12 is a member of the OATP1B family and a functional transporter

Malagnino V[1], Hussner J[1], Seibert I[1], Stolzenburg A[3], Sager CP[2], Meyer Zu Schwabedissen HE[1]. Biochemical Pharmacology. 2018

Laboratories of origin:

[1] Biopharmacy, Department of Pharmaceutical Sciences, University of Basel, Basel, Switzerland

[2] Molecular Modeling, Department of Pharmaceutical Sciences, University of Basel, Basel, Switzerland

[3] Department of General Pharmacology, Center of Drug Absorption and Transport (C_DAT), University of Medicine Greifswald, Germany

Contribution Malagnino V: Study design, acquisition, analysis and interpretation of data, drafting of manuscript.

Journal: Biochemical Pharmacology (2018) **148**: 75-87

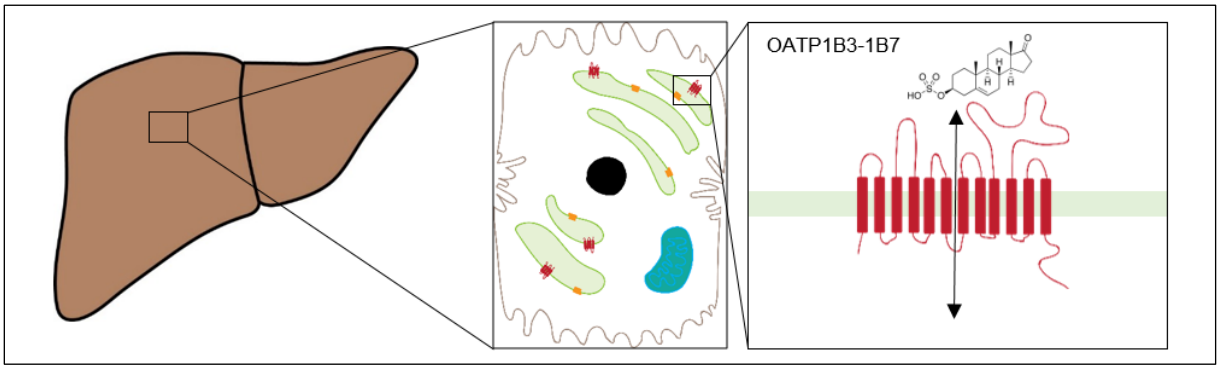

Graphical Abstract 1. LST-3TM12 is a member of the OATP1B family and a functional transporter. Artwork by V.Malagnino.

Biochemical Pharmacology 148 (2018) 75–87

Contents lists available at ScienceDirect

Biochemical Pharmacology

journal homepage: www.elsevier.com/locate/biochempharm

LST-3TM12 is a member of the OATP1B family and a functional transporter

Vanessa Malagnino [a], Janine Hussner [a], Isabell Seibert [a], Antje Stolzenburg [c], Christoph P. Sager [b], Henriette E. Meyer zu Schwabedissen [a,*]

[a] Biopharmacy, Department of Pharmaceutical Sciences, University of Basel, Basel, Switzerland
[b] Molecular Modeling, Department of Pharmaceutical Sciences, University of Basel, Basel, Switzerland
[c] Department of General Pharmacology, Center of Drug Absorption and Transport (C_DAT), University of Medicine Greifswald, Germany

ARTICLE INFO

Article history:
Received 10 November 2017
Accepted 13 December 2017
Available online 15 December 2017

Chemical compounds studied in this article:
Estrone 3-sulfate (PubChem CID: 3001028)
Dehydroepiandrosterone sulfate (PubChem CID: 12594)
Estradiol 17-β-D-glucuronide (PubChem CID: 66424)
Bromosulfophthalein (PubChem CID: 6282)

Keywords:
LST-3TM12
OATP1B transporter
Smooth endoplasmic reticulum entry
Dehydroepiandrosterone sulfate
Drug metabolism

ABSTRACT

Organic anion transporting polypeptides (OATPs) and particularly the two members of the OATP1B family are known for their role in pharmacokinetics. Both *SLCO1B3* and *SLCO1B1* are located on chromosome 12 encompassing the gene locus *SLCO1B7*. Hitherto, this particular gene has been assumed to be a pseudogene, even though there are published mRNA sequences linked to this chromosomal area. It was aim of this study to further investigate *SLCO1B7* and the associated mRNA *LST-3TM12*. In a first step, we aligned all mRNAs linked to the chromosomal region of *SLCO1B*-transporters. This *in silico* analysis revealed that *LST-3TM12* is a product of splicing of *SLCO1B3* and *SLCO1B7*, and encodes for a protein with twelve transmembrane domains. The existence of LST-3TM12 mRNA was verified by polymerase chain reaction showing liver enriched expression. In addition, immunohistological staining showed that LST-3TM12 protein was expressed in the endoplasmic reticulum (ER) of hepatocytes. Localization in the ER was further verified by immunoblot analysis showing high amounts of LST-3TM12 in liver microsomes. Function of LST-3TM12 was assessed by transport studies after heterologous expression in HeLa cells, where the transporter was shown to be expressed not only in the ER but also in the plasma membrane. Overexpression of LST-3TM12 was associated with enhanced cellular accumulation of dehydroepiandrosterone sulfate (V_{max} 300.2 pmol mg^{-1} min^{-1}; K_m 34.2 μm) and estradiol 17β-glucuronide (V_{max} 29.9 mol mg^{-1} min^{-1} and K_m 32.8 μM).

In conclusion, LST-3TM12 is a functional splice variant of *SLCO1B3* and *SLCO1B7* expressed in the ER of human liver.

1. Introduction

Membrane proteins facilitating transmembrane transport of xenobiotics play a pivotal role in drug absorption, distribution, and elimination. Both, cellular efflux and uptake of a certain compound can be modulated by the function of drug transporters. One family of membrane proteins mediating cellular uptake is the family of organic anion transporting polypeptides (OATPs) [1]. This protein family is part of the superfamily of the phylogenetically conserved *solute carrier* (SLC) transporters [2]. In 2004, the now commonly applied nomenclature of OATPs was introduced, where *SLCO* nominates the respective gene symbol of organic anion transporting polypeptides followed by identifiers for the subfamily and for the respective protein, the corresponding protein is identified by the prefix OATP instead of *SLCO* [3].

One subfamily of the OATPs is the OATP1B family of which the human representatives are OATP1B1 (LST-1, OATP-C, *SLCO1B1*) and OATP1B3 (LST-2, OATP-8, *SLCO1B3*) [3]. Both are expressed in the sinusoidal membrane of hepatocytes [4], where they facilitate cellular entry of a variety of endogenous and exogenous compounds [5]. Since their first description, various studies have provided evidence for the importance of OATP1B transporters in the hepatocellular handling of xenobiotics, finally resulting in the recommendation to include an assessment of interaction with OATP1B transporters in the process of drug development [1]. In 2012, OATP1B transporters were found to play a role in bilirubin homeostasis [6]. Van de Steeg and colleagues showed that the Rotor-syndrome, which is characterized by conjugated hyperbilirubinemia, coproporphyrinuria, and near-absent hepatic uptake

* Corresponding author at: Biopharmacy, Department of Pharmaceutical Sciences, University of Basel, Klingelbergstrasse 50, 4056 Basel, Switzerland.
E-mail address: h.meyerzuschwabedissen@unibas.ch (H.E. Meyer zu Schwabedissen).

https://doi.org/10.1016/j.bcp.2017.12.012
0006-2952/

of anionic diagnostics, is caused by the simultaneous presence of loss of function mutations in OATP1B1 and OATP1B3 [6].

In accordance with a role of OATP1B transporters in liver physiology are findings of a genome wide association (GWA) study, where genetic variants that are associated with total serum bilirubin levels in healthy individuals have been identified. The authors observed that the levels are not only linked to genetic variants in the region encoding for the uridine diphosphate glucuronosyl transferase 1A1 (UGT1A1), but also to polymorphisms located on chromosome 12.12, which is the chromosomal region where the OATP1B transporters are encoded [7]. While in the above-mentioned GWA study OATP1B1 was considered to be of major significance for bilirubin levels, Kang et al. reported OATP1B3 as key determinant based on the identified polymorphisms in a Korean population [8]. However, even though associated with bilirubin plasma levels, Buch *et al.* found only the polymorphisms rs6742078 (UGT1A1) and rs4149056 (OATP1B1) to be predictive for the presence of bilirubin in gallstones [9]. One of the polymorphisms identified in the aforementioned study of Johnson et al. is rs2417873. This particular polymorphism is located in the chromosomal area of *SLCO1B7* [7]. The same gene locus surfaced in a recent GWA study, where rs1546308 that also lies in this chromosomal region was linked to an increased risk of clozapine induced neutropenia [10].

There is nearly no information on the gene locus *SLCO1B7* or the encoded protein OATP1B7 in the literature. Analysis of the respective region on chromosome 12 revealed that *SLCO1B7* (GeneBank accession no. **NM_001009562.4**) lies between *SLCO1B3* and *SLCO1B1*. The gene is considered to be a pseudogene as there is no report on functional OATP1B7 [5]. Intrigued by the association of the above-mentioned GWAS to a non-functional gene, we performed an *in silico* domain prediction of the encoded protein OATP1B7. This *in silico* analysis suggested that OATP1B7 would consist of eleven transmembrane domains (TMDs) which conflicts with the premise that functional OATP transporters exhibit twelve TMDs [11]. However, in 2003 and 2005 Mizutamari H. and Abe T. published two mRNA sequences namely *LST-3b* (GeneBank accession no. **A442325.1**) and *LST-3TM12* (GeneBank accession no. **AY257470**), both linked to the chromosomal area of *SLCO1B7*. As there are no official nomenclature rules for these sequences we decided that in this manuscript the mRNA will be referred to in italics e.g. *LST-3TM12* and the translation products will have the same name but will be labelled in standard letters e.g. LST-3TM12.

It was the aim of the herein reported study to further analyze and characterize the mRNA sequences linked to *SLCO1B7* by *in silico* and *in vitro* approaches. We were able to show that the mRNA encoded by *SLCO1B7* is part of a functional transporter that may be involved in the hepatocellular handling of compounds.

2. Materials and methods

2.1. Materials

Unless stated otherwise chemicals were purchased from Sigma Aldrich, Buchs, Switzerland. Bovine serum albumin, Citric acid, EDTA, glycerol, glycin hematoxylin (hemalum solution acid acc. to Mayer), KCl, KH_2PO_4, 2-mercaptoethanol, NaCl, Na_2HPO_4, sodium citrate, SDS Tris-HCl, Tween 20, Roti®-Histokit II, Roti®-Mount FluorCare DAPI (4′,6-diamidino-2-phenylindole), Rotiszint®eco Plus, and HEPES were obtained from Carl Roth, Arlesheim, Switzerland.

2.2. In silico analyses

Basis for *in silico* analyses were the GeneBank entries publically available at the National Center for Biotechnology Information (NCBI). Sequence comparison was performed with Clone Manager Professional 8 (Sci-Ed Software, Denver, USA). 2D-structures were predicted using the open-source program TMpred [12]. For homology modelling, amino acid sequences were submitted to iTASSER [13]. Images of the 3D-models were generated with PyMOL (Schrödinger LLC, New York, NY, USA).

2.3. Polymerase chain reaction (PCR) for detection of the fused mRNA in human liver

For detection of *LST-3TM12* in human liver, 1 μg of total RNA pooled from 3 individuals (Ambion, LuBioScience, Lucerne, Switzerland) was reverse transcribed using the High-Capacity cDNA Reverse Transcription Kit (Thermo Fisher Scientific, LuBioScience, Lucerne, Switzerland). The resulting cDNA was template for a polymerase chain reaction (PCR) using the Phusion®-High-fidelity DNA Polymerase (Thermo Fisher Scientific) and primers located in *SLCO1B3* (Fusion_PCRfor 5′-CTTGGTATCTGTAGTTTAATA ATGGACCAACATC-′3) or *SLCO1B7* (Fusion_PCRrev 5′-CTTGAGATAA GAGATGCACTGTTGCAGAAC-′3). The PCR amplicon was ligated into pDrive® cloning vector (Qiagen, Hilden, Germany) and sequenced. The resulting sequence information was analyzed using the open access software BLAST® (https://blast.ncbi.nlm.nih.gov) and was finally compared to that of *LST-3TM12* by alignment.

2.4. Cloning of expression vectors

OATP1B7-pEF6 was generated amplifying the coding region with the primers OATP1B7for 5′-GCACTAGCTGGAATTTTTATGAAA ATATCAACCACTC-′3 and OATP1B7rev 5′-CTTAATTACATGCTTTACT GTTCTTCAGCAGAAGG-′3 by PCR, while OATP1B3-pEF6 has previously been reported [14]. Both plasmids were basis for the generation of LST-3TM12-pEF6 and LST-3TM12-isoform 2-pEF6, where the first 213 bp (base pairs) were extracted from OATP1B3-pEF6 using the restriction enzymes *BamHI* and *HindIII* (Thermo Fisher Scientific) and ligated into OATP1B7-pEF6. The resulting plasmid was template for generation of LST-3TM12-pEF6 and LST-3TM12-isoform 2-pEF6 by site directed mutagenesis using the QuikChange™ Multi Site Directed Mutagenesis Kit (Agilent, Basel, Switzerland) according to the manufacturer's instructions. In addition, a corresponding library of plasmids encoding for V5/His-tagged proteins was created by deletion of the TAA-Stop codon.

2.5. Expression analysis by real-time PCR

Total RNA extracted from liver and isolated hepatocytes was commercially obtained from PRIMACYT Cell Culture Technology (Schwerin, Germany), whereas RNA of different human tissues was purchased from BioChain (Newark, CA, USA). After reverse transcription of 1 μg RNA using the reverse transcription kit from Applied Biosystems Life Technologies™, Zug, Switzerland, a real-time PCR was performed using the ViiA™7 real-time PCR System (Thermo Fisher Scientific). Briefly, an equivalent of 20 ng mRNA of each sample was subjected to real-time PCR using TaqMan® Gene Expression Assays (Thermo Fisher Scientific) for quantification of *SLCO1B3* (Hs00251986_m1), *SLCO1B1* (Hs00272374_m1), *SLCO1B7* (Hs00991170_m1), or 18S rRNA (Hs99999901_s1). Transcription of the 5′UTR of *SLCO1B3* was determined using the primers 5′UTR for 5′-GAAGAGGTACATATGCTATGTGATCATTTCAAA CC-′3 and 5′UTRrev 5′-ATGTTGGTCCATTATTAAACTACAGATACCAA GTG-′3 and the SYBRgreen™ chemistry (Thermo Fisher Scientific). Relative expression was calculated by the $2^{-\Delta\Delta Ct}$ method, where ΔCt is the difference of the Ct-values (threshold of cycle) of the target gene and the gene for normalization (18S ribosomal RNA). The ΔCt value of each sample was related to the mean ΔCt-value of the indicated value, resulting in the ΔΔCt-value, which was then potentiated to the base of two ($2^{-\Delta\Delta Ct}$). No template controls were

included in all analyses. After the amplification, the amplicons were separated by a 3% agarose gel electrophoresis and visualized using ethidium bromide and the UVP GelDoc-It$^{TS2®}$ Imager (UVP Analytik Jena, Jena, Germany).

2.6. Immunoblot analysis

Protein expression was determined by immunoblot analysis using cell lysates or human tissue protein samples. Cell lysates for detection of V5-tagged proteins samples were obtained by solubilizing transfected cells in RIPA-buffer supplemented with proteinase inhibitor cocktail. For detection of transporters in human liver tissue, commercially obtained total normal liver protein (BioChain, Newark) and liver microsomes (Xenotech, Kansas City, KS, USA) were used. After quantification of the protein content using the Pierce™ BCA Protein Assay Kit (Thermo Fisher Scientific) proteins were supplemented with 4x Laemmli sample buffer (1 M Tris-HCl pH 6.8, 8% SDS, 40% glycerol, 8% 2-mercaptoethanol, bromophenol blue) and were incubated at 95 °C for 10 min. Then the samples were separated by SDS-PAGE and blotted onto nitrocellulose membranes (GE Healthcare, Glattbrugg, Switzerland). Prior incubation with the primary antibody at 4 °C overnight, membranes were placed in blocking buffer consisting of 5% fetal calf serum (FCS, Amimed, Allschwil, Switzerland) and 1% bovine serum albumin (BSA) in Tris-buffered saline with Tween 20 (TBS-T; 25 mM Tris, 140 mM NaCl, 2.6 mM KCl, 0.4% Tween 20) at room temperature for 1 h. After incubation with the primary antibody, membranes were washed with TBS-T and incubated with horseradish peroxidase-coupled secondary antibodies (BioRad Laboratories, Cressier, Switzerland). The primary antibodies are listed in Table 1. Binding of the antibodies was visualized with the Pierce ECL Plus Western Blotting substrate (Thermo Fisher Scientific) and the ChemiDoc MP imager (BioRad Laboratories AG).

2.7. Immunohistochemistry and immunofluorescent staining

For immunohistochemistry and immunofluorescent staining tissue slices of paraffin-embedded human liver (PRIMACYT Cell Culture Technology) were deparaffinized and rehydrated. Heat-induced epitope retrieval was performed in citrate buffer (0.1 M citric acid, 0.1 M sodium citrate, pH 6.0). In tissue dedicated for immunohistochemistry endogenous peroxidase was quenched with 3% H_2O_2 in methanol (Thermo Fisher Scientific). Subsequently, all samples were blocked in 5% FCS-1% BSA-phosphate buffered saline (PBS; 137 mM NaCl, 2.7 mM KCl, 8.1 mM Na_2HPO_4, 1.8 mM KH_2PO_4, pH 7.4) for 1 h. Afterwards, slides were incubated with the primary antibodies (Table 1). For immunohistochemistry and immunofluorescent staining horseradish peroxidase coupled antibodies from BioRad Laboratories and Alexa Fluor® labelled antibodies (Thermo Fisher Scientific) were used, respectively. For immunofluorescence the tissue was washed and mounted with cover slips using Roti®-Mount FluorCare DAPI. For immunohistochemistry the slides were submerged for 10 min in 50 mM Tris-buffer (pH 7.6, 37 °C), and then stained at 37 °C for 10 min with 1 mg/mL 3.3′-diaminobenzidine (Thermo Fisher Scientific) in 50 mM Tris-buffer supplemented with 0.02% H_2O_2. Nuclei were stained with hematoxylin and mounted with Roti®-Histokit II. The Leica DMi8 Microscope (Leica Microsystems, Heerbrugg, Switzerland) was used for image acquisition. For colocalization analysis the Zeiss LSM800 (Carl Zeiss Microscopy, Munich, Germany) was used. Z-stacks were recorded at a resolution of 40 nm/pixel with a distance of 130 nm of each section (Z-sectioning). Stacks were deconvolved with Huygens Essential deconvolution software (SVI, Hilversum, Netherlands), Pearson's and Mander's coefficient were estimated with Fiji [15].

Table 1
List summarizing the antibodies used for immunohistochemistry and Western blot analysis. The antibodies were commercially obtained from LabForce (Muttenz, Switzerland), Bio-Techne (Abingdon, UK), Santa Cruz Biotechnology Inc. (Heidelberg, Germany), LuBioscience (Lucerne, Switzerland), abcam (Cambridge UK) and Thermo Fisher Scientific Reinach, Switzerland.

Antibody (clone)	IF/IH dilution	WB dilution
Anti-OATP1B7 (LS-C110963)	1:50	1:2000
Anti-OATP1B7 (TA339136)	n. a.	1:2000
Anti-CYP3A4 (NBP2-37502)	n. a.	1:2000
Anti-OATP1B3 [4]	1:50	1:5000
Anti-LAMP2 (NBP2-22217)	1:100	1:1000
Anti-UGT1A1 (AF6490)	n. a.	1:200
Anti-G6PT (H00002542)	1:17	1:1000
Anti-PMP70 (NBP2-36770)	1:50	1:2000
Anti-V5-Tag (R960-25)	1:100	1:2000
Anti-GAPDH (sc-31915)	n. a.	1:1000
Anti-Actin (sc-1616)	n. a.	1:1000
Anti-Na^+K^+-ATPase (ab76020)	1:100	1:3000
Anti-Calnexin (ADI-SPA-865)	1:100	1:1000

2.8. Transport studies

Transport function was assessed after heterologous expression in HeLa cells (ATCC, CCL-2™ used in passage 10–24 in this study). Briefly, HeLa cells were seeded at a density of 4×10^4 cells/well in 24-well plates. One day after seeding, cells were transfected with 400 ng/well OATP1B7-pEF6, OATP1B3-pEF6, LST3TM12-pEF6, LST-3TM12-isoform 2-pEF6, or pEF6-control by using Lipofectin® Transfection Reagent (0.5 μL/well, Thermo Fisher Scientific). Expression was driven by T7 RNA-polymerase introduced into the cells by infection with the vTF7-3 virus (ATCC No. VR-2153) [16]. After 16 h in culture, cells were exposed to 0.1 nM estradiol 17-β-D-glucuronide (E_2G), estrone 3-sulfate (E_1S), dehydroepiandrosterone sulfate (DHEAS), or bromosulfophthalein (BSP) each supplemented with the respective tritiated tracer (100.000 DPM/well) obtained from Hartmann Analytics (Braunschweig, Germany) diluted in Hanks balanced salt solution (pH 7.4). After 10 min of incubation at 37 °C, cells were washed thrice with ice-cold PBS. Cellular accumulation of radioactivity was determined after lysis in 0.2% SDS-5 mM EDTA using Rotiszint®eco Plus and the scintillation counter Tri-Carb 2900TR (TopLab, Rickenbach, Switzerland). An aliquot of each sample was used for protein quantification. The ability of BSP to reduce transport of [^{3}H]-DHEAS was assessed over a range of 0.001–200 μM. To validate the vTF7-3 virus driven heterologous expression system immunofluorescent staining of treated HeLa cells was performed. For this HeLa cells were seeded at a density of 1×10^5 cells/well onto cover slips placed in 12-well culture plates. One day after seeding, cells were transfected with 500 ng plasmid/well using 3.0 μL Lipofectin® Transfection Reagent/well followed by infection with the vTF7-3 as described above. Sixteen hours after infection cells were washed with PBS and fixed in ice-cold 5% acetic acid-ethanol (Merck, Darmstadt, Germany) for 10 min, and cells were incubated with the respective antibodies as described above.

2.9. Biotinylation and enrichment of membrane proteins

HeLa cells were seeded in 10 cm dishes at a density of 1.8×10^6 cells per dish. After 24 h, cells were transfected with 8.4 μg plasmid per dish using 20.0 μL Lipofectin® Transfection Reagent® and infected with vTF7-3 vaccinia virus. Sixteen hours after transfection cells were washed with ice-cold Dulbecco's PBS (DPBS, containing Ca^{2+}/Mg^{2+} pH 7.2) and incubated with 2.5 mg EZ-Link™-Sulfo-NHS-SS-Biotin (Thermo Fisher Scientific) in DPBS at 4 °C on a rotating platform shaker (20 rpm, Polymax 1040, Heidolph, Sch-

wabach, Germany) for 30 min. Cells were washed twice with ice-cold PBS and non-reacted biotin was blocked with 100 mM glycin – DPBS at 4 °C for 20 min. After removal of the buffer solution, lysis buffer (50 mM HEPES, 150 mM NaCl, 1 mM EDTA, 2 mM $MgCl_2$, 1% (w/v) Triton-X-100) supplemented with 100 μM oxidized glutathione and proteinase inhibitor cocktail was added to the cells. Cells were gently scraped into solution, transferred into a 1.5 mL reaction tubes, and then disrupted with an ultrasonic homogenizer UP200S (Hielscher, Rottweil, Germany) by five one second bursts. After incubation on ice for 30 min and mixing every 5 min for 5 s, nuclei and cell debris were removed by centrifugation at 10.000×*g* at 4 °C for 2 min. An equivalent of 100 μg of protein was loaded onto 35 μL of NeutrAvidin Beads (Thermo Fisher Scientific) by continuous rotation for 1 h at room temperature. After this, the beads were washed three times with lysis buffer. Prior to SDS-PAGE samples were supplemented with 4x Laemmli sample buffer and incubated for 1 h at room temperature. Ten micrograms of each cell lysate was loaded as control. Western blot analysis was performed as described above.

2.10. Microsomal uptake

Human liver microsomes obtained from Xenotech were used for microsomal transport assays. The particle size of the microsomes in Tris-sucrose buffer (Tris 50 mM, 0.25 M sucrose, pH 7.5) was measured by dynamic light scattering (Zeta Sizer nano ZS, Malvern Instruments, Malvern, UK). Transport was performed in Tris-sucrose buffer supplemented with DHEAS (0.1 μM, 100.000 DPM/reaction) using 40 μg of microsomes. Microsomal accumulation of DHEAS was determined after incubation at 37 °C. After 10 min, the reaction mixture was filtered through a Millipore Durapore filter (pore size of 0.22 μm; Millipore, Zug, Switzerland) and washed three times with ice-cold PBS. Then the filters were incubated in 3 mL Rotiszint®eco Plus at room temperature under continuous shaking for 30 min. Finally, radioactivity was quantified using the liquid scintillation counter Tri-Carb 2900TR.

2.11. Statistical analysis

Statistical analyses were performed using GraphPad prism 6 (La Jolla, CA, USA). A p-value below .05 was considered statistically significant. Statistical analysis of hepatocyte vs. liver expression was performed with a Mann-Whitney test. In experiments identifying a substrate, uptake was compared to the control using the one-way ANOVA and Dunnett's multiple comparison test. The IC_{50} was estimated with a logistic function where the top was set to 100% and the bottom to 0% of the response assuming standard slope. V_{max} and K_m were estimated with a Michaelis-Menten fit. In microsomal uptake experiments, transport inhibition by addition of BSP was statistically evaluated with an unpaired *t*-test.

3. Results

3.1. In silico analysis of published mRNA sequences linked to the gene locus SLCO1B7

At first we analyzed the two mRNA sequences linked to the database entry of *SLCO1B7* (GeneBank accession no. **NM_001009562.4**), namely *LST-3b* (GeneBank accession no. **A442325.1**) and *LST-3TM12* (GeneBank accession no. **AY257470**) for sequence homology. Both mRNA sequences exhibited 100% overlap in the coding region, so that we focused on *LST-3TM12* in further analyses (Fig. 1A). Subsequent comparison of *LST-3TM12* with the coding mRNA sequences of OATP1B1 (*SLCO1B1*; GeneBank accession no **NM_006446.4**), or OATP1B3 (*SLCO1B3;* GeneBank accession no. **NM_019844.3**) revealed 83%, or 87% similarity, respectively. Furthermore, *LST-3TM12* exhibited 92% identity to the mRNA sequence encoded by *SLCO1B7*. The mRNA alignment of *LST-3TM12* (Fig. 1B) with that of *SLCO1B3* and of *SLCO1B7* suggested that *LST-3TM12* might be a product of splicing. Based on our sequence alignment the splicing occurs most likely at 333 bp in the mRNA sequence encoding for OATP1B3 and at 193 bp in the mRNA sequence encoding for OATP1B7 (Fig. 1B).

3.2. In silico prediction of a 2D model and 3D-homology model of the LST-3TM12 protein

We translated the mRNA sequence into the corresponding protein (LST-3TM12) and conducted an *in silico* prediction of TMDs using the TMpred software. In accordance with the common features of OATP transporters [2], this analysis suggested 12 TMDs and a large fifth extracellular loop (Fig. 2A) for LST-3TM12, while OATP1B7 would miss the first TMD. The assumed splicing would occur in the 3rd TMD of LST-3TM12. Subsequently a 3D-homology model was calculated. The program iTASSER proposed several structures for LST-3TM12, of which we choose the one forming a channel through the cytoplasmic membrane (Fig. 2C).

3.3. Analysis of mRNA expression in human tissue

In order to assess expression of *LST-3TM12* mRNA, we aimed to perform a real-time PCR. Notably, based on our alignment *LST-3TM12* is a splicing product of *SLCO1B3* and *SLCO1B7*. Because of the high sequence homology in the area of splicing (Fig. 1B), there is no segment of the mRNA sequence that could be used to specifically detect *LST-3TM12* by PCR. Thus, we were limited to use an assay for *SLCO1B7* that recognizes *LST-3TM12* and *SLCO1B7*, but that is not able to discriminate between both. Accordingly, we quantified the amount of mRNA in different human tissues by real-time PCR using assays for *SLCO1B3*, *SLCO1B7*, and the 5′UTR of *SLCO1B3*. As shown in Fig. 3, we observed high amounts of all mRNAs in human liver. However, there were also signals for *SLCO1B7* and *SLCO1B3* in kidney, intestine, brain, small intestine, pancreas, and colon, albeit close to detection limit. Subsequent visualization of the PCR products of the linear amplification phase by agarose gel electrophoresis revealed presence of the PCR amplicons of *SLCO1B7* and *SLCO1B3* in human liver only.

3.4. Verification of the existence of LST-3TM12 mRNA in human liver

Our real-time data showed signals for *SLCO1B7* mRNA in human liver which connotes that the gene locus is transcribed. However, this does not necessarily mean that *LST-3TM12* mRNA is formed. In order to prove the existence of the mRNA encoding for LST-3TM12, a PCR on reverse transcribed mRNA was conducted using primers, which are located at the beginning of *SLCO1B3* (−21 bp) and at position 1127 bp of *SLCO1B7*. Importantly, this particular region of *SLCO1B7* exhibits high sequence difference compared to other OATP1B transporters. As shown in Fig. 4, an amplicon of the predicted size (1267 bp) was generated, thereby supporting the notion that the mRNA encoding for *LST-3TM12* is present in human liver. The obtained amplicon, which is referred to as *LST-3TM12* isoform 2, was isolated, sequenced and compared to *LST-3TM12*. This comparison revealed seven nucleotide exchanges, namely *LST-3TM12* c.219 T>C (p.Phe73Phe), c.225 T>A (p.Ile75Ile), c.235C>T (p.Leu79Phe), c.304-307CTC>TTT (p.Leu102Phe), c.332-333CA>TG (p.Thr111Met), c.641C>T (p.Ala214Val), and c.1153A>G (p.Thr385Ala). Importantly, three of these exchanges are previously published polymorphisms namely rs758196707

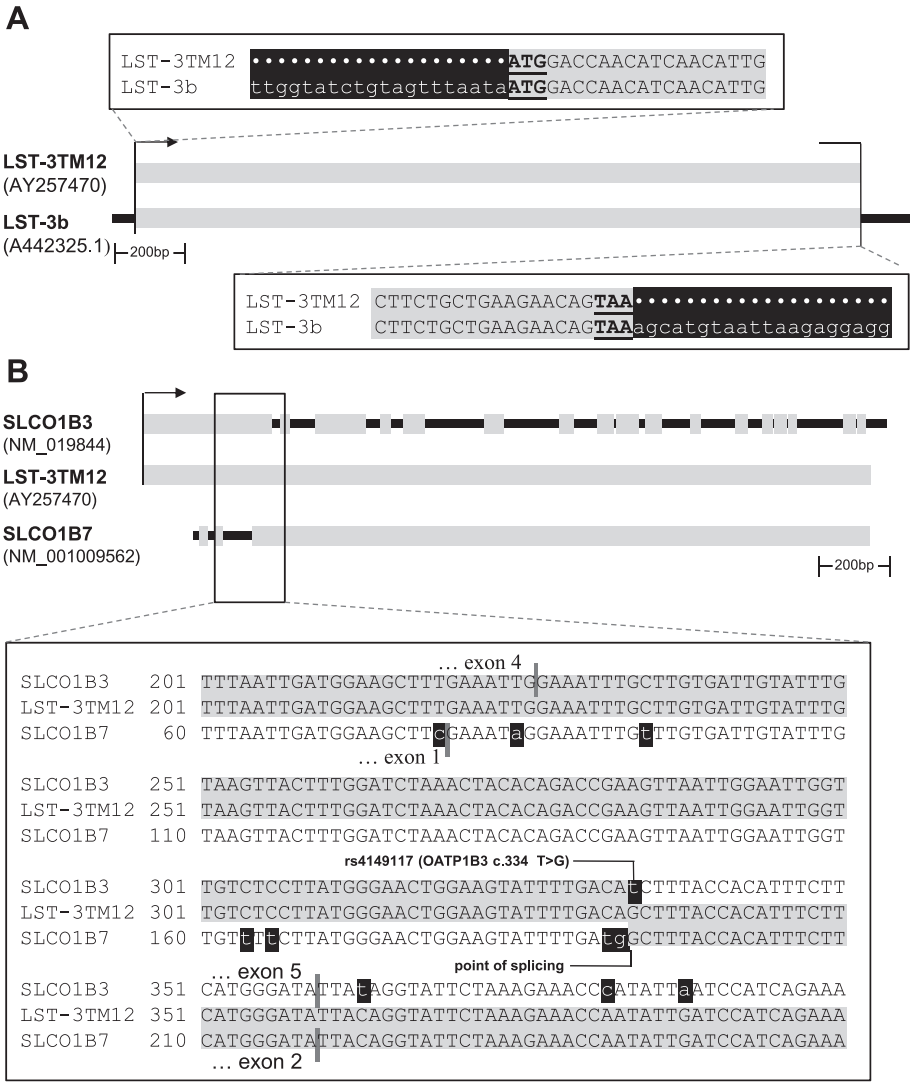

Fig. 1. Comparison of the mRNA sequences of *SLCO1B3*, *LST-3TM12*, *LST-3b*, and *SLCO1B7*. Aligning the mRNA sequences of *LST-3TM12* and *LST-3b* revealed 100% analogy of the coding sequences of *LST-3TM12* and *LST-3b* (A). For *LST-3b* additional information on the 5′-and 3′-untranslated region (UTR) is available as shown in the enlargement. Additionally, the alignment of *SLCO1B3*, *LST-3TM12*, and *SLCO1B7* showed identity of *LST-3TM12* and *SLCO1B3* until base pair 333, while the following part of *LST-3TM12* is identical to *SLCO1B7*, thereby suggesting that the point of splicing is located in this area. Depicted in the insert are the exon boundaries and the frequent polymorphism rs4149117 (OATP1B3 c.334 T>G) (B).

(*LST-3TM12* c. 219 T>C, p.Phe73Phe) with a published minor allele frequency (MAF) of 0.056, rs1546308 (*LST-3TM12* c.641C>T, p. Ala214Val, published MAF 0.04), and rs11045689 (*LST-3TM12* c.1153A>G, p.Thr385Ala, published MAF 0.33).

3.5. Determining the cellular origin of the SLCO1B7 transcript in human liver

To determine whether transcripts with *SLCO1B7* identity originate from hepatocytes or other cells in human liver, we used mRNA isolated from human hepatocytes or liver tissue of four or three individuals, respectively, for quantification by real-time PCR. As shown in Fig. 5, all OATP1B transporters determined in this analysis exhibited expression in liver tissue and isolated human hepatocytes. However, there was a trend for slightly higher amounts of the *SLCO1B1* transcript comparing isolated hepatocytes and liver tissue (mean expression normalized to human liver ± SD, hepatocytes [n = 4] vs. liver [n = 3], 2.14 ± 1.04 vs. 1.00 ± 0.07; Mann-Whitney test p = .057). No trend for enrichment was observed for *SLCO1B7* (0.70 ± 0.43 vs. 1.66 ± 2.00; p = .856), *SLCO1B3* (0.86 ± 0.52 vs. 1.16 ± 0.77, p = .856), or the 5′UTR of *SLCO1B3* (0.72 ± 0.81 vs. 1.04 ± 0.40; p = .400).

3.6. Immunohistochemical detection of LST-3TM12 in human liver tissue

Based on our findings suggesting transcription of *LST-3TM12* in hepatic tissue, we determined expression and localization of the protein in liver tissue by immunohistochemistry. As it is impossible to create an antibody specific for LST-3TM12, we used a commercially available anti-OATP1B7 antibody (LS-C110963), which is able to detect both LST-3TM12 and OATP1B7 without discriminating between them. Nevertheless, a specific staining of hepatocytes was observed with enhanced signals in perivenular areas (centrilobular) of liver tissue (Fig. 6A). Furthermore, the detected protein appeared to be present in intracellular vesicular structures. This finding differs from that observed for OATP1B3 which showed to be expressed in the plasma membrane of hepatocytes (Fig. 6A). However, similar to LST-3TM12, OATP1B3 was expressed in centrilobular hepatocytes.

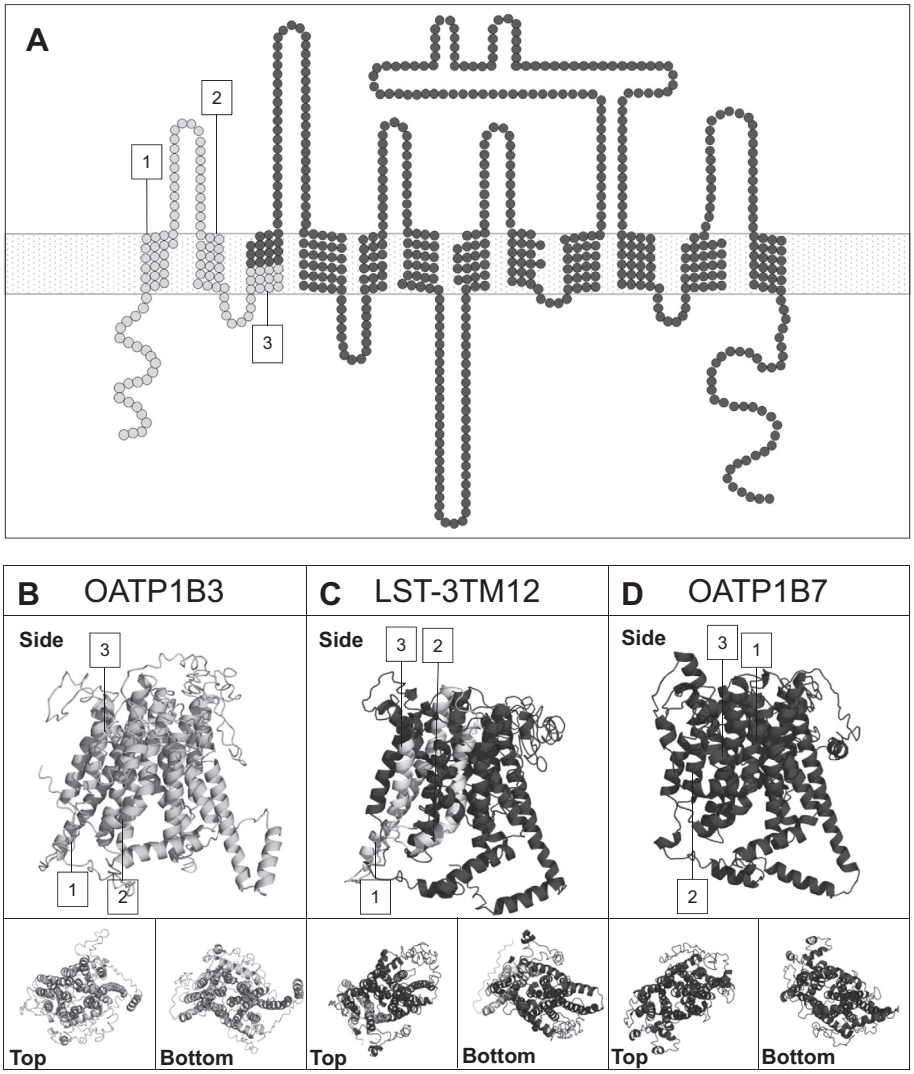

Fig. 2. Predicted 2D model and 3D-homology model of LST-3TM12. The 2D structure of LST-3TM12 was predicted using TMpred. Light grey indicates parts of the predicted protein deriving from OATP1B3, while amino acids labelled in dark grey are most likely originating from OATP1B7. The numbers indicate the respective transmembrane domain. Transition from OATP1B3 to OATP1B7 was predicted to occur most likely in transmembrane domain three of LST-3TM12 (A). The 3D-homology models of OATP1B3 (**Q9NPD5.1**), LST-3TM12 (**AAP81211.1**), and OATP1B7 (putative **NP_001009562.3**) were calculated with the iTASSER protein structure and function prediction platform. Both, the N- and C-terminus of the twelve transmembrane domain containing protein were predicted to be located intracellularly (B).

3.7. Determining the cellular localization of LST-3TM12

There are multiple vesicular intracellular structures in hepatocytes; one of particular importance in the hepatic function of drug metabolism is the smooth endoplasmic reticulum (SER). In order to evaluate whether LST-3TM12 is located in the SER, we compared protein amount in human liver tissue and enriched liver microsomes with the use of the anti-OATP1B7 antibody TA339136. As shown in Fig. 6B, an augmented signal for LST-3TM12 was detected in microsomes compared to liver. Importantly, hepatic enzymes known to be expressed in the SER, such as UGT1A1, CYP3A4 (cytochrome P450 3A4), and glucose-6-phosphatase (G6PT, *SLC37A4*) were observed to be enriched too. No such augmentation in protein amount was observed for OATP1B3, for the lysosomal associated membrane protein 2 (LAMP2, *LAMP2*), or for the peroxisomal membrane protein 70 (PMP70, *ABCD3*). To validate this observation an immunofluorescent colocalization study was performed using antibodies directed against LST-3TM12 and G6PT. As shown in Fig. 6C, we observed a distinct but not complete overlap. The extent of colocalization was evaluated calculating the Pearson's and the Mander's coefficient. The calculated Pearson's coefficient of 0.52 suggested a partial colocalization of both proteins. The Mander's coefficient, which estimates the portion of colocalization, was 0.97 for LST-3TM12 overlapping with G6PT, thereby suggesting a probability of 97% for a positive staining for G6PT in areas positive for LST-3TM12. In contrast, Mander's coefficient for G6PT overlapping with LST-3TM12 was estimated to be only 0.29, thereby reflecting the presence of G6PT in all hepatocytes, while the transporter only appeared in centrilobular hepatocytes.

3.8. Functional characterization of LST-3TM12, LST-3TM12 isoform 2, and OATP1B7 by heterologous expression

Quantification of the intracellular accumulation of previously reported OATP1B substrates namely DHEAS, E_2G, E_1S, or BSP (Fig. 7B-E) revealed significantly increased accumulation of E_2G and BSP in cells expressing OATP1B3, while presence of LST-3TM12 significantly enhanced uptake of E_2G and DHEAS. No significant change in cellular accumulation was observed for any of the tested compounds when OATP1B7 or LST-3TM12 isoform 2 were expressed in the cells.

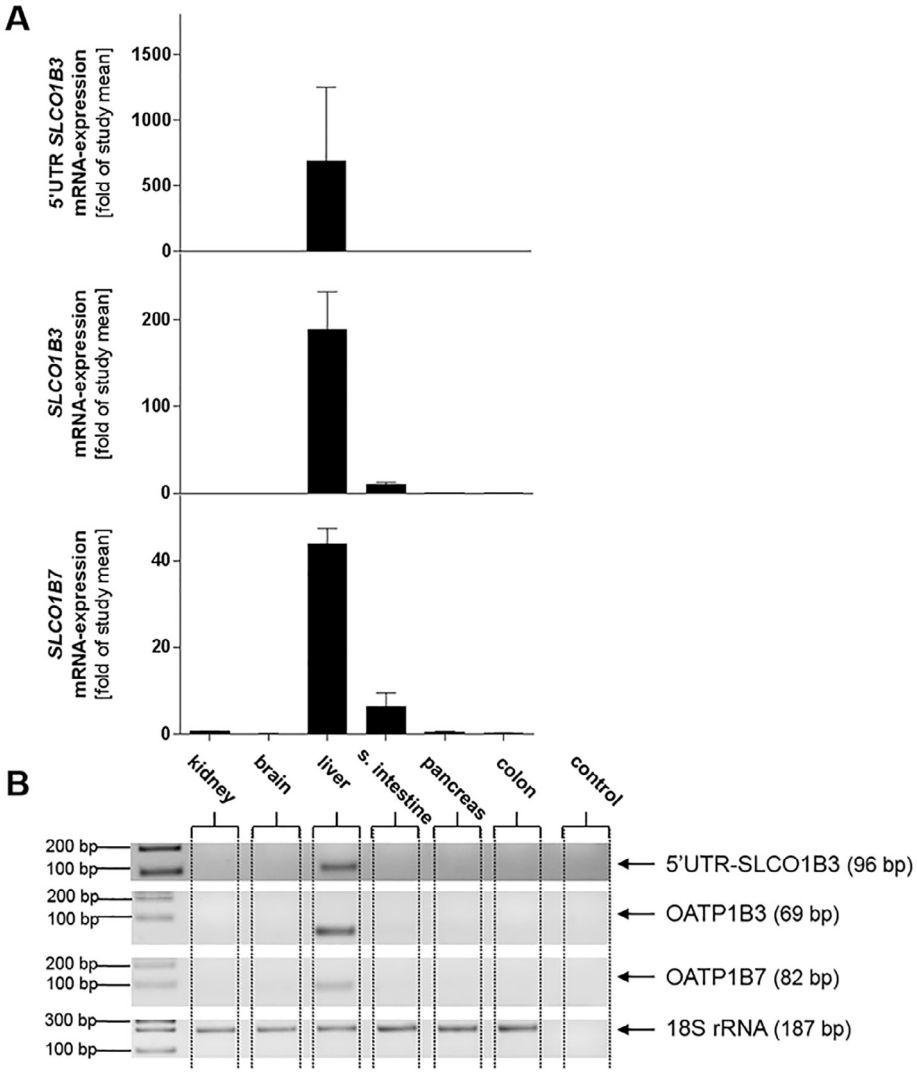

Fig. 3. Expression of *SLCO1B3* and *SLCO1B7* mRNA in human tissues. Amount of the 5′ untranslated region (UTR) of *SLCO1B3*, *SLCO1B3*, and *SLCO1B7* mRNA was quantified by real time-PCR in different tissues. Data are shown as fold of study mean ± SD of n = 3 experiments performed in duplicates, signals were first normalized to 18S rRNA and then related to the study mean (A). PCR products from the linear phase of amplification were separated by agarose gel electrophoresis and visualized with ethidium bromide (B).

Subsequent experiments performed to assess transport kinetics validated the finding of E_2G being transported by LST-3TM12 (Fig. 8A) and OATP1B3 (data not shown). The kinetic parameters of E_2G transport for both LST-3TM12 and OATP1B3 were estimated applying a Michaelis-Menten curve fitting. The estimated maximal transport rate (V_{max}) was 29.7 ± 6.5 or 12.9 ± 1.9 pmol mg^{-1} min^{-1}, while the affinity (K_m) was 32.8 ± 15.0 or 4.9 ± 3.9 μM for LST-3TM12 or OATP1B3, respectively. Additionally, the kinetics of DHEAS transport by LST-3TM12 were determined (Fig. 8B) showing a V_{max} of 300.2 ± 64.6 pmol mg^{-1} min^{-1} and a K_m of 34.2 ± 14.1 μM. No change in cellular uptake of DHEAS was observed in cells expressing OATP1B3 (data not shown).

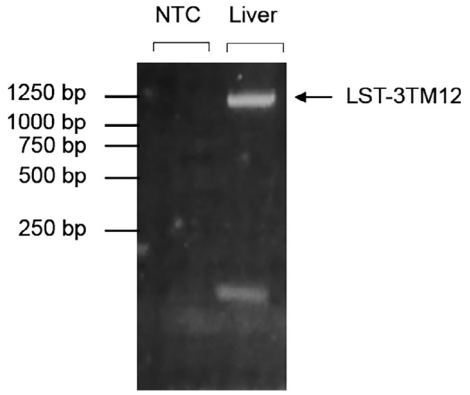

Fig. 4. Detection of LST-3TM12 mRNA in human liver. Existence of the *LST-3TM12* mRNA in human liver was verified by polymerase chain reaction using primers binding at −21 bp of *SLCO1B3* and at position 1127 bp of *SLCO1B7* for amplification followed by ethidium bromide agarose gel electrophoresis for detection. A no template control (NTC) was included in the analysis.

Subsequently we tested whether the selected OATP substrates inhibit DHEAS uptake. Here BSP was found to be a potent inhibitor of LST-3TM12. Indeed, incubation with BSP significantly decreased the uptake of DHEAS by LST-3TM12 with an estimated inhibitory potency of 11.97 μM (Fig. 8C).

3.9. Immunohistological staining and immunofluorescence of heterologous expressed LST-3TM12, LST-3TM12 isoform 2, and OATP1B7

As mentioned before, heterologous expression using the vTF7-3 based system was confirmed by immunoblot analysis. As shown in Fig. 7A, transfected OATP1B7 appeared at about 60 kDa, while the

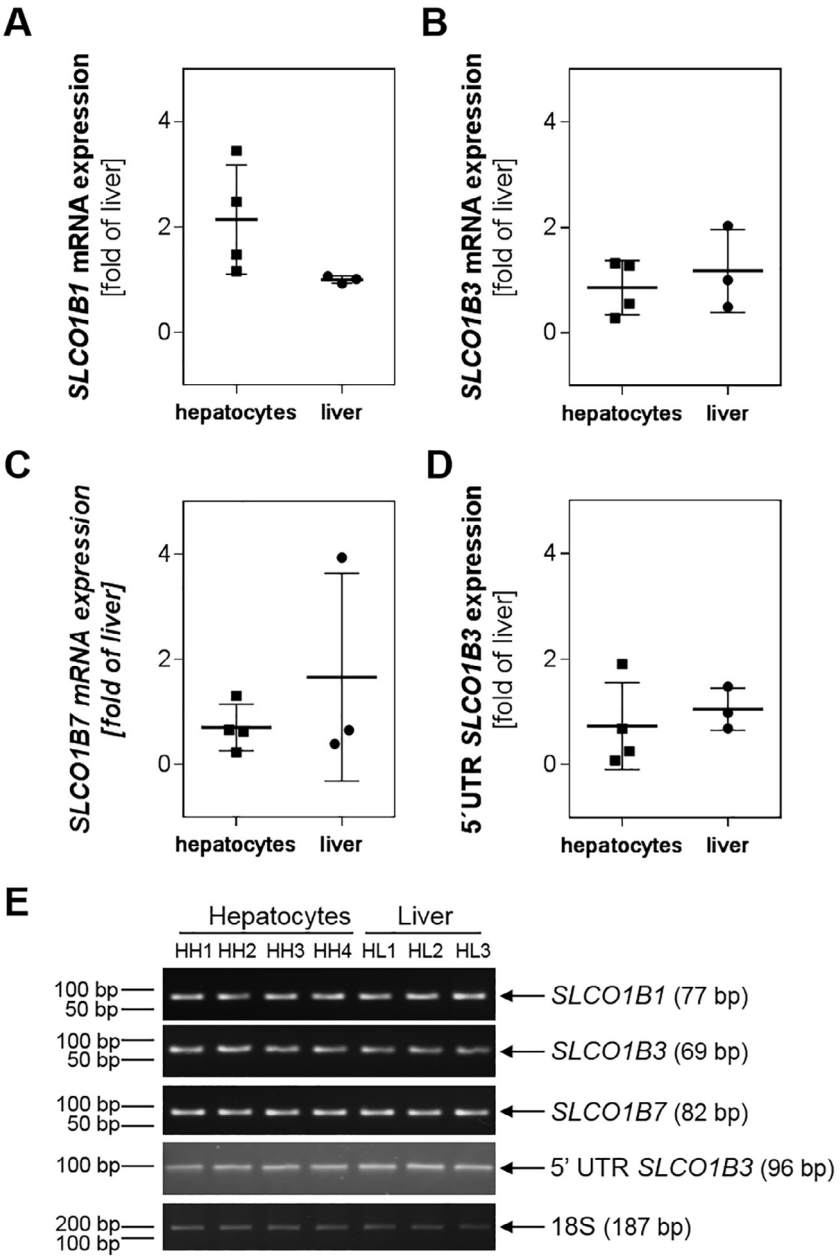

Fig. 5. Comparison of transporter expression in human liver and isolated human hepatocytes. The mRNA amount of *SLCO1B1* (A), *SLCO1B3* (B), *SLCO1B7* (C), and the 5′UTR (untranslated region) of *SLCO1B3* (D) was determined in mRNA samples of human liver (HL, n = 3 individuals) or of purified human hepatocytes (HH, n = 4 individuals). Data are presented as mean ± SD, measurement was performed in technical duplicates. Statistical analysis was performed with the Mann-Whitney test. Specificity of the resulting amplicon was controlled by ethidium bromide agarose gel electrophoresis (E).

bands of LST-3TM12, LST-3TM12 and OATP1B3 were located at about 90 kDa.

To evaluate localization of the transporters after heterologous expression a co-staining was performed. As shown in Fig. 9A, we did not only observe LST-3TM12 in the plasma membrane as shown by the colocalization with the Na^+/K^+-ATPase, but also in the endoplasmic reticulum (ER) after heterologous expression in HeLa cells. Localization in the ER was confirmed by colocalization analysis using calnexin as marker for this intracellular structure. The finding of heterologously expressed LST-3TM12 being also localized in the plasma membrane was further validated performing an analysis where surface proteins were biotinylated, subsequently enriched and then tested for presence of the transporter (Fig. 9B). Detection of LST-3TM12 in the fraction of biotinylated membrane proteins supported the notion of LST-3TM12 being present in the plasma membrane in this cell model. Similar results were obtained for OATP1B3.

3.10. Microsomal transport

In order to test whether there is an active component contributing to the microsomal uptake of DHEAS we performed studies with enriched liver microsomes. Notably, assessment of microsomal particle size by dynamic light scattering revealed a size of 287.6 ± 25.3 nm (mean ± SD), thereby allowing the application of a filter-based system as commonly applied for transport studies with membrane vesicles. Testing whether DHEAS accumulation in liver microsomes (mean DHEAS uptake ± SD; solvent control 2.33 ± 1.2 8 pmol mg^{-1}) is influenced by presence of the above-identified LST-3TM12 inhibitor BSP, revealed significant lower uptake in

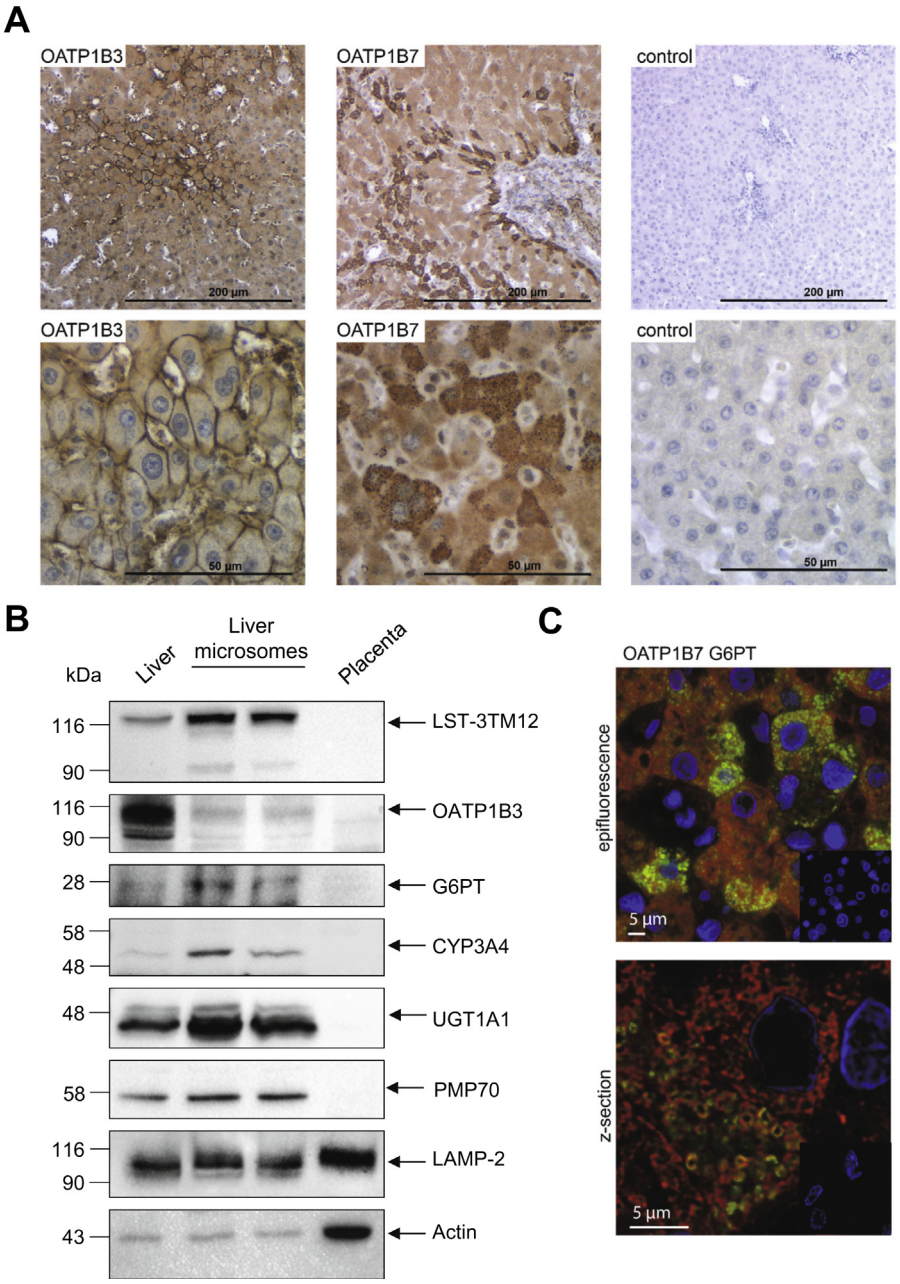

Fig. 6. Detection of LST-3TM12 and OATP1B3 protein in human liver. LST-3TM12 and OATP1B3 were visualized by immunohistochemistry (A). Protein expression of transporters (LST-3TM12, OATP1B3, G6PT, PMP70), metabolic enzymes (CYP3A4, UGT1A1), and LAMP2 was determined by Western blot analysis comparing human liver tissue and enriched hepatic microsomes. Placenta served as negative control (B). Localization in the SER was verified by co-staining of LST-3TM12 (green) with the SER-marker protein G6PT (red). The upper panel gives an impression of the co-staining (epifluorescence), whereas the lower panel shows the confocal deconvolved z-section (C).

presence of 100 µM BSP (0.66 ± 0.30 pmol mg^{-1}; unpaired *t*-test, n = 3 in triplicates, Fig. 8D).

4. Discussion

OATP1B1 and OATP1B3 are well known for their contribution to the hepatic handling of xenobiotics [1]. In the same chromosomal region lies another gene locus namely *SLCO1B7*. In contrast to *SLCO1B1* and *SLCO1B3, SLCO1B7* has previously been proposed to be a pseudogene [5]. This notion is in accordance with our *in silico* findings suggesting that the encoded OATP1B7 protein would exhibit only 11 TMDs, while currently known functional *SLCO* transporters consist of 12 TMDs [11]. The publication of the mRNA *LST-3TM12* (GeneBank entry no. **AY257470.1**) linked to the gene locus *SLCO1B7* gave rise to the hypothesis that *SLCO1B7* is not a pseudogene, but encodes for transcripts. By sequence alignment of *LST-3TM12* with *SLCO1B3* and *SLCO1B7*, it became evident that *LST-3TM12* is a product of mRNA splicing, resulting in a protein that was predicted to exhibit 12 TMDs.

To provide evidence for the assumed splicing, we inspected the sequences of *SLCO1B3* and *LST-3TM12* for classical splice donor and acceptor sites. However, in the region we assumed splicing, we found no classical splicing sites. Nevertheless, exon 5 of *SLCO1B3* could serve as splice donor and exon 3 of *SLCO1B7* as splice acceptor site, which might explain the formation of *LST-3TM12* mRNA. This assumption would be true, if the individual of which the published *LST-3TM12* mRNA was obtained, was carrier of the fre-

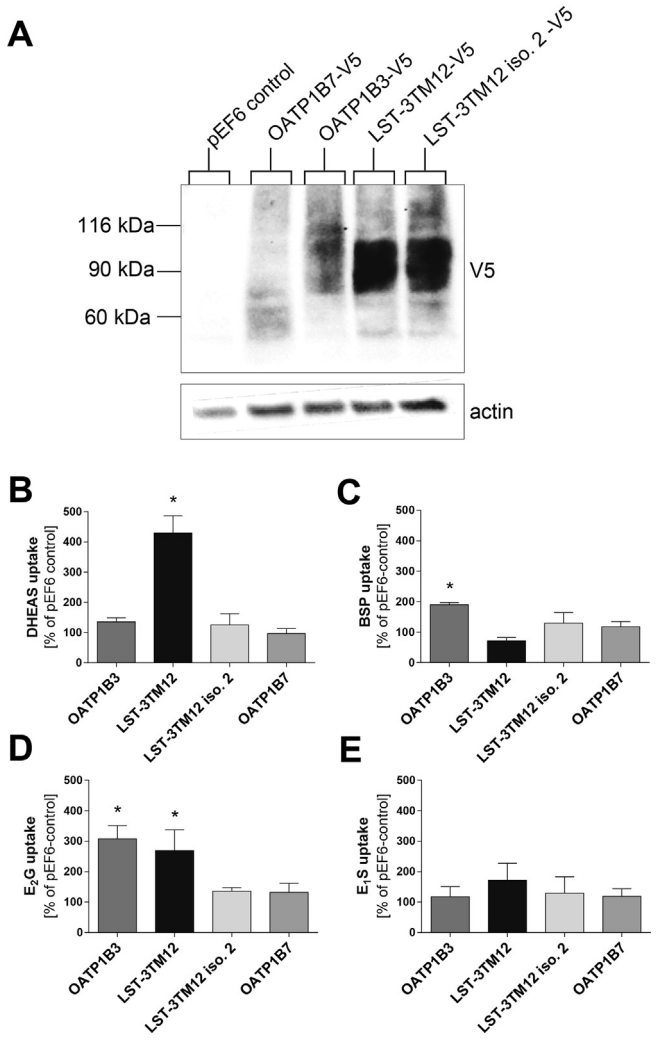

Fig. 7. Expression and function of transporters in transiently transfected HeLa cells. Expression of OATP1B7, OATP1B3, LST-3TM12, and LST-3TM12 isoform 2 (LST-3TM12 iso. 2) was verified by immunoblot analysis, showing presence of all transporter using the vTF7-based expression system. V5-tagged proteins were used to allow detection of the transporters with the same antibody (A). Function of the transporters was assessed determining the cellular accumulation of the known OATP substrates dehydroepiandrosterone sulfate (DHEAS, B), bromosulfophthalein (BSP, C), estradiol 17-β-D-glucuronide (E_2G, D), and estrone 3-sulfate (E_1S, E) in presence and absence of the respective transporter. Cell transfected with pEF6 served as control. Data are presented as mean ± SD of n = 4 independent experiments each conducted in triplicates. For statistical analysis the one-way ANOVA with Dunett's multiple comparison test was applied ($^*p < .05$).

quently occurring polymorphism rs4149117 (OATP1B3 c.334 T>G; p.Ser112Ala). Importantly, it is known that the minor G allele of this polymorphism occurs with a frequency of 0.52–0.89 in individuals of European ancestry [14], suggesting that our assumption is likely.

In this study, we amplified and sequenced the mRNA of *LST-3TM12* whereby we obtained a mRNA sequence very similar to the previously published one. The herein amplified mRNA sequence (*LST-3TM12 isoform 2*) exhibited a few nucleotide exchanges compared to the published version (*LST-3TM12*). Considering these variants, splicing would be expected to occur earlier. Here, the area of position 129 bp to 132 bp of *SLCO1B3* represents a classical splice donor acceptor site (AG/GT) combination. This splice donor acceptor site could also be the transition point between *SLCO1B3* and the sequence of *SLCO1B7*. Finally, it remains to be mentioned that there is the possibility that non-canonical splice sites are involved in the formation of the *LST-3TM12* mRNA [17], and that based on the NCBI single nucleotide polymorphism database the area exhibits various polymorphisms where in most cases allele frequencies have not been determined.

However, splicing represents an important mechanism to promote genetic diversity [18]. There are various examples in the family of SLC transporters where splicing alters transport function and even localization [19]. One example would be the *SLC2A9* gene coding for the glucose transporter GLUT9. This gene has two known splice variants which are both expressed in kidney, but are sorting to different poles of the tubular cell [20]. Another example phylogenetically closer to OATP1B3, is the murine Oatp1b2 transporter. This transporter has three different splice variants of which the shorter versions exhibit lower expression, while showing limited to no affinity to substrates of the full-length version [21].

Testing for transcripts containing *SLCO1B7* revealed high amounts in human liver, thereby suggesting that the mRNA encoding for *LST-3TM12* is liver enriched. This is in accordance with previous findings for other OATP1B transporters, where OATP1B1 has been shown to be liver specific [22,23], and OATP1B3 to be liver enriched [24]. In order to determine whether the detected mRNA in human liver originates from human hepatocytes we compared expression in liver and isolated (enriched) human hepatocytes. While we observed a tendency for elevated mRNA amounts of *SLCO1B1* in human hepatocytes, there was no specific enrichment when quantifying *SLCO1B3*, *SLCO1B7* or the 5′ UTR of *SLCO1B3* mRNA. This might be explained by findings of our subsequent immunohistological studies where a distinct expression pattern of OATP1B3 and LST-3TM12 in perivenular areas was observed. This is in accordance to the findings on the distribution of OATP1B3 by Sticova et al. [25]. In contrast, OATP1B1 is expressed in all hepatocytes [4] thus, the trend for enriched expression in hepatocytes may be deduced to this circumstance.

Furthermore, we observed that LST-3TM12 is not located in the cytoplasmic membrane of hepatocytes, but in vesicular structures within the cytoplasm. This is different to OATP1B1 and OATP1B3, which are both located in the plasma membrane [4]. The vesicular structures were investigated by co-staining of LST-3TM12 with antibodies directed against the lysosome marker LAMP2, the peroxisome marker PMP70, or the ER marker G6PT. Both, LAMP2 and PMP70 did not colocalize with LST-3TM12 (data not shown), whereas G6PT displayed similar localization to LST-3TM12. Indeed, if an area showed LST-3TM12 staining, it also exhibited presence of G6PT, but not all areas positive for G6PT were also positive for LST-3TM12. This observation may be explained by the fact that only perivenular hepatocytes express LST-3TM12 while G6PT is present in all hepatocytes. Localization in the SER was further validated by comparing the expression of LST-3TM12 in liver homogenate and liver microsomes. In accordance with enrichment in the ER, we observed an increased amount of LST-3TM12 in microsomal fractions compared to whole liver homogenate. Similar results were obtained for typical SER-bound marker proteins such as G6PT [26], CYP3A4 [27], or UGT1A1 [28].

The SER fulfils a manifold of functions including calcium storage, lipid metabolism, and drug metabolism [27]. We hypothesize that LST-3TM12 is involved in accumulation of substrates in the lumen of the SER. This is supported by our observation that accumulation of the herein identified LST-3TM12 substrate DHEAS in microsomes was significantly reduced by BSP. Especially for *in vitro* studies on UGTs, it is known that enriched microsomes have to be permeabilized to ensure maximal enzyme activity. This is currently explained by the intraluminal localization of the catalytic site of UGTs [28]. Accordingly, it may be speculated that active transport mediated by a transporter, such as the herein reported LST-3TM12, ensures access to the catalytic site of metabolizing enzymes under physiological conditions, whereby being a rate-limiting step in microsomal metabolism.

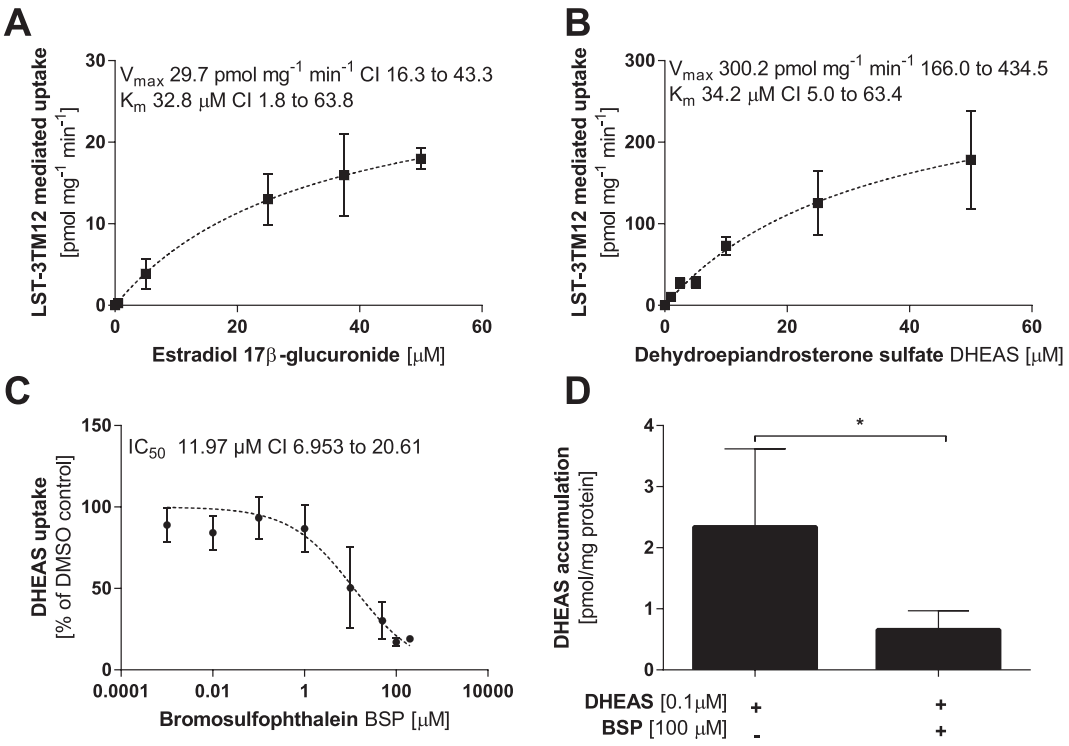

Fig. 8. Assessment of kinetic parameters for LST-3TM12 substrates. Concentration dependent uptake of estradiol 17-β-D-glucuronide (A) and dehydroepiandrosterone sulfate (DHEAS) (B) was quantified after heterologous expression of LST-3TM12 in HeLa cells. K_m and V_{max} were estimated with a Michaelis-Menten fit (n = 3 experiments performed triplicates). The inhibitory potency (IC_{50}) of bromosulfophthalein (BSP) was determined assessing cellular accumulation of DHEAS in presence of increasing amounts of the inhibitor (n = 5 experiments performed triplicates) (C). The IC_{50} was estimated with a logistic function where the top was set to 100% and the bottom to 0% of the response assuming standard slope. BSP significantly reduced the microsomal accumulation of DHEAS (n = 3 experiments performed in triplicates) (D). The impact of BSP was statistically evaluated with an unpaired *t*-test, $^{*}p < .05$. All data are presented as mean ± SD.

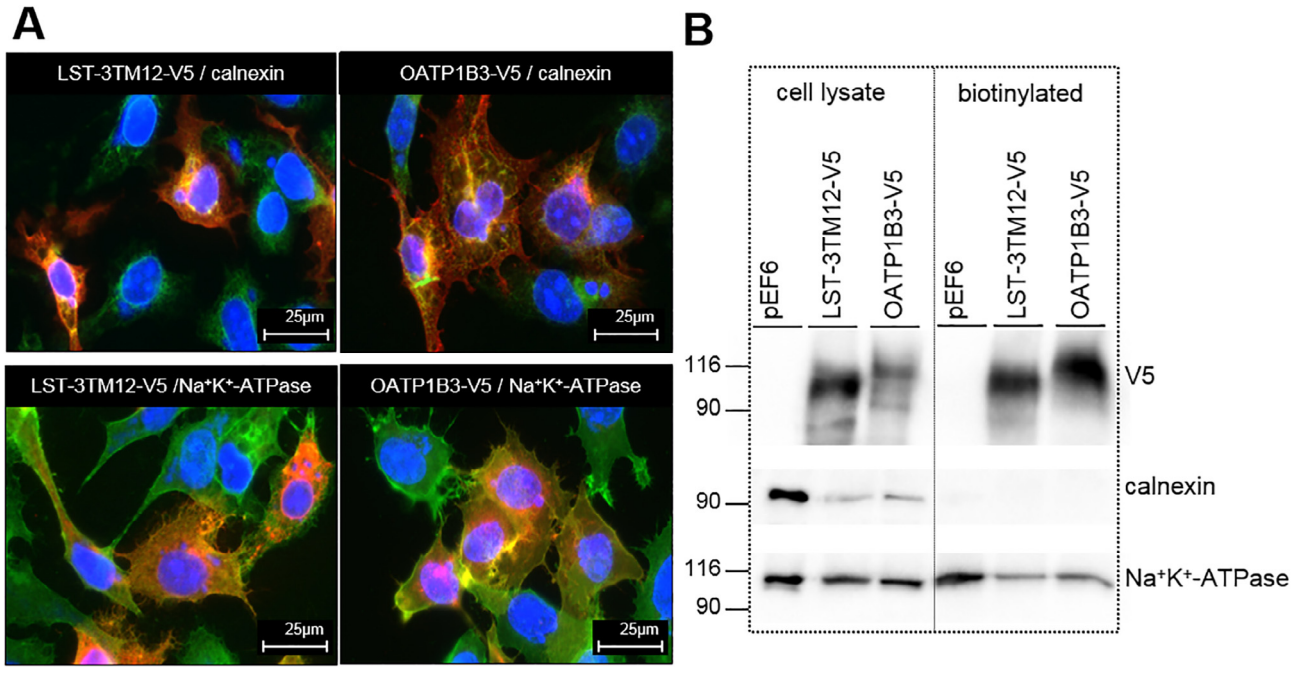

Fig. 9. Localization of LST-3TM12 and OATP1B3 after heterologous expression in HeLa cells. Localization of the V5-tagged transporters OATP1B3-V5 (red) or LST-3TM12-V5 (red) after heterologous expression in HeLa cells was determined by costaining with either the endoplasmic reticulum marker calnexin (green) or the membrane protein Na^+-K^+-ATPase (green) (A). To verify presence of OATP1B3 or LST-3TM12 in the plasma membrane, surface proteins were enriched by biotinylation and tested for expression of the respective transporter, calnexin, or Na^+-K^+-ATPase. Cells transfected with pEF6 served as control (B). (For interpretation of the references to colour in this figure legend, the reader is referred to the web version of this article.)

To identify substrates of LST-3TM12 we performed heterologous expression experiments. Assuming that LST-3TM12 is localized in intracellular vesicular structures, one may argue that a cellular system is not suitable to test transporter function, as there may be limited access to the tested protein. This argument is certainly true, if other mechanisms of cellular entry are completely neglected. In fact, even if only present in intracellular structures, the function of a SER-transporter would change the distribution equilibrium and thereby cellular accumulation of a substrate. In this context, the study by Chun et al. should be mentioned. Here the function of an additional splice variant of OATP1B3, the cancer-type OATP1B3, was also detectible in uptake assays, even if this particular variant of OATP1B3 does not sort to the plasma membrane [29]. It seems noteworthy, that in contrast to the intracellular localization in human hepatocytes we not only observed expression of LST-3TM12 intracellularly, but also in the cellular membrane after heterologous expression in HeLa cells. The latter finding was further supported by results of a biotinylation assay, where LST-3TM12 was detected after enrichment of biotinylated membrane proteins. However, we may have under- or overestimated transport velocity using the data from our expression system to estimate kinetic parameters, even though we were able to identify DHEAS and E_2G as LST-3TM12 substrates. The estimated V_{max} for DHEAS was 300.2 pmol mg^{-1} min^{-1} and the K_m was 34.2 μM. Even if previously reported [30–32] we were not able to show DHEAS uptake by OATP1B3 in our experimental setup. However, to our knowledge there are no complete kinetic parameters available for DHEAS-transport by OATP1B3 [30–32]. For E_2G we observed a V_{max} of 29.7 and 12.9 pmol mg^{-1} min^{-1} and a K_m of 32.8 and 4.9 μM for LST-3TM12 and OATP1B3, respectively. For OATP1B3 stably expressed in CHO-cells Gui et al. observed a V_{max} and K_m of 360 pmol mg^{-1} min^{-1} and 58 μM, respectively [33]. No transport activity was observed for OATP1B7, or the newly identified LST-3TM12 isoform 2. As mentioned before, the lack of transport by OATP1B7 might be due to the missing TMD, while the lack of activity of LST-3TM12 isoform 2 could be deduced to the presence of multiple nucleotide exchanges. In this context, it seems noteworthy to mention that single nucleotide exchanges significantly alter transport function of OATP1B3 and OATP1B1 [14,34].

The herein reported results may certainly be affected by the significant sequence overlap between *SLCO1B7* and *LST-3TM12,* which limits the specificity of the used detection methods, especially the real-time PCR and antibody-based methods, so that none of the reported results should be considered separately. However, taken together our data suggested that LST-3TM12 is a product of *SLCO1B3* and *SLCO1B7* splicing. Moreover, it is expressed in hepatocytes, where it is most likely localized in the SER and may facilitate the delivery of compounds to the active site of metabolizing enzymes. Importantly, this is the first report showing LST-3TM12 to be a functional transporter, as we observed a significant accumulation of DHEAS and E_2G in presence of the transporter.

Acknowledgements

The study has been fully financed by funds of the Biopharmacy at the Department of Pharmaceutical Sciences, University of Basel. We want to thank Prof. Richard B. Kim University of Western Ontario for kindly providing us the anti-OATP1B3 antiserum. Some experiments summarized in this study have been part of the diploma thesis of Antje Stolzenburg. Furthermore, this study will be part of the PhD thesis of Vanessa Malagnino.

Conflict of interest

There is no conflict of interest to declare by any author.

References

[1] K.M. Giacomini, S.M. Huang, D.J. Tweedie, L.Z. Benet, K.L. Brouwer, X. Chu, A. Dahlin, R. Evers, V. Fischer, K.M. Hillgren, K.A. Hoffmaster, T. Ishikawa, D. Keppler, R.B. Kim, C.A. Lee, M. Niemi, J.W. Polli, Y. Sugiyama, P.W. Swaan, J.A. Ware, S.H. Wright, S.W. Yee, M.J. Zamek-Gliszczynski, L. Zhang, Membrane transporters in drug development, Nat. Rev. Drug Discov. 9 (3) (2010) 215–236.
[2] B. Hagenbuch, P.J. Meier, The superfamily of organic anion transporting polypeptides, Biochim. Biophys. Acta 1609 (1) (2003) 1–18.
[3] B. Hagenbuch, P.J. Meier, Organic anion transporting polypeptides of the OATP/SLC21 family: phylogenetic classification as OATP/ SLCO superfamily, new nomenclature and molecular/functional properties, Pflugers Arch. 447 (5) (2004) 653–665.
[4] R.H. Ho, R.G. Tirona, B.F. Leake, H. Glaeser, W. Lee, C.J. Lemke, Y. Wang, R.B. Kim, Drug and bile acid transporters in rosuvastatin hepatic uptake: function, expression, and pharmacogenetics, Gastroenterology 130 (6) (2006) 1793–1806.
[5] B. Stieger, B. Hagenbuch, Organic anion-transporting polypeptides, Curr. Top. Membr. 73 (2014) 205–232.
[6] E. van de Steeg, V. Stranecky, H. Hartmannova, L. Noskova, M. Hrebicek, E. Wagenaar, A. van Esch, D.R. de Waart, R.P. Oude Elferink, K.E. Kenworthy, E. Sticova, M. Al-Edreesi, A.S. Knisely, S. Kmoch, M. Jirsa, A.H. Schinkel, Complete OATP1B1 and OATP1B3 deficiency causes human Rotor syndrome by interrupting conjugated bilirubin reuptake into the liver, J. Clin. Invest. 122 (2) (2012) 519–528.
[7] A.D. Johnson, M. Kavousi, A.V. Smith, M.H. Chen, A. Dehghan, T. Aspelund, J.P. Lin, C.M. van Duijn, T.B. Harris, L.A. Cupples, A.G. Uitterlinden, L. Launer, A. Hofman, F. Rivadeneira, B. Stricker, Q. Yang, C.J. O'Donnell, V. Gudnason, J.C. Witteman, Genome-wide association meta-analysis for total serum bilirubin levels, Hum. Mol. Genet. 18 (14) (2009) 2700–2710.
[8] T.W. Kang, H.J. Kim, H. Ju, J.H. Kim, Y.J. Jeon, H.C. Lee, K.K. Kim, J.W. Kim, S. Lee, J.Y. Kim, S.Y. Kim, Y.S. Kim, Genome-wide association of serum bilirubin levels in Korean population, Hum. Mol. Genet. 19 (18) (2010) 3672–3678.
[9] S. Buch, C. Schafmayer, H. Volzke, M. Seeger, J.F. Miquel, S.C. Sookoian, J.H. Egberts, A. Arlt, C.J. Pirola, M.M. Lerch, U. John, A. Franke, O. von Kampen, M. Brosch, M. Nothnagel, W. Kratzer, B.O. Boehm, D.C. Broring, S. Schreiber, M. Krawczak, J. Hampe, Loci from a genome-wide analysis of bilirubin levels are associated with gallstone risk and composition, Gastroenterology 139 (6) (2010) 1942–1951. e2.
[10] S.E. Legge, M.L. Hamshere, S. Ripke, A.F. Pardinas, J.I. Goldstein, E. Rees, A.L. Richards, G. Leonenko, L.F. Jorskog, K.D. Chambert, D.A. Collier, G. Genovese, I. Giegling, P. Holmans, A. Jonasdottir, G. Kirov, S.A. McCarroll, J.H. MacCabe, K. Mantripragada, J.L. Moran, B.M. Neale, H. Stefansson, D. Rujescu, M.J. Daly, P.F. Sullivan, M.J. Owen, M.C. O'Donovan, J.T. Walters, Genome-wide common and rare variant analysis provides novel insights into clozapine-associated neutropenia, Mol. Psychiatry (2016).
[11] B. Hagenbuch, C. Gui, Xenobiotic transporters of the human organic anion transporting polypeptides (OATP) family, Xenobiotica 38 (7–8) (2008) 778–801.
[12] P. Artimo, M. Jonnalagedda, K. Arnold, D. Baratin, G. Csardi, E. de Castro, S. Duvaud, V. Flegel, A. Fortier, E. Gasteiger, A. Grosdidier, C. Hernandez, V. Ioannidis, D. Kuznetsov, R. Liechti, S. Moretti, K. Mostaguir, N. Redaschi, G. Rossier, I. Xenarios, H. Stockinger, ExPASy: SIB bioinformatics resource portal, Nucleic Acids Res. 40 (Web Server issue) (2012) W597–W603.
[13] J. Yang, R. Yan, A. Roy, D. Xu, J. Poisson, Y. Zhang, The I-TASSER suite: protein structure and function prediction, Nat. Methods 12 (1) (2015) 7–8.
[14] U.I. Schwarz, H.E. Meyer zu Schwabedissen, R.G. Tirona, A. Suzuki, B.F. Leake, Y. Mokrab, K. Mizuguchi, R.H. Ho, R.B. Kim, Identification of novel functional organic anion-transporting polypeptide 1B3 polymorphisms and assessment of substrate specificity, Pharmacogenet. Genomics 21 (3) (2011) 103–114.
[15] J. Schindelin, I. Arganda-Carreras, E. Frise, V. Kaynig, M. Longair, T. Pietzsch, S. Preibisch, C. Rueden, S. Saalfeld, B. Schmid, J.Y. Tinevez, D.J. White, V. Hartenstein, K. Eliceiri, P. Tomancak, A. Cardona, Fiji: an open-source platform for biological-image analysis, Nat. Methods 9 (7) (2012) 676–682.
[16] T.R. Fuerst, E.G. Niles, F.W. Studier, B. Moss, Eukaryotic transient-expression system based on recombinant vaccinia virus that synthesizes bacteriophage T7 RNA polymerase, Proc. Natl. Acad. Sci. U.S.A. 83 (21) (1986) 8122–8126.
[17] M. Burset, I.A. Seledtsov, V.V. Solovyev, Analysis of canonical and non-canonical splice sites in mammalian genomes, Nucleic Acids Res. 28 (21) (2000) 4364–4375.
[18] Y. Xing, C. Lee, Alternative splicing and RNA selection pressure–evolutionary consequences for eukaryotic genomes, Nat. Rev. Genet. 7 (7) (2006) 499–509.
[19] F. Zhou, L. Zhu, K. Wang, M. Murray, Recent advance in the pharmacogenomics of human Solute Carrier Transporters (SLCs) in drug disposition, Adv. Drug Deliv. Rev. (2016).
[20] R. Augustin, M.O. Carayannopoulos, L.O. Dowd, J.E. Phay, J.F. Moley, K.H. Moley, Identification and characterization of human glucose transporter-like protein-9 (GLUT9): alternative splicing alters trafficking, J. Biol. Chem. 279 (16) (2004) 16229–16236.
[21] H.E. Meyer Zu Schwabedissen, J.A. Ware, R.G. Tirona, R.B. Kim, Identification, expression, and functional characterization of full-length and splice variants of murine organic anion transporting polypeptide 1b2, Mol. Pharm. 6 (6) (2009) 1790–1797.
[22] T. Abe, M. Kakyo, T. Tokui, R. Nakagomi, T. Nishio, D. Nakai, H. Nomura, M. Unno, M. Suzuki, T. Naitoh, S. Matsuno, H. Yawo, Identification of a novel gene

family encoding human liver-specific organic anion transporter LST-1, J. Biol. Chem. 274 (24) (1999) 17159–17163.
[23] J. Konig, Y. Cui, A.T. Nies, D. Keppler, A novel human organic anion transporting polypeptide localized to the basolateral hepatocyte membrane, Am. J. Physiol. Gastrointest. Liver Physiol. 278 (1) (2000) G156–G164.
[24] T. Abe, M. Unno, T. Onogawa, T. Tokui, T.N. Kondo, R. Nakagomi, H. Adachi, K. Fujiwara, M. Okabe, T. Suzuki, K. Nunoki, E. Sato, M. Kakyo, T. Nishio, J. Sugita, N. Asano, M. Tanemoto, M. Seki, F. Date, K. Ono, Y. Kondo, K. Shiiba, M. Suzuki, H. Ohtani, T. Shimosegawa, K. Iinuma, H. Nagura, S. Ito, S. Matsuno, LST-2, a human liver-specific organic anion transporter, determines methotrexate sensitivity in gastrointestinal cancers, Gastroenterology 120 (7) (2001) 1689–1699.
[25] E. Sticova, A. Lodererova, E. van de Steeg, S. Frankova, M. Kollar, V. Lanska, R. Kotalova, T. Dedic, A.H. Schinkel, M. Jirsa, Down-regulation of OATP1B proteins correlates with hyperbilirubinemia in advanced cholestasis, Int. J. Clin. Exp. Pathol. 8 (5) (2015) 5252–5262.
[26] C.J. Pan, B. Lin, J.Y. Chou, Transmembrane topology of human glucose 6-phosphate transporter, J. Biol. Chem. 274 (20) (1999) 13865–13869.
[27] M.D. Coleman, Human Drug Metabolism, 2nd ed., John Wiley & Sons Ltd, Chichester, 2010.
[28] M.B. Fisher, K. Campanale, B.L. Ackermann, M. VandenBranden, S.A. Wrighton, In vitro glucuronidation using human liver microsomes and the pore-forming peptide alamethicin, Drug Metab. Dispos. 28 (5) (2000) 560–566.
[29] S.E. Chun, N. Thakkar, Y. Oh, J.E. Park, S. Han, G. Ryoo, H. Hahn, S.H. Maeng, Y.R. Lim, B.W. Han, W. Lee, The N-terminal region of organic anion transporting polypeptide 1B3 (OATP1B3) plays an essential role in regulating its plasma membrane trafficking, Biochem. Pharmacol. 131 (2017) 98–105.
[30] Y. Cui, J. Konig, I. Leier, U. Buchholz, D. Keppler, Hepatic uptake of bilirubin and its conjugates by the human organic anion transporter SLC21A6, J. Biol. Chem. 276 (13) (2001) 9626–9630.
[31] G.A. Kullak-Ublick, M.G. Ismair, B. Stieger, L. Landmann, R. Huber, F. Pizzagalli, K. Fattinger, P.J. Meier, B. Hagenbuch, Organic anion-transporting polypeptide B (OATP-B) and its functional comparison with three other OATPs of human liver, Gastroenterology 120 (2) (2001) 525–533.
[32] J. Konig, Y. Cui, A.T. Nies, D. Keppler, Localization and genomic organization of a new hepatocellular organic anion transporting polypeptide, J. Biol. Chem. 275 (30) (2000) 23161–23168.
[33] C. Gui, Y. Miao, L. Thompson, B. Wahlgren, M. Mock, B. Stieger, B. Hagenbuch, Effect of pregnane X receptor ligands on transport mediated by human OATP1B1 and OATP1B3, Eur. J. Pharmacol. 584 (1) (2008) 57–65.
[34] R.G. Tirona, B.F. Leake, G. Merino, R.B. Kim, Polymorphisms in OATP-C: identification of multiple allelic variants associated with altered transport activity among European- and African-Americans, J. Biol. Chem. 276 (38) (2001) 35669–35675.

3.2 OATP1B3-1B7 (LST-3TM12) is a drug transporter that impacts endoplasmic reticulum gating and the metabolism of ezetimibe

Malagnino V[1], Duthaler U[2], Seibert I[1], Krähenbühl S[2], Meyer Zu Schwabedissen HE[1].Molecular Pharmacology. 2019

Laboratories of origin:

[1] Biopharmacy, Department of Pharmaceutical Sciences, University of Basel, Basel, Switzerland

[2] Division of Clinical Pharmacology and Toxicology, Department of Biomedicine, University of Basel and University Hospital Basel, Basel, Switzerland

Contribution Malagnino V: Study design, acquisition, analysis and interpretation of data, drafting of manuscript.

Journal: Molecular Pharmacology (2019), 96 (2) 128-137

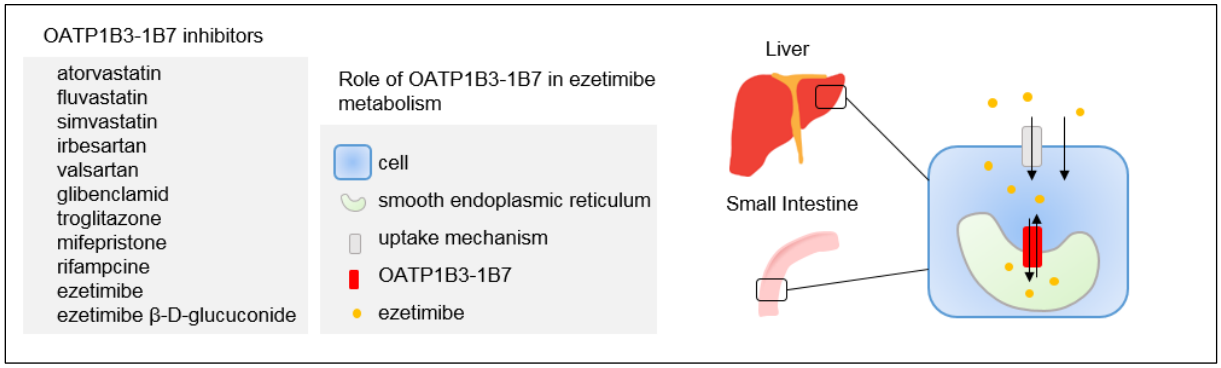

Graphical Abstract 2. OATP1B3-1B7 (LST-3TM12) is a drug transporter that impacts endoplasmic reticulum gating and the metabolism of ezetimibe. Artwork by V. Malagnino.

1521-0111/96/2/128–137$35.00
MOLECULAR PHARMACOLOGY

https://doi.org/10.1124/mol.118.114934
Mol Pharmacol 96:128–137, August 2019

OATP1B3-1B7 (LST-3TM12) Is a Drug Transporter That Affects Endoplasmic Reticulum Access and the Metabolism of Ezetimibe[S]

Vanessa Malagnino, Urs Duthaler, Isabell Seibert, Stephan Krähenbühl, and Henriette E. Meyer zu Schwabedissen

Biopharmacy, Department of Pharmaceutical Sciences, University of Basel (V.M., I.S., H.E.M.S.) and Division of Clinical Pharmacology and Toxicology, Department of Biomedicine, University of Basel and University Hospital Basel (U.D., S.K.), Basel, Switzerland

Received October 25, 2018; accepted May 15, 2019

ABSTRACT

Drug transporters play a crucial role in pharmacokinetics. One subfamily of transporters with proven clinical relevance are the OATP1B transporters. Recently we identified a new member of the OATP1B family named OATP1B3-1B7 (LST-3TM12). This functional transporter is encoded by *SLCO1B3* and *SLCO1B7*. OATP1B3-1B7 is expressed in hepatocytes and is located in the membrane of the smooth endoplasmic reticulum (SER). One aim of this study was to test whether OATP1B3-1B7 interacts with commercial drugs. First, we screened a selection of OATP1B substrates for inhibition of OATP1B3-1B7–mediated transport of dehydroepiandrosterone sulfate and identified several inhibitors. One such inhibitor was ezetimibe, which not only inhibited OATP1B3-1B7 but is also a substrate, as its cellular content was significantly increased in cells heterologously expressing the transporter. In humans, ezetimibe is extensively metabolized by hepatic and intestinal uridine-5′-diphospho-glucuronosyltransferases (UGTs), the catalytic site of which is located within the SER lumen. After verification of OATP1B3-1B7 expression in the small intestine, we determined in microsomes whether SER access can be modulated by inhibitors of OATP1B3-1B7. We were able to show that these compounds significantly reduced accumulation in small intestinal and hepatic microsomes, which influenced the rate of ezetimibe β-D-glucuronide formation as determined in microsomes treated with bromsulphthalein. Notably, this molecule not only inhibits the herein reported transporter but also other transport systems. In conclusion, we report that multiple drugs interact with OATP1B3-1B7; for ezetimibe, we were able to show that SER access and metabolism is significantly reduced by bromsulphthalein, which is an inhibitor of OATP1B3-1B7.

SIGNIFICANCE STATEMENT

OATP1B3-1B3 (LST-3TM12) is a transporter that has yet to be fully characterized. We provide valuable insight into the interaction potential of this transporter with several marketed drugs. Ezetimibe, which interacted with OATP1B3-1B7, is highly metabolized by uridine-5′-diphospho-glucuronosyltransferases (UGTs), whose catalytic site is located within the smooth endoplasmic reticulum (SER) lumen. Through microsomal assays with ezetimibe and the transport inhibitor bromsulphthalein we investigated the interdependence of SER access and the glucuronidation rate of ezetimibe. These findings led us to the hypothesis that access or exit of drugs to the SER is orchestrated by SER transporters such as OATP1B3-1B7.

Introduction

Transporters play a major role in pharmacokinetics and pharmacodynamics, as their influx and efflux function influences absorption, distribution, and elimination of their substrates. Moreover, drug transporters are assumed to be key determinants in the compartmentalization of the organism, governing transbarrier transport and modulating the cellular amount of drugs at intracellular drug targets or metabolizing enzymes (Hillgren et al., 2013). In the last two decades, membrane proteins facilitating cellular entry have extended our understanding of drug transport. Findings on their role in adverse drug events and drug-drug interactions finally resulted in the recommendation to also test new drug entities for interactions with a selection of influx transporters (Giacomini et al., 2010).

Part of this recommendation pertains to members of the 1B-subfamily of the organic anion transporting polypeptides (OATPs), namely OATP1B1 and OATP1B3. Both transporters are highly expressed in the liver (Abe et al., 1999, 2001) and transport a variety of compounds, including statins, sartans, angiotensinogen-converting enzyme inhibitors, and glinides (Maeda, 2015). Tirona et al. (2001) reported on function-impairing genetic polymorphisms of OATP1B1, setting the

https://doi.org/10.1124/mol.118.114934.
[S] This article has supplemental material available at molpharm.aspetjournals.org.

ABBREVIATIONS: BSP, bromsulphthalein; CI, confidence interval; CYP, cytochrome P450 isoform; DHEAS, dehydroepiandrosterone sulfate; G6PT, glucose-6-phosphatase; HBSS, Hanks' balanced salt solution; IS, internal standard; OATP, organic anion transporting polypeptide; SER, smooth endoplasmic reticulum; UGT, 5′-diphospho-glucuronosyltransferase.

stage for in vivo studies on the relevance of OATP1B1 in the hepatocellular entry of substrate drugs. In particular, the rs4149056 polymorphism (c.521T > C; p.Val174Ala) was shown to be linked to changes in pharmacokinetics (Kalliokoski and Niemi, 2009). For OATP1B3, there is less evidence from pharmacogenetic studies for its relevance in vivo. Even if there are polymorphisms that influence transport function in vitro (Picard et al., 2010; Schwarz et al., 2011), there are only limited reports on their impact on pharmacokinetics in humans. However, one variant—rs4149117 (c.334G > T; p.Ala112Ser)—has been reported to be predictive for altered pharmacokinetics of mycophenolic acid and mycophenol-glucuronide (Miura et al., 2008; Picard et al., 2010). However, considering that OATP1B transporters share most substrates and that OATP1B1 is more abundant in hepatocytes (Kunze et al., 2014), the impact of impaired OATP1B3 function is expected to only manifest for molecules that exhibit low affinity toward OATP1B1 (Yoshida et al., 2012).

Most of the hitherto characterized drug transporters are located in the plasma membrane. However, the organization of a cell with intracellular compartments surrounded by lipid layers suggests that there are similar mechanisms directing a compound to the lumen of a compartment (Petzinger and Geyer, 2006). One intracellular compartment where mechanisms of entry and efflux are most likely is the smooth endoplasmic reticulum (SER). This organelle contains several drug-metabolizing enzymes such as cytochrome P450 enzymes (CYP) or the uridine-5′-diphosphoglucuronosyltransferases (UGT) (Matern et al., 1984; Coleman, 2010). Hepatocytes in particular exhibit a sophisticated SER that contains high amounts of metabolizing enzymes (Alberts et al., 2002). Among these, UGT enzymes are known to have their active site located within the lumen (Coleman, 2010). In regard to hepatic drug metabolism, cellular entry is often followed by functionalization and/or intramicrosomal glucuronidation (Coleman, 2010). This implies that a compound has to overcome not only the plasma membrane but also the SER membrane to be directed to its metabolic fate.

In terms of transporters that facilitate SER entry, we have recently reported on OATP1B3-1B7 (LST-3TM12). This novel member of the OATP1B family is a variant encoded by two gene loci. In detail, the first five exons of OATP1B3-1B7 (LST-3TM12, NCBI#AY257074 containing 2064 base pairs) originate from *SLCO1B3*, while *SLCO1B7* provides the remaining exons (exons 3–13 of *SLCO1B7*). The resulting OATP1B3-1B7 mRNA encodes for a functional transporter (687 AA), which recognizes dehydroepiandrosterone sulfate (DHEAS) and estradiol 17β-D-glucuronide as substrates. Furthermore, we showed that the abundance of OATP1B3-1B7 is expressed in the liver, with localization in the SER of hepatocytes (Malagnino et al., 2018). Due to its localization, we hypothesized that OATP1B3-1B7 has a SER gateway function and influences metabolism by SER enzymes.

In the present study we tested whether OATP1B3-1B7 also interacts with molecules used in drug therapy. Thus, a selection of 19 compounds that have previously been reported to interact with OATP1B transporters was tested for their effect on OATP1B3-1B7 function. In addition, clozapine was included in the screening as adverse events during clozapine treatment have been associated with polymorphism in the *SLCO1B7* gene region (Legge et al., 2017). One of the identified inhibitors was ezetimibe, which acts as a cholesterol uptake inhibitor that is extensively glucuronidated (Kosoglou et al., 2005). As we assumed that OATP1B3-1B7 could mediate access to the SER lumen and thus to the active site of UGTs, we investigated the putative SER gateway function of OATP1B3-1B7 on the example of ezetimibe.

Materials and Methods

Unless stated otherwise, all materials were purchased from Sigma-Aldrich (Buchs, Switzerland).

Cell Culture. HeLa cells (CCL-2 in passage 6–27; American Type Culture Collection, Manassas, VA) were grown in Dulbecco's modified Eagle's medium supplemented with 10% fetal calf serum (Amimend, Allschwil, Switzerland) and 1% glutamine (Bioconcept, Allschwil, Switzerland) in a humidified atmosphere at 37°C and 5% CO_2. Cell lines were assayed for mycoplasma with the PCR Mycoplasma Test Kit I/C (Promokine, Heidelberg, Germany) before experimentation.

Transport Inhibition Studies. HeLa cells were seeded at a density of 4×10^5 cells/well, which corresponds to a confluence of 80%, and were then transfected with OATP1B3-1B7-pEF6 or pEF6-control and infected with vTF-7 (VR-2153; American Type Culture Collection) as described elsewhere (Malagnino et al., 2018). Importantly, in this experimental system OATP1B3-1B7 also sorts to the plasma membrane (Malagnino et al., 2018). Cells were exposed to 0.1 nM DHEAS supplemented with [^{3}H]-DHEAS as a tracer (specific activity 81.3 Ci/mmol, 100,000 DPM/well, NET860250UC; PerkinElmer, Schwerzenbach, Switzerland) in commercially obtained Hanks' balanced salt solution (HBSS, pH 7.4; Sigma-Aldrich).

In a preliminary screening, the test compound was added at a concentration of 25 or 100 μM. After 10 minutes of incubation at 37°C, the cells were washed twice with ice-cold PBS and lysed in 0.2% SDS-5 mM EDTA (Carl Roth AG, Arlesheim, Switzerland). Five volume percent of the lysate was used for protein quantification by bicinchoninic acid assay (Pierce BCA Protein Assay Kit; Thermo Scientific, Reinach, Switzerland). The remaining lysate was transferred to a Rotiszinteco Plus scintillation buffer (Carl Roth AG). The β-decay was quantified with the liquid scintillation counter Tri-Carb 2900TR (TopLab, Rickenbach, Switzerland).

Compounds that exhibited statistically significant inhibition of OATP1B3-1B7–mediated DHEAS accumulation were further characterized by determining the respective half-maximal inhibitor concentration (IC_{50}). Here, cells were treated with ascending concentrations (ranges shown in Figs. 1 and 2) of the identified inhibitor. Data were analyzed by subtracting the transport rates of control transfected cells from the rates observed for the cells expressing OATP1B3-1B7. Data are shown as percent of solvent control, where the observed net transport rate was normalized to that of the solvent control. By using the statistical program GraphPad Prism version 6 (La Jolla, CA), the IC_{50} was estimated with a "log (inhibitor) versus normalized response" curve fitting using a fixed slope of -1.

Transport Experiments with Ezetimibe. HeLa cells, which transiently express OATP1B3-1B7, were prepared to validate the transport of ezetimibe. Ten minutes before exposure to ezetimibe, the cells were preincubated with HBSS. The cells were then exposed to 100 nM unlabeled ezetimibe supplemented with [^{3}H]-labeled tracer (specific activity 20–40 Ci/mmol, 100,000 DPM/well, ART 1463; Hartmann ANALYTIC, Braunschweig, Germany). The cells were incubated for 10 minutes at 37°C and were subsequently washed twice with ice-cold PBS. The amount of radiolabel was quantified by liquid scintillation counting as described earlier.

Western Blot Analysis. For Western blot analysis we used 5–10 μg of protein of liver homogenate from healthy human subjects

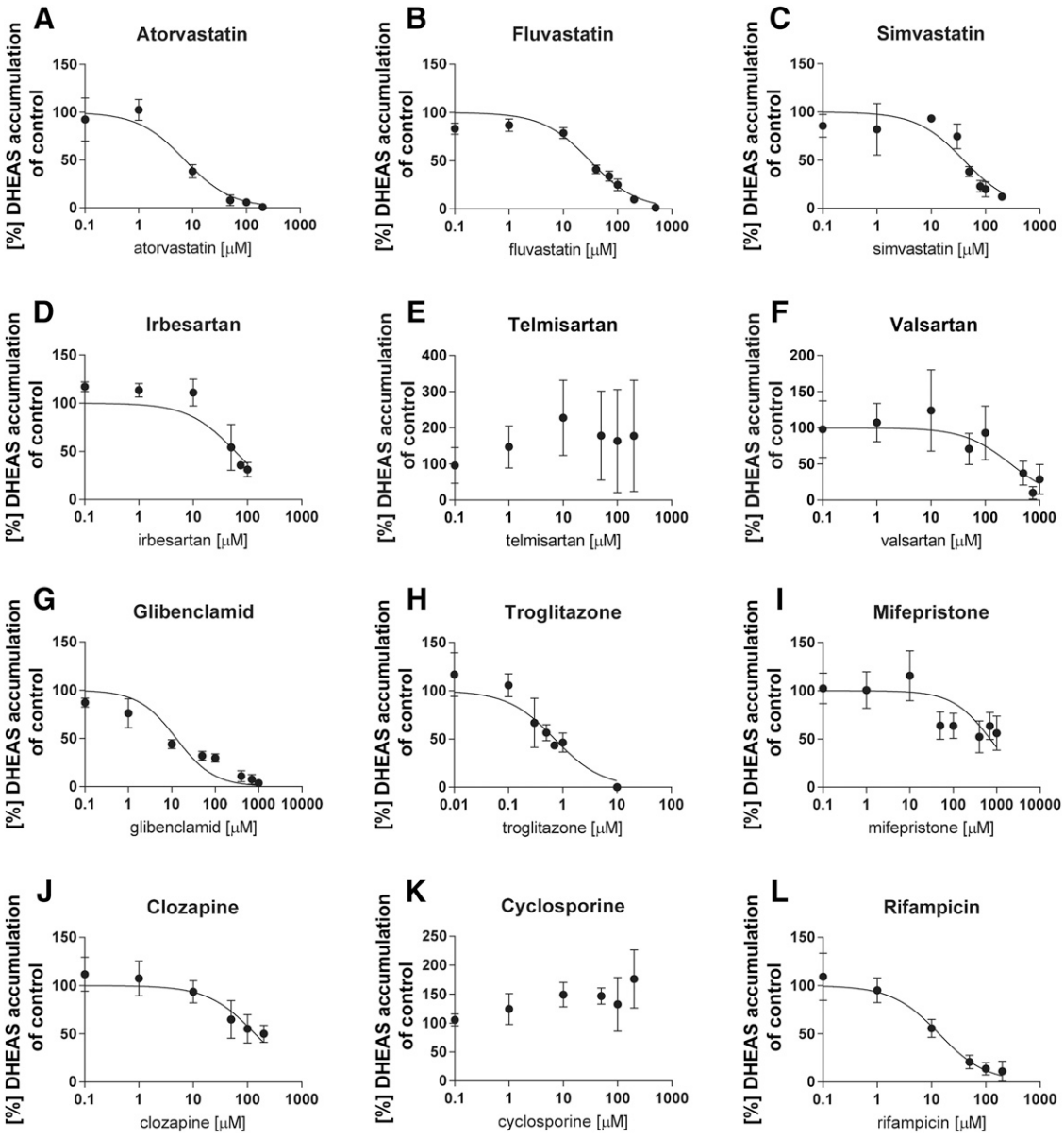

Fig. 1. Concentration-dependent effects of selected therapeutic agents on OATP1B3-1B7–mediated DHEAS transport. The concentration-dependent impact of atorvastatin (A), fluvastatin (B), simvastatin (C), irbesartan (D), telmisartan (E), valsartan (F), glibenclamide (G), troglitazone (H), mifepristone (I), clozapine (J), cyclosporine (K), and rifampicin (L) on the OATP1B3-1B7–mediated accumulation of DHEAS was determined. Normalized data were used to estimate the IC_{50} with a "log (inhibitor) versus normalized response" curve fitting that uses a fixed slope of −1. Data are shown as mean % of solvent control ± S.D. of at least three independent experiments, each performed in triplicate.

(BioChain, Newark, NJ), pooled microsomes from human liver (Ultra Pool; Corning/Thermo Fisher Scientific, Corning, NY), duodenum (BioChain), or pooled human small intestinal microsomes (Corning). The Western blot analysis was performed as described elsewhere (Malagnino et al., 2018). Equal loading of the samples was ascertained by Ponceau S staining (Carl Roth AG). The commercial supplier and the dilutions of the antibodies are listed in Supplemental Table 1.

Immunohistological and Immunofluorescent Staining of Human Tissue Samples. Localization of OATP1B3-1B7 was determined by immunohistochemistry and immunofluorescent staining of liver (male; PRIMACYT Cell Culture Technology, Schwerin, Germany) or duodenum (male; AMSBIO, Abingdon, United Kingdom) tissue slides, performed as described elsewhere (Malagnino et al., 2018) and using the antibodies summarized in Supplemental Table 1. In controls, serum of rabbits not exposed to the epitope was used. The images were acquired with a Leica DMi8 Microscope (Leica Microsystems, Heerbrugg, Switzerland).

The cellular localization of OATP1B3-1B7 in duodenum slices was tested by analyzing its colocalization with the SER marker glucose-6-phosphatase (G6PT, *SLC37A4*). A Zeiss LSM800 (Carl Zeiss Microscopy, Munich, Germany) was used for image acquisition. Z-stacks were recorded at a resolution of 123 nm/pixel with a section distance of 50 nm (Z-sectioning). Images were processed with the Zeiss Airyscan method, which directly deconvolves the images. Pearson's correlation coefficient and Mander's overlap coefficient were calculated with the open source program Fiji and the JACoP plugin (Bolte and Cordelieres, 2006; Schindelin et al., 2012).

Microsomal Transport Assays. Human liver microsomes (Corning) and pooled human small intestinal microsomes (Corning) were used for microsomal transport assays. The mean diameter of the

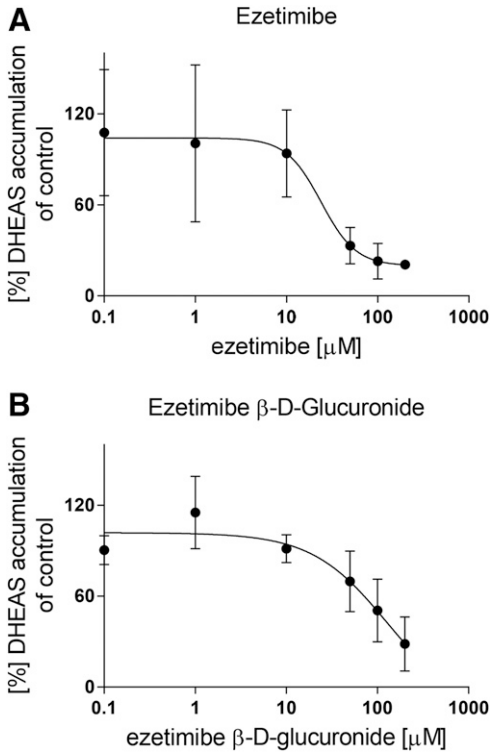

Fig. 2. Interaction of ezetimibe and ezetimibe β-D-glucuronide with OATP1B3-1B7. The concentration-dependent inhibition of DHEAS transport in OATP1B3-1B7 overexpressing HeLa cells was determined for ezetimibe (A) and ezetimibe β-D-glucuronide (B). The IC_{50} of ezetimibe and ezetimibe β-D-glucuronide were estimated by "log (inhibitor) versus normalized response" curve fitting with a fixed slope of −1. Data are shown as mean % of solvent control ± S.D. of four independent experiments, each conducted in triplicate.

microsomes was determined by dynamic light scattering with a Zeta Sizer nano ZS (Malvern Instruments, Malvern, United Kingdom). For the microsomal transport assay, 40 μg (hepatic) or 20 μg (intestinal) of microsomes were suspended in a Tris-Sucrose buffer containing 0.1 μM ezetimibe (^{3}[H]-tracer, 100,000 DPM/reaction). Uptake was inhibited by the addition of 100 μM of the OATP inhibitors/substrates atorvastatin, bromsulphthalein (BSP), or DHEAS to the reaction mix. After incubating the microsomes for 10 minutes at 37°C and 620 rpm, we stopped the reaction by filtering the solution through a Millipore Durapore filter (pore size of 0.22 μm; Millipore, Zug, Switzerland) followed by a washing step using 3 ml of ice-cold PBS. The filters were transferred to a 3-ml Rotiszinteco Plus scintillation fluid (Carl Roth AG) and incubated for at least 30 minutes at room temperature under constant shaking. Accumulation was determined by scintillation counting with the Tri-Carb 2900TR.

Estimation of Enzymatic Activity of UGTs by Microsomal Assays. Hepatic and small intestinal microsomes, UGT reaction mixture solution A, and the UGT reaction mix solution B with alamethicin were obtained from Corning. In addition, UGT reaction mix solution B without alamethicin was prepared according to the manufacturer's protocol (250 mM Tris-HCl, 40 mM $MgCl_2$, pH 7.5). The UGT reaction mix solution A, UGT reaction mix solution B (with or without alamethicin), and ezetimibe were mixed according to the manufacturer's protocol and preheated to 37°C (ThermoMixer Comfort; Eppendorf, Hamburg, Germany). The reaction was started by adding microsomes to the mixture, which resulted in a protein content of 0.5 and 0.25 mg/ml for hepatic and small intestinal microsomes, respectively. At indicated time points an aliquot of 50 μl was drawn and combined with 250 μl methanol supplemented with the internal standard (IS) efavirenz-d5 (concentration 100 ng/ml; Toronto Research Chemicals, Ontario, Canada).

The samples were vigorously mixed and then centrifuged for 30 minutes at 3200*g* and 10°C. An aliquot of 2.5 μl supernatant was injected into the high-pressure liquid chromatography with tandem mass spectrometry system, which consisted of a Shimadzu (Kyoto, Japan) high-pressure liquid chromatography connected to an API 4000 Qtrap mass spectrometer (AB Sciex, Concord, ON, Canada). The system was operated with the Analyst software 1.6.2 (AB Sciex).

Ezetimibe, ezetimibe β-D-glucuronide, and efavirenz-d5 (IS) were separated on a Luna PFP(2) analytical column (50 × 2 mm, 3 μm; Phenomenex, Torrance). Mobile phase A and B were water and methanol, respectively. Both mobile phases were supplemented with 0.1% formic acid. The samples were loaded at 5% mobile B onto the analytical column. Mobile phase B was increased to 95% between 0.5 and 2 minutes. The column was washed for 1 minute at 95% B and reconditioned at 5% B for another 0.5 minutes. Ezetimibe, ezetimibe β-D-glucuronide, and efavirenz-d5 eluted after 2.17, 2.28, and 2.31 minutes, respectively.

The analytes were ionized in the negative mode by electrospray ionization and detected by multiple reaction monitoring. A transition of 584 → 271 *m/z*, 408 → 271 *m/z*, 319 → 248 *m/z* was used for ezetimibe, ezetimibe β-D-glucuronide, and efavirenz-d5, respectively. The calibration curves of ezetimibe, ezetimibe β-D-glucuronide were prepared in PBS plus 0.05% Triton X. The calibration covered a range of 5–10,000 nM for ezetimibe and ezetimibe β-D-glucuronide. The calibration samples were processed as the samples of the microsomal assay.

Ezetimibe and ezetimibe β-D-glucuronide were quantified based on a linear regression of the analyte to IS peak area ratio (y) and the nominal concentration (x). The regressions were weighted by $1/x^2$ and a coefficient of variation (R) above 0.99 was accepted. The glucuronidation rates of the different experimental conditions were calculated with a nonlinear one-phase-association curve fit (eq. 1) with GraphPad Prism version 6:

$$y = y_0 + \text{Plateau}\,(1 - \exp(-kx)) \quad (1)$$

where y_0 is the y value when the time is zero, Plateau is the y value at infinite times, and k is the rate constant.

Statistical Analysis. $P<0.05$ was considered to be statistically significant. GraphPad prism version 6 was used for all statistical analyses.

Results

Inhibitor Screening and IC_{50} Determination. We screened 19 compounds shown to interact with OATP1B1 or OATP1B3 and clozapine (20 compounds in total) for their impact on OATP1B3-1B7–mediated cellular accumulation of DHEAS. Clozapine was included in our analysis, as occurrence of adverse events during clozapine treatment is associated with polymorphisms in the gene region of *SLCO1B7* (Fig. 1J) (Legge et al., 2017).

As summarized in Table 1, atorvastatin, troglitazone, and rifampicin inhibited OATP1B3-1B7 significantly at 25 μM, while 13 of the 20 test compounds—namely, atorvastatin, fluvastatin, simvastatin, irbesartan, telmisartan, valsartan, glibenclamide, troglitazone, mifepristone, cyclosporine, rifampicin, ezetimibe, and, ezetimibe β-D-glucuronide—significantly changed the amount of DHEAS in the cells at a concentration of 100 μM (Table 1), suggesting rather low inhibitory potency.

For all compounds exhibiting a statistical significant influence at 100 μM concentration and clozapine, we assessed the concentration-dependence of their impact on OATP1B3-1B7–mediated DHEAS transport (Figs. 1 and 2). In our

TABLE 1

Overview of the 20 compounds tested for interaction with OATP1B3-1B7 mediated uptake of dehydroepiandrosterone sulfate (DHEAS)

The data are reported as mean percent of solvent control ± S.D. Each compound was tested at two concentrations (25 and 50 μM) in three to four independent experiments each performed in triplicate. For statistical analysis of the data, the one-sample t test for normalized data was used.

Compound	Mean DHEAS Accumulation, Percentage of Solvent Control ± S.D.	
	Tested at 25 μM	Tested at 100 μM
Statins		
Atorvastatin[a]	38.8 ± 8.9[b]	8.3 ± 10.5[b]
Fluvastatin[a]	90.9 ± 22.6	20.5 ± 14.1[b]
Rosuvastatin	100.9 ± 31.6	62.9 ± 25.9
Simvastatin[a]	91.1 ± 15.0	4.9 ± 9.5[b]
Angiotensin II receptor antagonists		
Irbesartan[a]	63.9 ± 38.9	41.9 ± 24.5[b]
Telmisartan[a]	146.5 ± 27.9	63.5 ± 14.7[b]
Valsartan[a]	114.1 ± 36.6	56.0 ± 6.3[b]
Angiotensin-converting enzyme inhibitors		
Enalapril	100.9 ± 18.5	100.5 ± 25.7
Sulfonylureas		
Glibenclamide[a]	69.7 ± 14.4	45.1 ± 24.4[b]
Thiazolidinediones		
Troglitazone[a]	1.6 ± 3.0[b]	3.0 ± 6.3[b]
Steroidal antiprogestogens		
Mifepristone[a]	68.1 ± 30.0	43.9 ± 11.1[b]
Anticonvulsives		
Carbamazepine	72.2 ± 21.5	75.0 ± 23.2
Atypical antipsychotics		
Clozapine[a]	131.4 ± 30.2	103.8 ± 54.1
Immunosuppressives		
Cyclosporine[a]	137.5 ± 24.1	135.6 ± 16.1[b]
Chemotherapeutics		
Paclitaxel	106.3 ± 29.6	81.1 ± 12.5
Erythromycin	65.7 ± 54.4	109.3 ± 12.9
Antibiotics		
Doxorubicin	150.9 ± 109.3	82.6 ± 18.1
Rifampicin[a]	37.8 ± 17.8[b]	35.2 ± 16.1[b]
Azetidinones		
Ezetimibe[a]	96.7 ± 29.4	43.8 ± 32.0[b]
Ezetimibe β-D-glucuronide[a]	72.1 ± 24.7	29.9 ± 5.7[b]

[a]Compound selected for determination of concentration dependence of the effect.
[b]Indicates $P < 0.05$.

experimental set up, only atorvastatin, fluvastatin, glibenclamide, troglitazone, and rifampicin reached 90% inhibition of DHEAS accumulation, and the experimental data were used to calculate the respective IC_{50} value. For simvastatin, irbesartan, valsartan, mifepristone, clozapine ezetimibe, and ezetimibe β-D-glucuronide the IC_{50} values were computed based on the obtained experimental data. The IC_{50} values were estimated applying a "log (inhibitor) versus normalized response" curve fitting using a fixed slope of -1. The fixed slope was used as fewer than 12 experimental data points were used to fit the data.

Table 2 summarizes the obtained IC_{50} values, the 95% confidence intervals (CI), and the respective R^2 values for each compound included in the analysis. Although telmisartan and cyclosporine enhanced DHEAS accumulation, this effect was not dose dependent.

Transport Experiments with Ezetimibe. Another identified inhibitor was ezetimibe, for which the reported IC_{50} was of the same magnitude as observed for OATP1B1 and OATP1B3 (Oswald et al., 2008). Considering that glucuronidation mediated by UGTs is a major metabolic pathway of ezetimibe (Ghosal et al., 2004) and that formation of ezetimibe β-D-glucuronide occurs in the SER, we selected this compound to further investigate the influence of OATP1B3-1B7 on SER access. At first, we determined the concentration-dependent influence of ezetimibe and of ezetimibe β-D-glucuronide on OATP1B3-1B7–mediated cellular accumulation of DHEAS. The IC_{50} was 37.5 μM (95% CI, 18.7–75.1 μM) for ezetimibe and 99.7 μM (95% CI, 66.7–149 μM) for ezetimibe β-D-glucuronide (Fig. 2; Table 2).

In the next step, we tested whether OATP1B3-1B7 transports ezetimibe. First, the ezetimibe uptake experiments had to be extensively optimized as ezetimibe exhibited extensive unspecific binding (see Supplemental Fig. 1; Supplemental Methods). Eventually we were able to show a statistically significant increase in cellular accumulation at an ezetimibe concentration of 0.1 μM of about 16% compared with control (mean % of pEF6-control ± S.D.; 116.4% ± 14.8% $n = 6$ independent experiments each performed in triplicates, $P < 0.05$ one sample t test).

Abundance of OATP1B3-1B7 in the SER. Expression of OATP1B3-1B7 in the microsomal preparations of human liver and small intestine was verified by Western blot analysis, showing an enriched band at around 90 kDa (Fig. 3A). Similar results had been previously observed for the transporter, of which the molecular size was predicted to be 76 kDa (Clone Manager Professional 8; Sci-Ed Software, Denver). Moreover, Western blot analysis of the V5-tagged transporter revealed

TABLE 2

Summary of estimated half-maximal inhibitory concentration (IC_{50})

The IC_{50} was estimated with the log (inhibitor) versus normalized response curve applying a fixed slope of −1. Provided are the obtained values for each compound, the respective 95% confidence interval (CI), and the goodness of fit (R^2 value).

Compound	IC_{50} (μM)	CI (μM)	Number of Independent Experiments	R^2 Value
Atorvastatin	7.2	4.2–11.6	3	0.93
Fluvastatin	30.7	24.4–38.8	3	0.92
Simvastatin	39.6[a]	27.3–57.8	3	0.78
Irbesartan	59.0[a]	35.5–97.4	3	0.80
Valsartan	293.0[a]	136.6–628.4	4	0.56
Glibenclamide	12.7	7.7–20.9	3	0.79
Troglitazone	0.6	0.5–1.1	3	0.83
Mifepristone	706.7[a]	381.6–1309.0	3	0.33
Clozapine	137.5[a]	91.0–207.7	4	0.7
Rifampicin	13.6	9.6–19.6	5	0.89
Ezetimibe	37.5[a]	18.7–75.1	5	0.63
Ezetimibe β-D-glucuronide	99.7[a]	66.7–149.4	5	0.69

[a]Indicates where IC_{50} values were computed without reaching 90%.

an intense band at around 90 kDa and a faint band at around 58 kDa, when lysates of heterologously expressing cells were probed for V5 (Malagnino et al., 2018). Importantly, for the liver we observed an enrichment of the known SER proteins CYP3A4 and UGT1A1, comparing liver lysate with hepatic microsomes.

In accordance with OATP1B3 being localized in the plasma membrane, we observed a depletion of OATP1B3 in the microsomal fraction. In small intestinal microsomes we detected the microsomal enzymes and OATP1B3-1B7. However, we were not able to show enrichment of any of the tested markers compared with a commercially obtained total protein sample from human duodenum. Because the microsomes are prepared from mature jejunal and duodenal enterocytes, the total duodenum protein may not be a representative sample to control for ER enrichment.

We performed immunohistological and immunofluorescent stainings of human duodenal sections to investigate the cellular localization of OATP1B3-1B7 in the small intestine. Figure 3B shows that OATP1B3-1B7 is expressed in the liver and duodenum; in both tissues OATP1B3-1B7 is mostly located intracellularly. This finding was corroborated when we made an immunofluorescent staining of OATP1B3-1B7 in the duodenum (Fig. 3C). To verify that the intracellular structure is part of the intestinal SER we detected OATP1B3-1B7 in a costaining with the SER marker G6PT.

Figure 3D depicts a Z-section of the colocalization study, which was analyzed calculating the Pearson's and Mander's coefficient of colocalization of the fluorophores. The Pearson's coefficient (0.59 ± 0.14 S.D.) indicated that 59% of the detected proteins share the same localization, while the Mander's overlap coefficient for OATP1B3-1B7 was 0.80 ± 18.0 (± S.D.), suggesting that 80% of all areas positive for OATP1B3-1B7 were also positive for G6PT. In contrast, the Mander's overlap coefficient for G6PT was 0.48 ± 13.0, which showed that 48% of the G6PT-positive areas also contained OATP1B3-1B7. This seems reasonable, considering that G6PT marks the entire SER, while OATP1B3-1B7 would be expected to be present in specialized regions of the SER.

Microsomal Accumulation of Ezetimibe. Before assessing the accumulation of ezetimibe, we determined the diameters of hepatic and small intestinal microsomes to be 234.9 and 243.7 nm, respectively, suggesting that vesicle transport studies could be conducted. To test whether accumulation of ezetimibe into microsomes may be influenced by OATP1B3-1B7 inhibition, we measured the accumulation of ezetimibe in hepatic or small intestinal microsomes in the presence and absence of the OATP inhibitors atorvastatin and BSP, or the reported OATP1B3-1B7 substrate (DHEAS) (Malagnino et al., 2018). For both the hepatic (Fig. 4A) and intestinal (Fig. 4B) microsomes, we observed a statistically significant reduction of the intramicrosomal accumulated amount of ezetimibe in the presence of the tested compounds.

Inhibition of OATP1B3-1B7 Transport and Its Consequences for UGT-Mediated Metabolism. We have conducted metabolism studies in microsomes in which we determined the conversion rate of ezetimibe to ezetimibe β-D-glucuronide by UGT isoforms. Drugs have to overcome the SER membrane to be glucuronidated because the enzymatically active sites of UGT isoforms lie inside the SER. Therefore, it is standard procedure to permeabilize microsomes for glucuronidation assays with the intention to increase the metabolic rates. To test whether the transmembrane transport is the rate-limiting step in the glucuronidation process of ezetimibe, we compared the formation of ezetimibe β-D-glucuronide in the presence and absence of the pore-forming agent alamethicin, which is commonly used in microsomal studies.

When we subjected ezetimibe to nonpermeabilized microsomes, we saw that the initial conversion rate dropped by more than half in hepatic and small intestinal microsomes. In liver microsomes, the glucuronidation rate was 0.19 nmol mg^{-1} min^{-1} (95% CI, 0.18–0.22 nmol mg^{-1} min^{-1}) and 0.03 nmol mg^{-1} min^{-1} (95% CI, 0.02–0.06 nmol mg^{-1} min^{-1}) in the case of permeabilized and nonpermeabilized membranes, respectively (Fig. 5A). In permeabilized intestinal microsomes, the rate was 0.023 nmol mg^{-1} min^{-1} (95% CI, 0.01–0.04 nmol mg^{-1} min^{-1}) and in intact membranes 0.012 nmol mg^{-1} min^{1} (95% CI, 0.00–0.03 nmol mg^{-1} min^{-1}) (Fig. 5C).

To estimate the contribution of a SER transporter, we added BSP to the nonpermeabilized microsomes. Here, we observed a significant decrease in the conversion rates in hepatic as well as small intestinal microsomes (Fig. 5, B and D), suggesting that a BSP inhibitable protein grants access to the metabolic site of UGT isoforms.

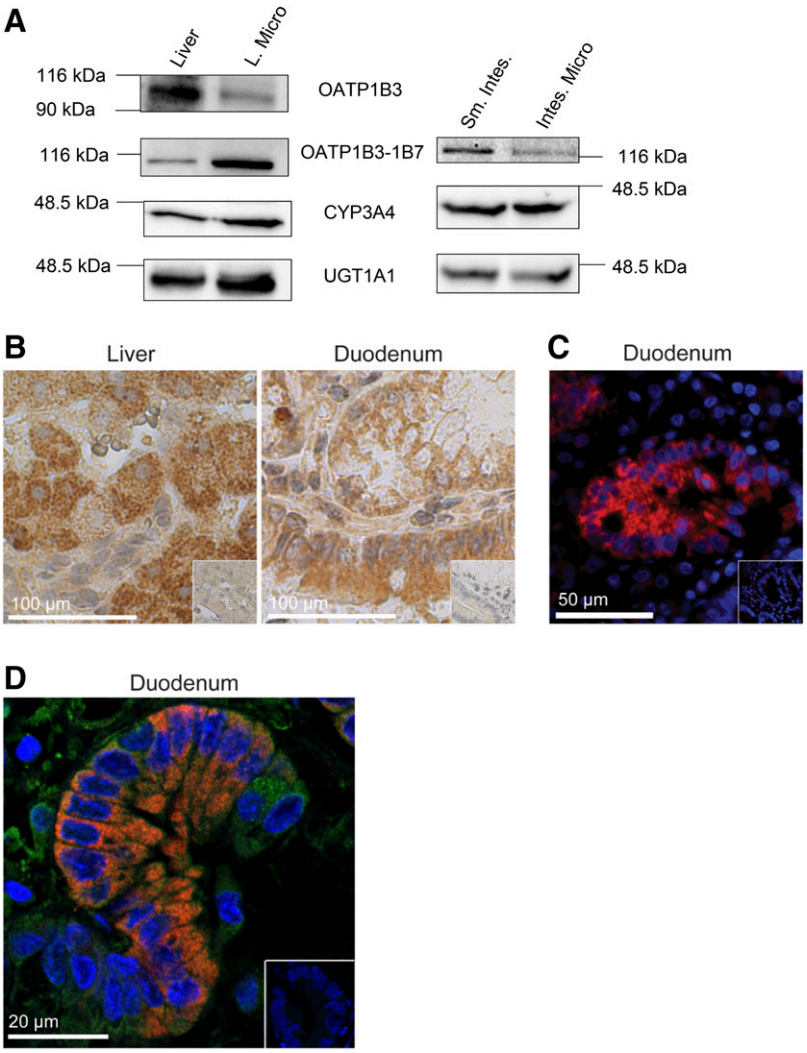

Fig. 3. Detection of OATP1B3-1B7 in liver and small intestinal tissue. (A) Western blot analysis of total liver, hepatic microsomes (L. Micro) (6-3 blots), small intestine duodenum (Sm. Intes.), and small intestinal microsomes (Intes. Micro) (three blots) was performed to assess the amount of OATP1B3-1B7, CYP3A4, and UGT1A1. Moreover, in samples derived from the liver, OATP1B3 was quantified. The proteins were detected on single films (single exposure), and the protein load was 10 μg for all investigated proteins except CYP3A4, for which the load was 5 μg. (B) Detection of OATP1B3-1B7 localization in the human liver or duodenum by immunohistochemistry. (C) Immunofluorescent staining of OATP1B3-1B7 (red) in the duodenum. Nuclei are labeled with 4′,6-diamidino-2-phenylindole (blue). In control images, rabbit serum was used instead of the primary antiserum, and these are shown in the right corner of each image. (D) Representative Z section of a costaining showing the transporter OATP1B3-1B7 in red and the smooth endoplasmic reticulum marker G6PT in green. In the control image the primary antibodies were omitted.

Discussion

In this study, we report that various drugs interact with OATP1B3-1B7 (LST-3TM12), a novel member of the OATP1B-family that is located in the SER membrane of liver tissue. For a preliminary screening, we selected drugs described to act as either substrates or inhibitors of OATP1B1 and OATP1B3, and identified several inhibitors of OATP1B3-1B7. Moreover, we have also assessed the interaction between clozapine and OATP1B3-1B7 because polymorphisms in the gene region of *SLCO1B7* have been associated with an increased risk for adverse events (Legge et al., 2017).

For all identified inhibitors and clozapine we determined the IC_{50}. Notably, the obtained experimental data allowed the calculation of the IC_{50} for five compounds while for the other compounds the respective data were computed as they did not reach 90% inhibition in our experimental setup. On average the observed IC_{50} values were two magnitudes above the expected maximal plasma concentrations (Heikinheimo, 1997; Siekmeier et al., 2001; Goodman et al., 2005; Masubuchi, 2006; Guo et al., 2015).

However, it would be too early to consider the interaction with OATP1B7-1B3 as of no relevance for the in vivo situation because we do not know the intracellular concentration of the compounds. According to Matsuda et al. (2012), the intestinal and portal concentrations of orally administered compounds may be higher than the maximal systemic concentrations. Moreover, in the employed expression system OATP1B3-1B3 is not only expressed at the cell membrane but also intracellularly (Malagnino et al., 2018), which may have resulted in an underestimation of the inhibitory potency.

In accordance with recent findings by Dickens et al. (2018) for OATP1B1 and OATP1B3, we did not observe inhibition of OATP1B3-1B7–mediated DHEAS transport by clozapine. However, considering the function of OATP1B3-1B7 as a SER access mechanism, one may speculate that the contribution of transporters to an adverse event is not driven by the interaction with the parent compound but with its metabolite *N*-desmethylclozapine, which is known to undergo hepatic glucuronidation (Schaber et al., 2001).

For the tested HMG-CoA reductase inhibitors, we observed that those statins known to be highly metabolized by CYPs and/or by UGTs (Dain et al., 1993; Prueksaritanont et al., 2002; Lennernäs, 2003) interact with OATP1B3-1B7, while rosuvastatin, for which metabolism plays a minor role in elimination (Martin et al., 2003), did not impact OATP1B3-1B7 mediated transport. However, for the angiotensin II type 1 receptor inhibitors tested in this study, the association of metabolism with OATP1B3-1B7 interaction no longer holds.

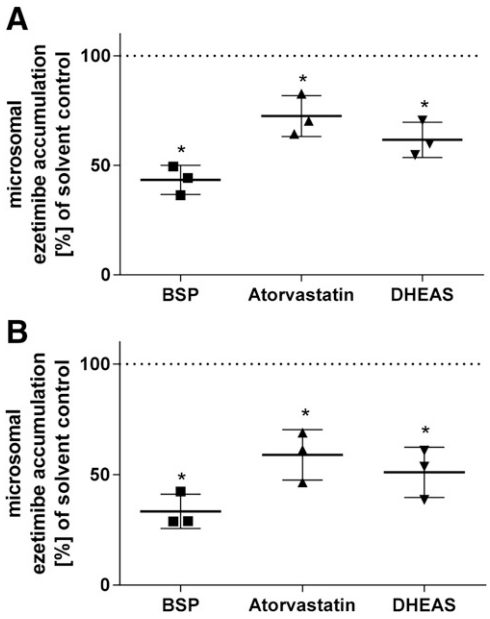

Fig. 4. Impact of known inhibitors of OATP1B3-1B7 on microsomal accumulation of ezetimibe. Hepatic (A) and small intestinal microsomes (B) were exposed to 0.1 μM ezetimibe in the absence or presence of 100 μM bromsulphthalein, atorvastatin, or dehydroepiandrosterone sulfate, and the microsomal accumulation was quantified. Data of $n = 3$ independent experiments are shown as mean % of solvent control ± S.D. For statistical analysis, the one-sample t test was applied (*$P < 0.05$).

Here we found inhibition of OATP1B3-1B7 by irbesartan and valsartan. Irbesartan undergoes extensive hydroxylation and glucuronidation (Chando et al., 1998), whereas valsartan is only minimally metabolized (Nakashima et al., 2005). Taken together, this suggests that microsomal metabolism is not a valid criterion to predict interaction with OATP1B3-1B7.

One feature that may be predictive is the presence of a steroid scaffold. Indeed, mifepristone, a progesterone receptor antagonist (Wildschut et al., 2011), was identified as an OATP1B3-1B7 inhibitor. However, it was the weakest inhibitor, with a maximal inhibition of about 50% at the maximum concentration (1000 μM) tested. Nevertheless, the steroid scaffold in mifepristone appears in the previously reported OATP1B3-1B7 substrates DHEAS and estradiol 17β-D-glucuronide (Malagnino et al., 2018). Further studies would certainly be warranted to strengthen this assumption.

Troglitazone exhibited the highest inhibitory potency in our primary screening with an IC_{50} value of about 0.6 μM. This peroxisome proliferator-activated receptor-γ agonist developed for the treatment of diabetes was withdrawn from the market in 2000 due to severe idiosyncratic hepatotoxicity (Ogimura et al., 2017). The mechanisms underlying the drug-induced liver injury are still a focus of ongoing research programs, but they are assumed to involve interactions with multiple cellular pathways (Masubuchi, 2006). Considering that troglitazone itself is highly metabolized (He et al., 2004), it could be possible that OATP1B3-1B7 plays a role in its metabolism. However, this remains to be determined.

In this study, we further investigated the role of OATP1B3-1B7 in SER access and metabolism using ezetimibe, for which the reported IC_{50} value was similar to that observed for OATP1B1 (14.8 μM) or OATP1B3 (8.9 μM) (Oswald et al., 2008). Moreover, ezetimibe is extensively glucuronidated (Ghosal et al., 2004), which allows indirect testing of the relation between SER access and the glucuronidation rate of a compound. Ezetimibe not only impaired OATP1B3-1B7–mediated DHEAS uptake, but our data also suggested that it is a substrate of OATP1B3-1B7. Once absorbed, ezetimibe is extensively metabolized by glucuronidation (Patel et al., 2003). The major metabolite created is ezetimibe β-D-glucuronide, which not only exhibits pharmacologic activity comparable to the parent compound but also is known to be part of the extensive enterohepatic recycling of ezetimibe (Patel et al., 2003; Kosoglou et al., 2005).

Importantly, glucuronidation of ezetimibe is not limited to the liver; it has also been shown for the small intestine. Considering that SER access would also be of relevance in the intestine, we confirmed the presence of OATP1B3-1B7 in enterocytes and small intestinal microsomes. In accordance with previously published findings where OATP1B3-1B7 was found to be located in the SER of hepatocytes (Malagnino et al., 2018), we observed the majority of the transporter to be present in the SER. Also important is that SER access is a rate-limiting step for glucuronidation. In metabolic studies with microsomes the pore-forming substance alamethicin is commonly used, which results in an increase of the observed glucuronidation rates (Fisher et al., 2000). By testing the influence of alamethicin on the glucuronidation of ezetimibe, we observed this effect of alamethicin in both small intestinal and hepatic microsomes.

To link OATP1B3-1B7 to SER access of ezetimibe, we tested the influence of OATP inhibitors or substrates of the transporter on the accumulation of ezetimibe in liver and small intestine microsomes. We observed a significant reduction of ezetimibe accumulation in their presence. This finding suggested that an OATP transporter might be involved in the SER entry of ezetimibe in the intestine and liver. Furthermore, we were able to show that the diminished accumulation of ezetimibe into microsomes also affected glucuronidation rates of ezetimibe. Indeed, in the presence of BSP, a nonglucuronidated OATP-inhibitor (Grodsky et al., 1959; Guofeng and Morris, 2014), the glucuronidation rates of ezetimibe were significantly decreased.

Taken together, our data suggest that ezetimibe is a substrate of OATP1B3-1B7, for which OATP1B3-1B7 could mediate SER access of ezetimibe and thereby facilitate admission to the active site of UGT isoforms. Considering that ezetimibe β-D-glucuronide is the major metabolite, we tested whether this molecule also interacts with the transport function of OATP1B3-1B7. Here, we observed moderate inhibition. Although we were able to link glucuronidation of ezetimibe with OATP inhibition in the SER, we are not able to define whether OATP1B3-1B7 mediates SER entry or exit; both processes would have an influence on the enzymatic rates of glucuronidation, considering the possibility of product inhibition of the involved UGT enzymes.

In conclusion, we showed that OATP1B3-1B7 interacts with several drugs. One of the identified inhibitors was ezetimibe, which is also a substrate of OATP1B3-1B7. Moreover, ezetimibe glucuronidation rates were decreased by BSP, which is a OATP1B3-1B7 inhibitor. Thus, we hypothesize, that OATP1B3-1B7 may function as a SER gateway for ezetimibe.

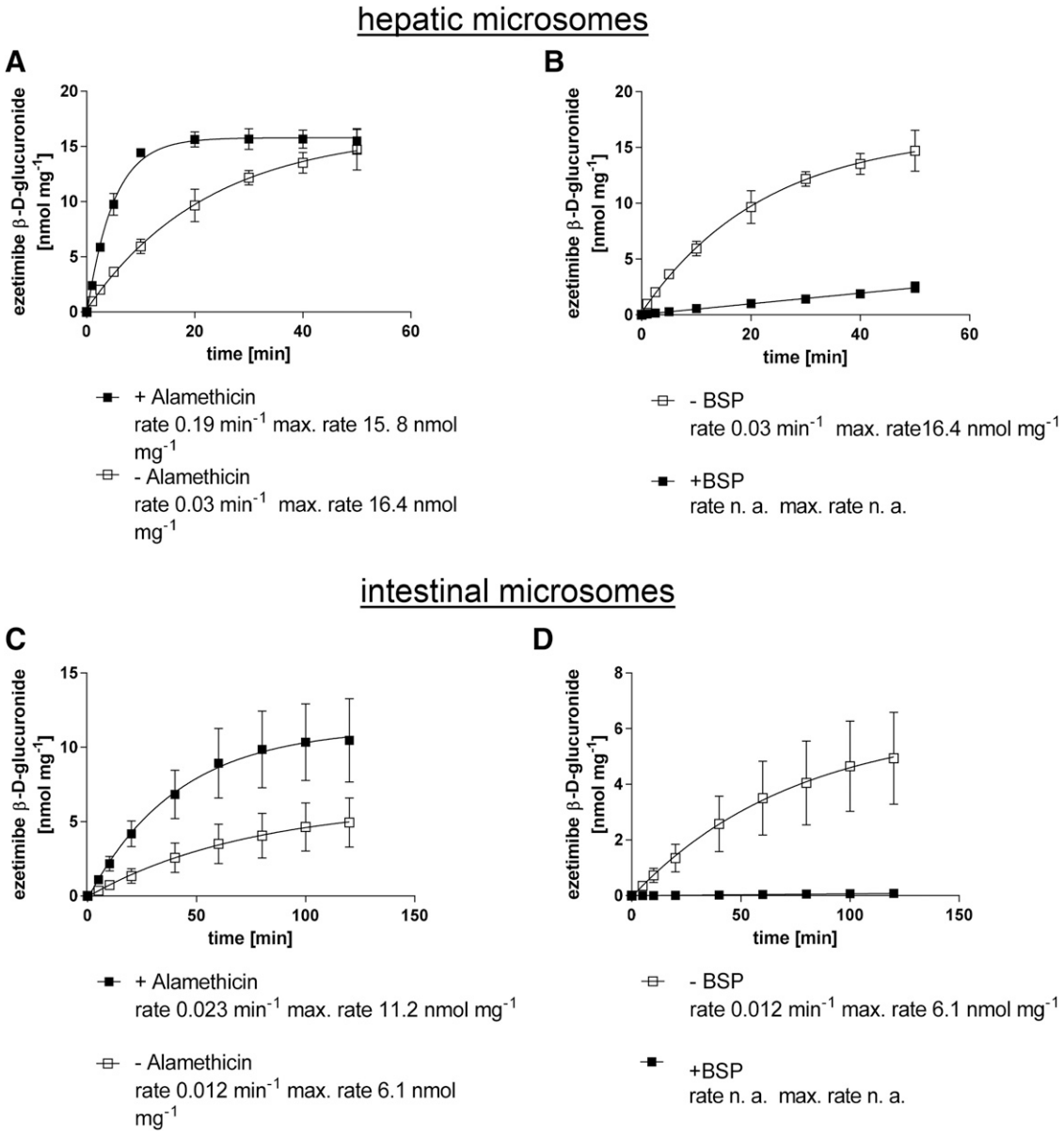

Fig. 5. Ezetimibe glucuronidation in microsomes. The ezetimibe glucuronidation rates in hepatic (A and B) and small intestinal microsomes (C and D) were assessed in the presence or absence of the pore-forming molecule alamethicin (A and C) and in the presence or absence of the OATP inhibitor BSP (B and D). The rate of ezetimibe glucuronidation was calculated applying the nonlinear one-phase association curve fit. Data are reported as mean ± S.D. of $n = 3$ independent experiments. n.a., not applicable.

Acknowledgments

This study will be part of the thesis of V.M. The confocal light microscopy and image analysis was performed at the Imaging Core Facility at the Biozentrum of the University of Basel, and we thank the staff members for their expert advice.

Authorship Contributions

Participated in research design: Malagnino, Duthaler, Meyer zu Schwabedissen.

Conducted experiments: Malagnino, Duthaler, Seibert.

Contributed new reagents or analytic tools: Krähenbühl, Meyer zu Schwabedissen.

Performed data analysis: Malagnino, Duthaler, Meyer zu Schwabedissen.

Wrote or contributed to the writing of the manuscript: Malagnino, Duthaler, Meyer zu Schwabedissen.

References

Abe T, Kakyo M, Tokui T, Nakagomi R, Nishio T, Nakai D, Nomura H, Unno M, Suzuki M, Naitoh T, et al. (1999) Identification of a novel gene family encoding human liver-specific organic anion transporter LST-1. *J Biol Chem* **274**: 17159–17163.

Abe T, Unno M, Onogawa T, Tokui T, Kondo TN, Nakagomi R, Adachi H, Fujiwara K, Okabe M, Suzuki T, et al. (2001) LST-2, a human liver-specific organic anion transporter, determines methotrexate sensitivity in gastrointestinal cancers. *Gastroenterology* **120**:1689–1699.

Alberts BJA, Johnson A, Lewis J, Raff M, Roberts K, and Walter P (2002) *Molecular Biology of the Cell*, 4th ed, Garland Science, New York.

Bolte S and Cordelières FP (2006) A guided tour into subcellular colocalization analysis in light microscopy. *J Microsc* **224**:213–232.

Chando TJ, Everett DW, Kahle AD, Starrett AM, Vachharajani N, Shyu WC, Kripalani KJ, and Barbhaiya RH (1998) Biotransformation of irbesartan in man. *Drug Metab Dispos* **26**:408–417.

Coleman MD (2010) *Human Drug Metabolism*, 2nd ed, John Wiley & Sons Ltd, Chichester, United Kingdom.

Dain JG, Fu E, Gorski J, Nicoletti J, and Scallen TJ (1993) Biotransformation of fluvastatin sodium in humans. *Drug Metab Dispos* **21**:567–572.

Dickens D, Rädisch S, Chiduza GN, Giannoudis A, Cross MJ, Malik H, Schaeffeler E, Sison-Young RL, Wilkinson EL, Goldring CE, et al. (2018) Cellular uptake of the

atypical antipsychotic clozapine is a carrier-mediated process. *Mol Pharm* **15**: 3557–3572.
Fisher MB, Campanale K, Ackermann BL, VandenBranden M, and Wrighton SA (2000) In vitro glucuronidation using human liver microsomes and the pore-forming peptide alamethicin. *Drug Metab Dispos* **28**:560–566.
Ghosal A, Hapangama N, Yuan Y, Achanfuo-Yeboah J, Iannucci R, Chowdhury S, Alton K, Patrick JE, and Zbaida S (2004) Identification of human UDP-glucuronosyltransferase enzyme(s) responsible for the glucuronidation of ezetimibe (Zetia). *Drug Metab Dispos* **32**:314–320.
Giacomini KM, Huang SM, Tweedie DJ, Benet LZ, Brouwer KL, Chu X, Dahlin A, Evers R, Fischer V, Hillgren KM, et al.; International Transporter Consortium (2010) Membrane transporters in drug development. *Nat Rev Drug Discov* **9**: 215–236.
Goodman LS, Gilman A, Brunton LL, Lazo JS, and Parker KL (2005) *Goodman & Gilman's the Pharmacological Basis of Therapeutics*, 11th ed, McGraw-Hill Medical Pub. Division, New York.
Grodsky GM, Carbone JV, and Fanska R (1959) Identification of metabolites of sulfobromophthalein. *J Clin Invest* **38**:1981–1988.
Guo L, Wang MM, He M, Qiu FR, and Jiang J (2015) Simultaneous determination of ezetimibe and its glucuronide metabolite in human plasma by solid phase extraction and liquid chromatography-tandem mass spectrometry. *J Chromatogr B Analyt Technol Biomed Life Sci* **986–987**:108–114.
Guofeng Y and Morris ME (2014) *Drug Transporters Molecular Characterization and Role in Drug Disposition*, John Wiley & Sons Inc., Hoboken, NJ.
He K, Talaat RE, Pool WF, Reily MD, Reed JE, Bridges AJ, and Woolf TF (2004) Metabolic activation of troglitazone: identification of a reactive metabolite and mechanisms involved. *Drug Metab Dispos* **32**:639–646.
Heikinheimo O (1997) Clinical pharmacokinetics of mifepristone. *Clin Pharmacokinet* **33**:7–17.
Hillgren KM, Keppler D, Zur AA, Giacomini KM, Stieger B, Cass CE, and Zhang L; International Transporter Consortium (2013) Emerging transporters of clinical importance: an update from the International Transporter Consortium. *Clin Pharmacol Ther* **94**:52–63.
Kalliokoski A and Niemi M (2009) Impact of OATP transporters on pharmacokinetics. *Br J Pharmacol* **158**:693–705.
Kosoglou T, Statkevich P, Johnson-Levonas AO, Paolini JF, Bergman AJ, and Alton KB (2005) Ezetimibe: a review of its metabolism, pharmacokinetics and drug interactions. *Clin Pharmacokinet* **44**:467–494.
Kunze A, Huwyler J, Camenisch G, and Poller B (2014) Prediction of organic anion-transporting polypeptide 1B1- and 1B3-mediated hepatic uptake of statins based on transporter protein expression and activity data. *Drug Metab Dispos* **42**: 1514–1521.
Legge SE, Hamshere ML, Ripke S, Pardinas AF, Goldstein JI, Rees E, Richards AL, Leonenko G, and Jorskog LF; Clozapine-Induced Agranulocytosis Consortium (2017) Genome-wide common and rare variant analysis provides novel insights into clozapine-associated neutropenia. *Mol Psychiatry* **22**:1509.
Lennernäs H (2003) Clinical pharmacokinetics of atorvastatin. *Clin Pharmacokinet* **42**:1141–1160.
Maeda K (2015) Organic anion transporting polypeptide (OATP)1B1 and OATP1B3 as important regulators of the pharmacokinetics of substrate drugs. *Biol Pharm Bull* **38**:155–168.
Malagnino V, Hussner J, Seibert I, Stolzenburg A, Sager CP, and Meyer Zu Schwabedissen HE (2018) LST-3TM12 is a member of the OATP1B family and a functional transporter. *Biochem Pharmacol* **148**:75–87.
Martin PD, Warwick MJ, Dane AL, Hill SJ, Giles PB, Phillips PJ, and Lenz E (2003) Metabolism, excretion, and pharmacokinetics of rosuvastatin in healthy adult male volunteers. *Clin Ther* **25**:2822–2835.
Masubuchi Y (2006) Metabolic and non-metabolic factors determining troglitazone hepatotoxicity: a review. *Drug Metab Pharmacokinet* **21**:347–356.
Matern S, Matern H, Farthmann EH, and Gerok W (1984) Hepatic and extrahepatic glucuronidation of bile acids in man. Characterization of bile acid uridine 5′-diphosphate-glucuronosyltransferase in hepatic, renal, and intestinal microsomes. *J Clin Invest* **74**:402–410.
Matsuda Y, Konno Y, Satsukawa M, Kobayashi T, Takimoto Y, Morisaki K, and Yamashita S (2012) Assessment of intestinal availability of various drugs in the oral absorption process using portal vein-cannulated rats. *Drug Metab Dispos* **40**:2231–2238.
Miura M, Kagaya H, Satoh S, Inoue K, Saito M, Habuchi T, and Suzuki T (2008) Influence of drug transporters and UGT polymorphisms on pharmacokinetics of phenolic glucuronide metabolite of mycophenolic acid in Japanese renal transplant recipients. *Ther Drug Monit* **30**:559–564.
Nakashima A, Kawashita H, Masuda N, Saxer C, Niina M, Nagae Y, and Iwasaki K (2005) Identification of cytochrome P450 forms involved in the 4-hydroxylation of valsartan, a potent and specific angiotensin II receptor antagonist, in human liver microsomes. *Xenobiotica* **35**:589–602.
Ogimura E, Nakagawa T, Deguchi J, Sekine S, Ito K, and Bando K (2017) Troglitazone inhibits bile acid amidation: a possible risk factor for liver injury. *Toxicol Sci* **158**:347–355.
Oswald S, König J, Lütjohann D, Giessmann T, Kroemer HK, Rimmbach C, Rosskopf D, Fromm MF, and Siegmund W (2008) Disposition of ezetimibe is influenced by polymorphisms of the hepatic uptake carrier OATP1B1. *Pharmacogenet Genomics* **18**:559–568.
Patel J, Sheehan V, and Gurk-Turner C (2003) Ezetimibe (Zetia): a new type of lipid-lowering agent. *Proc Bayl Univ Med Cent* **16**:354–358.
Petzinger E and Geyer J (2006) Drug transporters in pharmacokinetics. *Naunyn Schmiedebergs Arch Pharmacol* **372**:465–475.
Picard N, Yee SW, Woillard JB, Lebranchu Y, Le Meur Y, Giacomini KM, and Marquet P (2010) The role of organic anion-transporting polypeptides and their common genetic variants in mycophenolic acid pharmacokinetics. *Clin Pharmacol Ther* **87**:100–108.
Prueksaritanont T, Subramanian R, Fang X, Ma B, Qiu Y, Lin JH, Pearson PG, and Baillie TA (2002) Glucuronidation of statins in animals and humans: a novel mechanism of statin lactonization. *Drug Metab Dispos* **30**:505–512.
Schaber G, Wiatr G, Wachsmuth H, Dachtler M, Albert K, Gaertner I, and Breyer-Pfaff U (2001) Isolation and identification of clozapine metabolites in patient urine. *Drug Metab Dispos* **29**:923–931.
Schindelin J, Arganda-Carreras I, Frise E, Kaynig V, Longair M, Pietzsch T, Preibisch S, Rueden C, Saalfeld S, Schmid B, et al. (2012) Fiji: an open-source platform for biological-image analysis. *Nat Methods* **9**:676–682.
Schwarz UI, Meyer zu Schwabedissen HE, Tirona RG, Suzuki A, Leake BF, Mokrab Y, Mizuguchi K, Ho RH, and Kim RB (2011) Identification of novel functional organic anion-transporting polypeptide 1B3 polymorphisms and assessment of substrate specificity. *Pharmacogenet Genomics* **21**:103–114.
Siekmeier R, Lattke P, Mix C, Park JW, and Jaross W (2001) Dose dependency of fluvastatin pharmacokinetics in serum determined by reversed phase HPLC. *J Cardiovasc Pharmacol Ther* **6**:137–145.
Tirona RG, Leake BF, Merino G, and Kim RB (2001) Polymorphisms in OATP-C: identification of multiple allelic variants associated with altered transport activity among European- and African-Americans. *J Biol Chem* **276**:35669–35675.
Wildschut H, Both MI, Medema S, Thomee E, Wildhagen MF, and Kapp N (2011) Medical methods for mid-trimester termination of pregnancy. *Cochrane Database Syst Rev* (1):CD005216.
Yoshida K, Maeda K, and Sugiyama Y (2012) Transporter-mediated drug--drug interactions involving OATP substrates: predictions based on in vitro inhibition studies. *Clin Pharmacol Ther* **91**:1053–1064.

Address correspondence to: Dr. Henriette E. Meyer zu Schwabedissen, Biopharmacy, Department of Pharmaceutical Sciences, University of Basel, Klingelbergstrasse 50, 4056 Basel, Switzerland. E-mail: h.meyerzuschwabedissen@unibas.ch

OATP1B3-1B7 (LST-3TM12) is a drug transporter that affects endoplasmic reticulum access and the metabolism of ezetimibe

Vanessa Malagnino, Urs Duthaler, Isabel Seibert, Stephan Krähenbühl, Henriette E. Meyer zu Schwabedissen

Supplemental Methods

Transport experiments with ezetimibe

HeLa cells, which transiently express OATP1B3-1B7, were prepared to validate the transport of ezetimibe. Ten minutes before exposure to ezetimibe, the cells were pre-incubated with HBSS containing 1 µM of α-cyclodextrin. α-Cyclodextrin, a mild solvent that is commonly used for dissolution of poorly soluble drugs (Challa et al., 2005), was utilized to diminish unspecific binding of ezetimibe. The cells were then exposed to 10 nM of unlabeled ezetimibe supplemented with [^{3}H]-labeled tracer (specific activity 20-40 Ci/mmol, 100'000 DPM/well, ART 1463, Hartmann ANALYTIC, Braunschweig, Germany). The cells were incubated for 10 min at 37 °C and were subsequently washed twice with ice-cold PBS. The amount of radiolabel was quantified by liquid scintillation counting as described above.

Ezetimibe transport was also assessed in suspended HeLa cells: In detail, cells were cultivated in 6 cm dishes containing 8 x 10^5 cells. One day after seeding, transfection was performed with 21.2 µL Lipofectin® Transfection Reagent (Thermo Fisher Scientific) and 3.6 µg of OATP1B3-1B7-pEF6 or pEF6-control plasmid per dish. Expression was driven by a T7 RNA-polymerase introduced by simultaneous infection with the vTF7-3 virus (American Type Culture Collection, VR-2153) (Fuerst et al., 1986). 16 h after transfection, cells were detached with trypsin, the number of cells was determined (CASY, OMNI Life Sciences, Basel, Switzerland), and 10^5 cells in medium were aliquoted into 1.5 mL tubes. Then, 25 µM of ezetimibe supplemented with [^{3}H]-tracer (100,000DPM/well) in 50 mM Tris 0.25 M sucrose buffer (pH 7.5) were added to the cells and incubated at 37 °C and 620 rpm (MS-100 Thermoshaker,

Labgene Scientific Sa, Châtel-Saint-Denis, Switzerland) for 10 min. The reaction was stopped by filtration through Millipore Durapore filters (pore size 0.22 µM, Millipore, Zug, Switzerland) followed by washing of the filters with 3 mL ice-cold PBS. The filters were removed, immerged in Rotiszint®eco Plus scintillation fluid, and then ezetimibe accumulation was assessed by scintillation counting with the Tri-Carb 2900TR. The ezetimibe uptake rate in presence of OATP1B3-1B7 was normalized to that observed in pEF6-control transfected cells.

Supplemental Figure 1

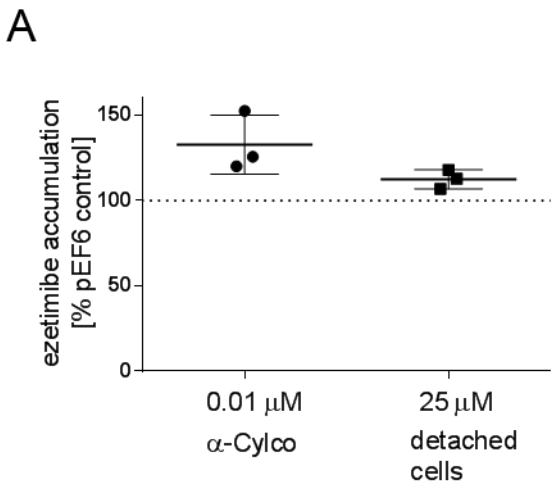

Supplemental Figure 1. Mean uptake of ezetimibe in OATP1B3-1B7 transfected HeLa cells. (A, 0.01µM α-CyclO) After treatment of HeLa cells expressing OATP1B3-1B7with 1 µM α-cyclodextrin, uptake of 10 nM ezetimibe was determined. Data are reported as mean % of pEF6-control ± SD of three independent replicates performed in biological triplicates. (A, 25 µM detached cells) Uptake in detached cells expressing OATP1B3-1B7 was measured at a concentration of 25 µM ezetimibe. Data are reported as mean % of pEF6-control ± SD of three independent replicates performed in biological duplicates. For statistical analysis the one

sample t-test was applied; None of the applied conditions is significantly different from the control.

Supplemental Table 1. List summarizing the antibodies used for immunohistochemistry and Western blot analysis. Except from the OATP1B3 antibody (Ho et al., 2006) all antibodies were commercially obtained from LifeSpan Biotechnologies[*] (Seattle, USA), Origene[α] (Rockville, USA), Novus Biologicals[β] (Littleton, USA), R & D Systems[ɣ] (Minneapolis, USA) LabForce (Muttenz, Switzerland), Santa Cruz Biotechnology Inc.[ε] (Dallas, USA), Bio-Techne (Abingdon, UK), Enzo Life Sciences[ω] (Lörrach, Germany), and Biorad Laboratories AG[Δ] (Cressier, Switzerland).

antibody (clone)	IF/IH dilution	WB dilution
anti-OATP1B7 (LS-C110963)[*]	1:50	n. a.
anti-OATP1B7 (TA339136)[α]	1:50	1:2000
anti-CYP3A4 (NBP2-37502)[β]	n. a.	1:2000
anti-OATP1B3	1:50	1:5000
anti-UGT1A1 (AF6490)[ɣ]	n. a.	1:200
anti-G6PT (H00002542)[β]	1:17	1:1000
anti-Calnexin (ADI-SPA-865)[ω]	1:100	1:1000
Goat Anti-Mouse IgG HRP[Δ]	1:200	1:1000-2000
Rabbit Anti-Goat IgG HRP[Δ]	1:200	1.1000-2000
Goat Anti-Rabbit IgG HRP[Δ]	1:200	1:1000

3.3 OATP1B3-1B7, a novel Organic Anion Transporting Polypeptide is modulated by FXR ligands and transports bile acids

Malagnino V[1], Hussner J[1], Issa A[1], Midzic A[1], Meyer zu Schwabedissen HE[1].

Laboratories of origin:

[1] Biopharmacy, Department of Pharmaceutical Sciences, University of Basel, Basel, Switzerland

Contribution Malagnino V: Study design, acquisition, analysis and interpretation of data, drafting of manuscript.

Journal: American Journal of Physiology-Gastrointestinal and Liver Physiology (2019) 317: G751-G762

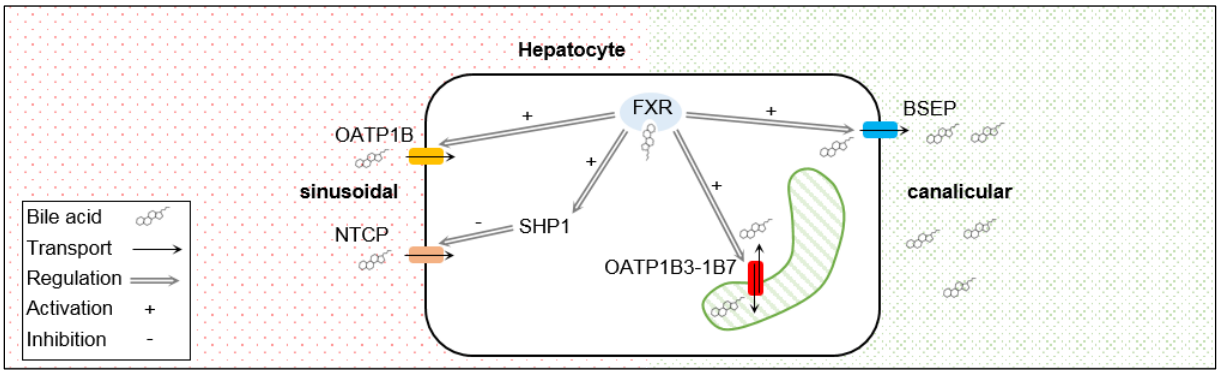

Graphical Abstract 3. OATP1B3-1B7, a novel Organic Anion Transporting Polypeptide is modulated by FXR ligands and transports bile acids. Artwork by V. Malagnino.

Am J Physiol Gastrointest Liver Physiol 317: G751–G762, 2019.
First published September 11, 2019; doi:10.1152/ajpgi.00330.2018.

RESEARCH ARTICLE | *Liver and Biliary Tract Physiology/Pathophysiology*

OATP1B3-1B7, a novel organic anion transporting polypeptide, is modulated by FXR ligands and transports bile acids

Vanessa Malagnino, Janine Hussner, Ali Issa, Angela Midzic, and Henriette E. Meyer zu Schwabedissen

Biopharmacy, Department of Pharmaceutical Sciences, University Basel, 4056 Basel, Switzerland

Submitted 5 October 2018; accepted in final form 2 September 2019

Malagnino V, Hussner J, Issa A, Midzic A, Meyer zu Schwabedissen HE. OATP1B3-1B7, a novel organic anion transporting polypeptide, is modulated by FXR ligands and transports bile acids. *Am J Physiol Gastrointest Liver Physiol* 317: G751–G762, 2019. First published September 11, 2019; doi:10.1152/ajpgi.00330.2018.—Organic anion transporting polypeptide (OATP) 1B3–1B7 (LST-3TM12) is a member of the OATP1B [solute carrier organic anion transporter (*SLCO*) *1B*] family. This transporter is not only functional but also expressed in the membrane of the smooth endoplasmic reticulum of hepatocytes and enterocytes. OATP1B3–1B7 is a splice variant of *SLCO1B3* in which the initial part is encoded by *SLCO1B3*, whereas the rest of the mRNA originates from the gene locus of *SLCO1B7*. In this study, we not only showed that *SLCO1B3* and the mRNA encoding for OATP1B3–1B7 share the 5′ untranslated region but also that silencing of an initial *SLCO1B3* exon lowered the amount of *SLCO1B3* and of *SLCO1B7* mRNA in Huh-7 cells. To validate the assumption that both transcripts are regulated by the same promoter we tested the influence of the bile acid sensor farnesoid X receptor (FXR) on their transcription. Treatment of Huh-7 and HepaRG cells with activators of this known regulator of OATP1B3 not only increased *SLCO1B3* but also OATP1B3–1B7 mRNA transcription. Applying a heterologous expression system, we showed that several bile acids interact with OATP1B3–1B7 and that taurocholic acid and lithocholic acid are OATP1B3–1B7 substrates. As OATP1B3–1B7 is located in the smooth endoplasmic reticulum, it may grant access to metabolizing enzymes. In accordance are our findings showing that the OATP1B3–1B7 inhibitor bromsulphthalein significantly reduced uptake of bile acids into human liver microsomes. Taken together, we report that OATP1B3–1B7 transcription can be modulated with FXR agonists and antagonists and that OATP1B3–1B7 transports bile acids.

NEW & NOTEWORTHY Our study on the transcriptional regulation of the novel organic anion transporting polypeptide (OATP) 1B3–1B7 concludes that the promoter of solute carrier organic anion transporter (*SLCO*) *1B3* governs *SLCO1B3–1B7* transcription. Moreover, the transcription of OATP1B3–1B7 can be modulated by farnesoid X receptor (FXR) agonists and antagonists. FXR is a major regulator in bile acid homeostasis that links OATP1B3–1B7 to this physiological function. Findings in transport studies with OATP1B3–1B7 suggest that this transporter interacts with the herein tested bile acids.

farnesoid X receptor; LST-3TM12; OATP1B3-1B7; *SLCO1B7*; *SLCO1B3*

INTRODUCTION

Proteins facilitating transmembrane transport are determinants of a variety of physiological processes. Considering that cellular accumulation is a prerequisite for intracellular mechanisms, including receptor binding, metabolism, or transcellular transport, uptake transporters play a key role in various pathways. One family of transporters that has repeatedly been associated with liver functions is the family of the organic anion transporting polypeptide (OATP) 1B transporters.

The OATPs are classified on the basis of their amino acid identities and divided into families that share ≥40% identity, which is represented by their first denominator in Arabic numbers (e.g., OATP1). The transporters are further divided in subfamilies with ≥60% identity that have one Latin letter as identifier (e.g., OATP1B) (9). The last denominator identifies the individual transporter and is again an Arabic number (e.g., OATP1B1) (9). The genes encoding the OATPs are written in italics and identified with the solute carrier organic anion transporter (*SLCO*) prefix with the same identifiers used for the proteins (9). For example, OATP1B1 is encoded by *SLCO1B1*.

The subfamily of the OATP1B transporters comprises the two members OATP1B1 (gene *SLCO1B1*) and OATP1B3 (gene *SLCO1B3*). These two transporters are not only involved in pharmacokinetics of their substrate drugs but also in the hepatocellular handling of endogenous molecules (13, 29). Recently, we were able to show that OATP1B3–1B7 (also known as LST-3TM12 under National Center for Biotechnology Information (NCBI) accession no. AY257470 and SLCO1B3-SLCO1B7 readthrough) is an additional member of the OATP1B family (16). In detail, the OATP1B3–1B7 protein is a variant of OATP1B3, as the N-terminal part of its mRNA derives from *SLCO1B3*, whereas the remaining part of the transcript originates from the neighboring *SLCO1B7* gene locus. According to the Human Gene Nomenclature, the mRNA is named SLCO1B3-SLCO1B7 readthrough.

The encoded protein OATP1B3–1B7 is a functional protein that transports the steroid hormones dehydroepiandrosterone sulfate (DHEAS), estradiol 17 β-D-glucuronide (E_2G), and ezetimibe (15, 16). Furthermore, OATP1B3–1B7 is expressed in the smooth endoplasmic reticulum (SER) of hepatocytes and enterocytes, and we hypothesize that it influences the access to metabolizing enzymes in the SER, as recently shown in the context of ezetimibe glucuronidation (15). The SLCO1B3-SLCO1B7 readthrough mRNA extends the number of variants associated with the *SLCO1B3* gene locus (24, 27). In terms of splice variants, *SLCO1B3* has also been reported to encode for multiple NH_2 terminally truncated versions (28), of which the

Address for reprint requests and other correspondence: H. E. Meyer zu Schwabedissen, Biopharmacy, Dept. of Pharmaceutical Sciences, Univ. of Basel, Klingelbergstrasse 50, 4056 Basel, Switzerland (e-mail: h.meyerzuschwabedissen@unibas.ch).

cancer-specific OATP1B3 is studied the most. This particular variant lacks the first NH_2-terminal 28 amino acids, or, more precisely, it does not include the first exon of *SLCO1B3* and is exclusive for malignant cells (20, 27).

Taking into account that the *SLCO1B3* part of SLCO1B3-SLCO1B7 readthrough (NCBI no. AY257470) includes exon 1 and that the transporter is expressed in healthy tissue, we assumed that transcriptional regulation of this splice variant might be regulated by similar mechanisms as those known for OATP1B3. Expression of the latter is controlled by multiple transcription factors, including the hepatocyte nuclear factor homeobox A (T cell factor 1), the forkhead box protein A2 (also known as hepatocyte nuclear factor 3β), and the farnesoid X receptor (FXR; nuclear receptor subfamily 1 group G member 4) (21). FXR binds directly to an inverted hexanucleotide repeat motif (IR-1 element) located 70–82 bp upstream of the transcriptional start site at exon 1 (11) and is ligand activated as it senses the intracellular levels of bile acids (14). Once activated, FXR translocates into the nucleus, in which it binds to FXR response elements, thereby modulating the transcription of its target genes (21). In general, the gene network modulated by FXR is involved in the regulation of bile acids (18). It is assumed that the overall function of the regulated genes is the protection of the organism, or at least the hepatocytes, from excessive bile acid exposure (30). In accordance are findings showing that activation of FXR directly increases the expression of the canalicular located efflux transporters bile salt export pump [ATP-binding cassette subfamily B member 11 (*ABCB11*)] and the multidrug resistance-associated protein 2 (*ABCC2*), both are efficiently excreting conjugated bile acids into the bile (10). Additionally, the expression of organic solute transporter α [OSTα; solute carrier (SLC) 51A] and β (OSTβ; SLC51B), which facilitate bidirectional transport of bile acids at the sinusoidal/basolateral membrane of hepatic, intestinal, and renal cells, is also induced by FXR (3, 4). However, with the differential regulation of hepatic uptake transporters of bile acids by FXR, the complexity of the gene network is revealed. Indeed, exposure to FXR activators has been shown to increase expression of OATP1B3 (11) and OATP1B1 (19) while reducing that of the Na^+-taurocholate cotransporting polypeptide (NTCP; SLC10A1) (7). NTCP is the most efficient bile acid uptake mechanism in human hepatocytes (18), and its suppression by FXR is indirect via the small heterodimer partner 1 [SHP; nuclear receptor subfamily 0 group B member 2 (*NR0B2*)] (10). This exceptional member of the family of nuclear receptors does not exhibit a DNA-binding site but efficiently represses genes by direct interaction with other transcription factors, finally resulting in lower transcription (23). SHP is a target of FXR and mediator of the restricted de novo formation of bile acids by cytochrome *P*450 7A1, which is the rate-limiting enzyme in bile acid synthesis (8).

Taken together, FXR is a major regulator of bile acid homeostasis and a known modulator of *SLCO1B3* transcription. Considering that OATP1B3–1B7 partially originates from *SLCO1B3*, we hypothesized that OATP1B3–1B7 could also be part of this gene network contributing to the SER handling of bile acids. We treated the hepatoma cell lines Huh-7 and HepaRG with the FXR agonists chenodeoxycholic acid (CDCA) (11) and GW4064 (32) and quantified the expression of OATP1B3–1B7 and known FXR target genes. Moreover, we treated the Huh-7 cells with the FXR antagonist DY268 and measured alteration in gene expression of OATP1B3–1B7 (31). Additionally, we assessed whether OATP1B3–1B7 functions as bile acid transporter.

MATERIALS AND METHODS

Materials. Unless stated otherwise, all substances were purchased from Sigma-Aldrich, Buchs, Switzerland.

Rapid amplification of the 5′ untranslated region of SLCO1B3-SLCO1B7 readthrough. Amplification of the 5′ untranslated region (5′UTR) was performed using the SMARTer rapid amplification of cDNA ends (RACE) 5′/3′ kit, and Human Liver Marathon-Ready cDNA both obtained from Takara Bio Europe (Saint-Germain-en-Laye, France), and the primer RACE 5′-CACCAGCACGGAATAT-GAGGTAAGTCC-′3 (Microsynth, Balgach, Switzerland) located in position 1,651 bp to 1,677 bp of the SLCO1B3-SLCO1B7 readthrough reference sequence (NCBI no. AY257470). The PCR products were visualized by agarose gel electrophoresis, isolated, and subcloned into pDrive (Qiagen, Hombrechtikon, Switzerland). After transformation in *Escherichia coli*, plasmids were isolated using the NucleoSpin Plasmid Kit (Macherey-Nagel, Oensingen, Switzerland) according to the manufacturer's instruction. After sequencing using the T7 or M13R primers (Microsynth), the obtained information was first analyzed by a database search using the open access software BLAST (https://blast.ncbi.nlm.nih.gov/Blast.cgi), followed by sequence alignment using the software Clone Manager 8 (Scientific & Educational Software).

Cell culture. Huh-7 cells (Japanese Collection of Research Bioresources Cell Bank), HepG2 cells (American Type Culture Collection, HB8065), and HeLa cells (American Type Culture Collection, CCL2) were cultivated in DMEM supplemented with 10% FCS (Amimed, Allschwil, Switzerland) and 1% stable glutamine (BioConcept, Allschwil, Switzerland). HepaRG (6) cells kindly provided by Prof. S. Krähenbühl (Clinical Pharmacology and Toxicology, University Hospital of Basel), were cultivated in Eagle's medium (Invitrogen, Carlsbad) in which 10% FCS, 2 mM glutamine (Bioconcept), 100 μg/mL penicillin-streptomycin (Bioconcept), 5 μg/mL human insulin, and 50 μM hydrocortisone hemisuccinate were added. In all experiments, the HepaRG cells were nondifferentiated: treatment of them was always started 4 h after seeding, as recommended by the supplier Thermo Fisher Scientific (Reinach, Switzerland). All cells were cultivated in a humidified atmosphere at 37°C and 5% CO_2. Before experimentation, all cell lines were tested for contamination with mycoplasma using the PCR Mycoplasma Test Kit I/C (Promokine, Heidelberg, Germany).

Quantification of mRNA expression by real-time PCR. To analyze endogenous expression, Huh-7, HepG2, and HeLa cells were seeded at a density of 2.6×10^4 cells/cm^2 and HepaRG cells at a density of 1.8×10^6cells/cm^2. For characterization of endogenous OATP1B3–1B7 expression in human liver, we used RNA isolated from three individuals (BioChain, Newark, CA). Cells were treated with 100 μM CDCA, 10 μM GW4064 (32), 1 μM DY268 (Tocris, Bristol, UK) (31), or DMSO 24 h (Huh-7) or 4 h (HepaRG) after seeding. RNA was isolated after 24 h (Huh-7) or 18 h (HepaRG) with peqGOLD (VWR, Dietikon, Switzerland) following the manufacturer's instructions. A volume corresponding to 1 μg RNA was treated with the DNase I kit from Thermo Fisher Scientific to avoid genomic DNA contamination. For reverse transcription, the High-Capacity cDNA Reverse Transcription Kit was applied. Quantitative real-time PCR was performed with an RNA-equivalent of 20 ng, the Viia 7 (Thermo Fisher Scientific), TaqMan Gene Expression Master Mix, and TaqMan gene expression assays for *SLCO1B7* (Hs00991170_m1), *SLCO1B3* (Hs00251986_m1), *SLCO1B1* (Hs00251986_m1), *NR0B2* (Hs0022267_m1), *ABCB11* (Hs00994811), OATP1B3–1B7-pre-mRNA (Hs03825569_s1) and eukaryotic 18s rRNA (Hs99999901_s1) from Thermo Fisher Scientific. To quantify the amount of the 5′UTR of *SLCO1B3*, the SYBR green Master Mix (Thermo Fisher Scientific) and the primers 5′UTR-forward (5′GAAGAGGTACATATGC-

AJP-Gastrointest Liver Physiol • doi:10.1152/ajpgi.00330.2018 • www.ajpgi.org

TATGTGATCATTTCAAACC′3) and 5′UTR-reverse (5′ATGTTG-GTCCATTATTAAACTACAGATACCAAGTG′3), both from Microsynth, were used. Expression of the target genes was calculated applying the $2^{-\Delta\Delta Ct}$ method in which the C_t value was normalized to 18s rRNA (ΔC_t) and then to the indicated control ($\Delta\Delta C_t$).

siRNA transfection. Knockdown of *SLCO1B3* with Silencer siRNA (ID 27960, Ambion, Thermo Fisher Scientific) targeting exon 4 was performed by reverse transfection using Lipofectamine RNAiMAX transfection reagent (Thermo Fisher Scientific). In brief, 10 pmol of each siRNA was mixed with 3 μL of Lipofectamine RNAiMAX both diluted in Opti-Mem I Reduced Serum Medium (Gibco, Thermo Fisher Scientific). After incubation for 5 min at room temperature (RT), the mixture was added to each well of a 12-well plate and incubated for a further 30 min at RT before seeding of Huh-7 cells on top at a density of 4.5×10^5 cells/cm^2. The medium was changed 24 h after transfection. For positive or negative control, cells were transfected with Silencer Select GAPDH siRNA (AM4605) or Silencer Negative Control No. 1 siRNA (4611G), respectively. After 48 h, total RNA was extracted. Then, the RNA was reversely transcribed and cDNA was applied to quantitative real-time PCR.

Transport assays with Huh-7 and HepaRG cells. One day or 4 h after seeding of Huh-7 (2.6×10^4 cells/cm^2) or HepaRG (1.8×10^6 cells/cm^2), respectively, cells were treated with CDCA (100 μM) or GW4064 (1 μM) for 24 h or 18 h for the Huh-7 cells or HepaRG cells, respectively. After treatment, cells were washed and incubated with nonradiolabeled 0.1 nM E_2G or 0.1 nM DHEAS diluted in Hanks' balanced salt solution (HBSS, Sigma-Aldrich) supplemented with the respective tritiated tracer (100,000 disintegrations/min/well; [^{3}H]E_2G: specific activity 52.9 Ci/mmol, ART 1320, Hartmann Analytic, Braunschweig, Germany; [^{3}H]DHEAS: specific activity 81.3 Ci/mmol, NET860250UC, PerkinElmer, Schwerzenbach, Switzerland). After incubation for 10 min at 37°C, cells were washed twice with ice-cold phosphate-buffered saline solution (PBS) and lysed in 0.2% SDS-5 mM EDTA. Five volume percent of each sample were used for protein determination by bicinchoninic acid assay (Pierce BCA Protein Assay Kit, Thermo Scientific). The remaining lysate was dissolved in Rotiszint eco plus (Carl Roth, Arlesheim, Switzerland), and accumulation of each compound was measured with the liquid scintillation counter Tri-Carb 2900TR (TopLab, Rickenbach, Switzerland).

Estimation of the inhibitory potency of bile acids. HeLa cells were seeded at a density of 1.2×10^5 cells/cm^2. One day after seeding, cells were transfected with 400 ng/well of OATP1B3–1B7-pEF6 or pEF6-control, as described elsewhere (16). After 16 h in culture, cells were exposed to 0.1 nM of nonradiolabeled DHEAS diluted in HBSS supplemented with the tritiated compound ([^{3}H]DHEAS, 100,000 disintegrations·min^{-1}·well^{-1}) in the presence of each bile acid [100 μM; lithocholic acid (LCA); CDCA; ursodeoxycholic acid (UDCA); and taurocholic acid (TCA)]. For determination of the half-maximal inhibitory concentrations (IC_{50}s) values, cells were incubated with nonradiolabeled 0.1 nM DHEAS diluted in HBSS supplemented with [^{3}H]DHEAS (100,000 disintegrations·min^{-1}·well^{-1}) in the presence of an ascending concentration series of each bile acid. Here, it is important to mention that transiently transfected HeLa cells partially sort OATP1B3–1B7 to the cytoplasm membrane (15). Subsequently, the amount of DHEAS was quantified processing the cells as described above.

Estimation of transport kinetics. For determination of TCA transport kinetics by OATP1B3–1B7, HeLa cells were seeded and transfected as described elsewhere (16). Before incubation with TCA, the transfected cells were incubated with 1 μM albumin fraction V (Carl Roth) diluted in HBSS for 10 min. Cells were then exposed to nonradiolabeled TCA supplemented with 100,000 disintegrations·min^{-1}·well^{-1} of the tritiated tracer ([^{3}H]TCA, specific activity 8 ci/mmol, ART 1368, Hartmann Analytic) diluted in 1 μM albumin fraction V-HBSS. Transport kinetics were determined by the use of ascending concentrations of TCA. Accumulation of TCA was measured by liquid scintillation counting. For analysis, the amount of TCA detected in control cells was subtracted from that obtained in OATP1B3–1B7 uptake. Net uptake of accumulated radiolabeled TCA was related to the protein content of each sample (calculated as pmol·mg^{-1}·min^{-1}).

Uptake of LCA. Transport of LCA was determined in suspended transfected HeLa cells to reduce unspecific binding of LCA. For this, 8×10^5 cells were seeded in 6-cm dishes and transfected as described above using 3.6 μg/dish of each plasmid and 21.2 μL/dish of Lipofectin. Sixteen hours after transfection, cells were detached using trypsin-EDTA solution, and then trypsin was quenched with culture medium. For each measurement, 1×10^5 cells suspended in 80 μL culture medium were transferred into 1.5 mL Eppendorf tubes (Eppendorf, Schönenbuch, Switzerland). Transport reaction was started by adding 1 nM of LCA diluted in Tris-sucrose buffer (Tris 50 mM, 0.25 M sucrose, pH 7.5) supplemented with [^{3}H]LCA (100,000 disintegrations·min^{-1}·well^{-1}, specific activity 30–60 Ci/mmol, ART 1263, Hartmann Analytic) to the cells. The mixture was incubated for 10 min at 37°C and 620 revolutions/min using an MS-100 Thermo-Shaker (Labgene Scientific SA, Châtel-Saint-Denis, Switzerland). The mixture was then filtered through Millipore Durapore filters (pore size of 0.22 μm; Millipore, Zug, Switzerland), and collected cells were washed with 3 mL ice-cold PBS. The filters were transferred into scintillation fluid, and accumulated radioactivity was measured by liquid scintillation counting with the Tri-Carb 2900TR.

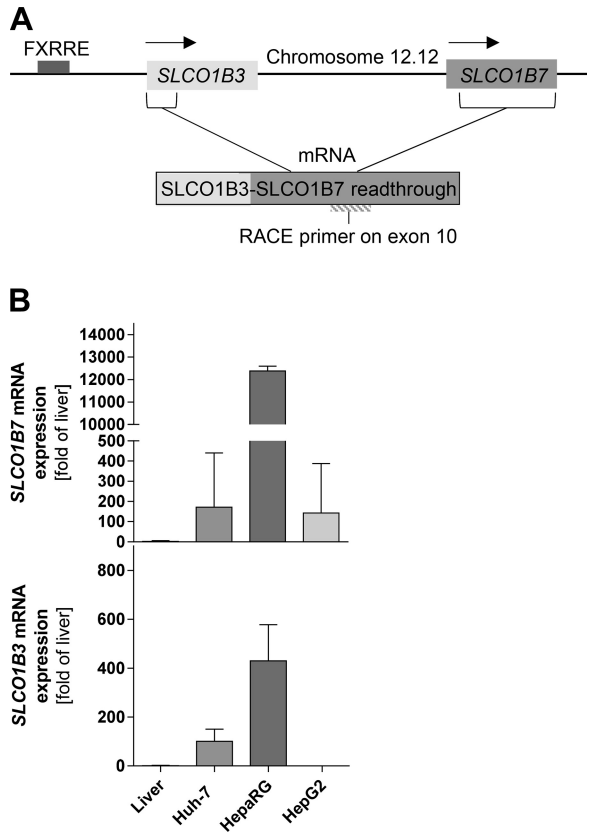

Fig. 1. Principle of rapid amplification of cDNA ends (RACE) and selection of a suitable cell model. *A*: scheme of 5′RACE of SLCO1B3-SLCO1B7 readthrough showing the binding site of the reverse primer in exon 10 of the gene *SLCO1B7*. *B*: expression of *SLCO1B3* and *SLCO1B7* mRNA was determined by quantitative real-time PCR in human liver and the human hepatoma-derived cell lines Huh-7, HepaRG, and HepG2. Relative expression was quantified using the $2^{-\Delta\Delta Ct}$ method, in which the expression was normalized to liver. Data are shown as means ± SD (n = 3). FXRRE, farnesoid X receptor response element.

AJP-Gastrointest Liver Physiol • doi:10.1152/ajpgi.00330.2018 • www.ajpgi.org

Microsome transport. Corning UltraPool (Thermo Scientific) microsomes (enriched SER of liver tissue) were used for microsomal uptake assays. For each experiment, 40 μg of microsomes were diluted in ice-cold Tris-sucrose buffer (Tris 50 mM, 0.25 M sucrose, pH 7.5) to a final volume of 30 μL. Precisely, before incubation with 0.1 nM TCA or 0.1 nM LCA supplemented with the respective radiolabeled tracer ([^{3}H]TCA or [^{3}H]LCA, 100,000 disintegrations·min^{-1}·well^{-1}), the samples were prewarmed in a thermomixer (Labgene, 620 revolutions/min, 37°C) and the TCA- or LCA-Tris-sucrose solution was added to the samples. After 10 min of incubation, the reaction mix was applied onto a Millipore Durapore filter (Millipore, Merck, Darmstadt, Germany) and then washed once with 3 mL of ice-cold PBS. Dynamic light scattering (Zetasizer Nano ZS, Malvern Instruments, Malvern, UK) quantified a diameter of 0.28 μm for the microsomes, suggesting that the majority of the microsomes would be retained by the filter. After filtration, the membranes were recovered and placed into scintillation vials filled with 3 mL Rotiszint eco plus (Carl Roth). The samples were shaken for 30 min at RT and then measured using the Tri-Carb 2900TR. Bromsulphthalein (BSP; 100 μM) was used as an OATP1B3–1B7 inhibitor.

Statistical analysis. Results were considered to be statistically significant with a P value below 0.05. All statistical analyses were performed with Prism 6 (GraphPad, La Jolla, CA).

RESULTS

Analysis of 5′RACE products. At first, we evaluated the 5′UTR of SLCO1B3-SLCO1B7 readthrough by performing a 5′RACE. The fragments were amplified from human liver cDNA using a primer binding to a sequence in OATP1B3–1B7 that originates from *SLCO1B7* (see Fig. 1*A*). The obtained PCR amplicons were subcloned into pDrive and sequenced. Analysis of the sequences of 7 clones containing a fragment of expected size showed not only the presence of the first exons of *SLCO1B3* but also parts of the 5′UTR of *SLCO1B3*, thereby suggesting that formation of the readthrough transcript may indeed be controlled by the promoter of *SLCO1B3*.

Selection of an appropriate cell model to determine transcriptional regulation of OATP1B3–1B7. To investigate the transcriptional regulation of *OATP1B3–1B7*, a cell system expressing OATP1B3 and OATP1B3–1B7 was needed. Three commonly used human hepatoma-derived cell lines, Huh-7, HepG2, and HepaRG, were assessed for presence of *SLCO1B3* and *SLCO1B7*-derived transcripts by real-time PCR. As depicted in Fig. 1*B*, the highest expression of *SLCO1B7* was detected in HepaRG when compared with human total liver (mean transcription normalized to liver ± SD; 12,384.0 ± 211.6), followed by a strong expression in Huh-7 (171.9 ± 268.3), whereas HepG2 cells exhibited the lowest amount of *SLCO1B7* (142.7 ± 245.5). Similar findings were obtained for *SLCO1B3* in the analysis (Fig. 1*B*; mean *SLCO1B3* transcription normalized to liver ± SD, HepaRG: 429.9 ± 148.0; Huh-7: 100.8 ± 49.7; HepG2: 0.05 ± 0.10). Accordingly, we chose Huh-7 and HepaRG cells for our further studies.

Silencing of SLCO1B3 transcription influences amount of SLCO1B7 expression. As we assumed that the transcription of OATP1B3–1B7 is linked to the *SLCO1B3* promoter, we expected that silencing of exon 4 of *SLCO1B3*, which is part of both transcripts SLCO1B3-SLCO1B7 readthrough and of *SLCO1B3*, would lead to the diminished transcription of both. Accordingly, we silenced exon 4 of *SLCO1B3* in Huh-7 cells and assessed the effect on the transcription using an *SLCO1B7* probe that recognizes the transcript encoding for OATP1B3–1B7 but also other *SLCO1B7* transcripts. The localization of

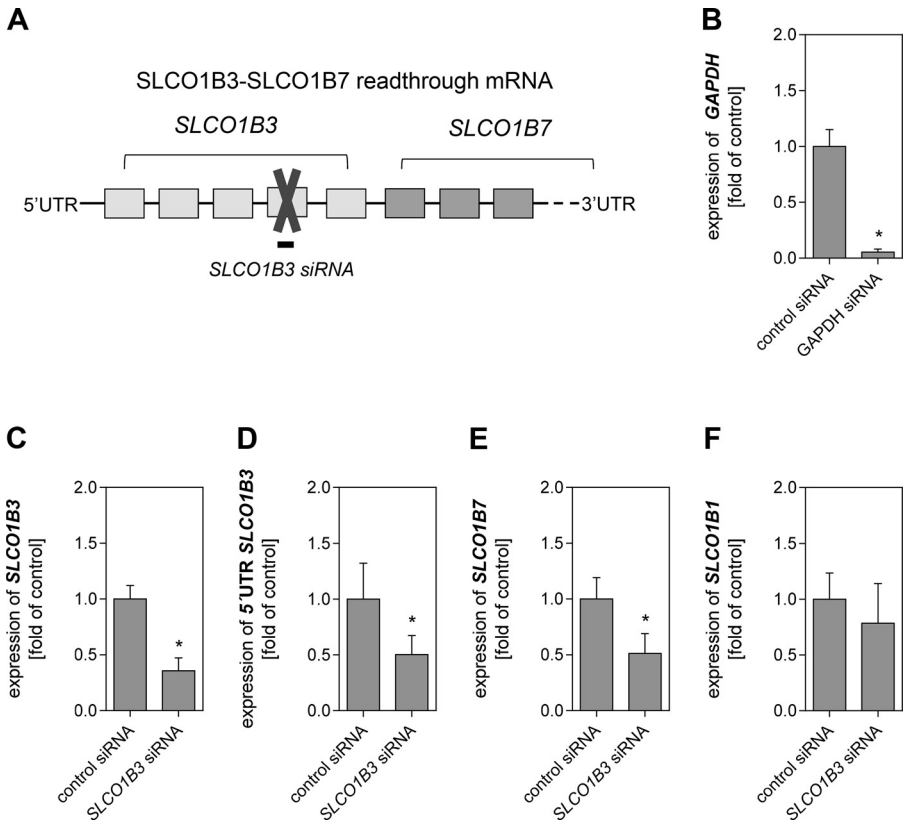

Fig. 2. Effects of silencing exon 4 of *SLCO1B3*. *A*: scheme showing the binding site (X) of the siRNA (48 h) used for silencing. *C–F*: influence of siRNA on endogenous mRNA expression was analyzed by quantitative real-time PCR. *F*: specificity of the siRNA was validated by quantification of *SLCO1B1* mRNA. *B*: siRNA directed against GAPDH served as experimental control. Relative expression was quantified using the $2^{-\Delta\Delta Ct}$ method, in which the expression was normalized to control siRNA. Data are shown as means ± SD (n = 4, Kruskal-Wallis with Dunn's multiple comparison test, $^*P < 0.05$). SLCO, solute carrier organic anion transporter; UTR, untranslated region.

AJP-Gastrointest Liver Physiol • doi:10.1152/ajpgi.00330.2018 • www.ajpgi.org

the siRNA binding site is schematically depicted in Fig. 2*A*. The *SLCO1B3* siRNA reduced the amount of *SLCO1B3* and 5′UTR *SLCO1B3* mRNA significantly (Fig. 2, *C* and *D*). Importantly, the same siRNA significantly reduced transcription of *SLCO1B7* (Fig. 2*E*; means ± SD, silencer negative control 1.00 ± 1.80 vs. *SLCO1B3* siRNA 0.50 ± 0.18). No such reduction was observed when we quantified the expression of *SLCO1B1* (Fig. 2*F*). A siRNA silencing GAPDH was used as quality control for the reverse transfection protocol (Fig. 2*B*).

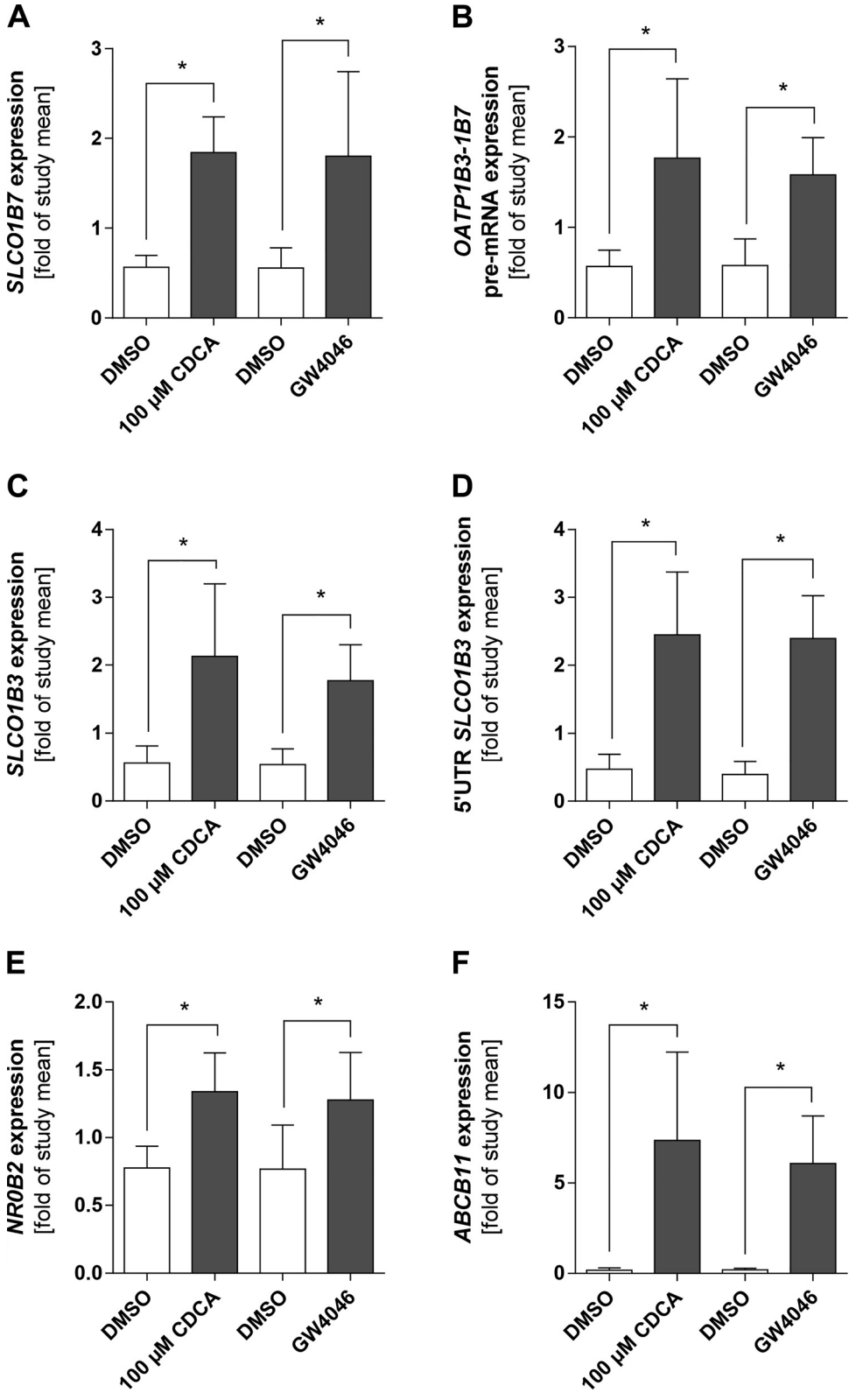

Fig. 3. Expression change in Huh-7 cells when treated with farnesoid X receptor (FXR) agonists [chenodeoxycholic acid (CDCA) 100 μM and GW4064 10 μM] or antagonist (DY268 1 μM). Relative expression of target transcripts was normalized to the study mean (average of Δct-DMSO and Δct-treatment). Significant induction was determined with the Mann-Whitney nonparametric test ($n \leq 4$, $^*P < 0.05$). Data are presented as means ± SD. ABCB11, ATP-binding cassette subfamily B member 11. NR0B2, nuclear receptor subfamily 0 group B member 2. SLCO, solute carrier organic anion transporter; UTR, untranslated region.

AJP-Gastrointest Liver Physiol • doi:10.1152/ajpgi.00330.2018 • www.ajpgi.org

Influence of known FXR agonists/antagonists on the expression of SLCO1B3-SLCO1B7 readthrough. OATP1B3 is transcriptionally regulated by FXR (11). To provide evidence for the assumption that transcription of SLCO1B3-SLCO1B7 readthrough is also controlled by the promoter of *SLCO1B3*, we assessed the impact of the known FXR activators CDCA (14), and GW4064 (32) or the FXR inhibitor DY268 (31) on the transcription of *SLCO1B3* and SLCO1B3-SLCO1B7 readthrough in Huh-7 cells. As OATP1B3 and SLCO1B3-SLCO1B7 readthrough have a high similarity, we measured SLCO1B3-SLCO1B7 readthrough expression with the exonic *SLCO1B7* assay, which could potentially also detect other *SLCO1B7* transcripts, and the intronic *OATP1B3–1B7*-pre-mRNA that is specific for SLCO1B3-SLCO1B7 readthrough, even if it is not as stable as mRNA (22).

As shown in Fig. 3, the transcription of *SLCO1B7*, *OATP1B3–1B7*-pre-mRNA, *SLCO1B3*, and 5′UTR *SLCO1B3* increased significantly after treatment with 100 μM CDCA and 10 μM GW4064. Significant induction of transcription was determined using the nonparametric Mann-Whitney test, in which the expression of the target gene was normalized to the study mean ($n \leq 5$). Importantly, the treatment with the FXR

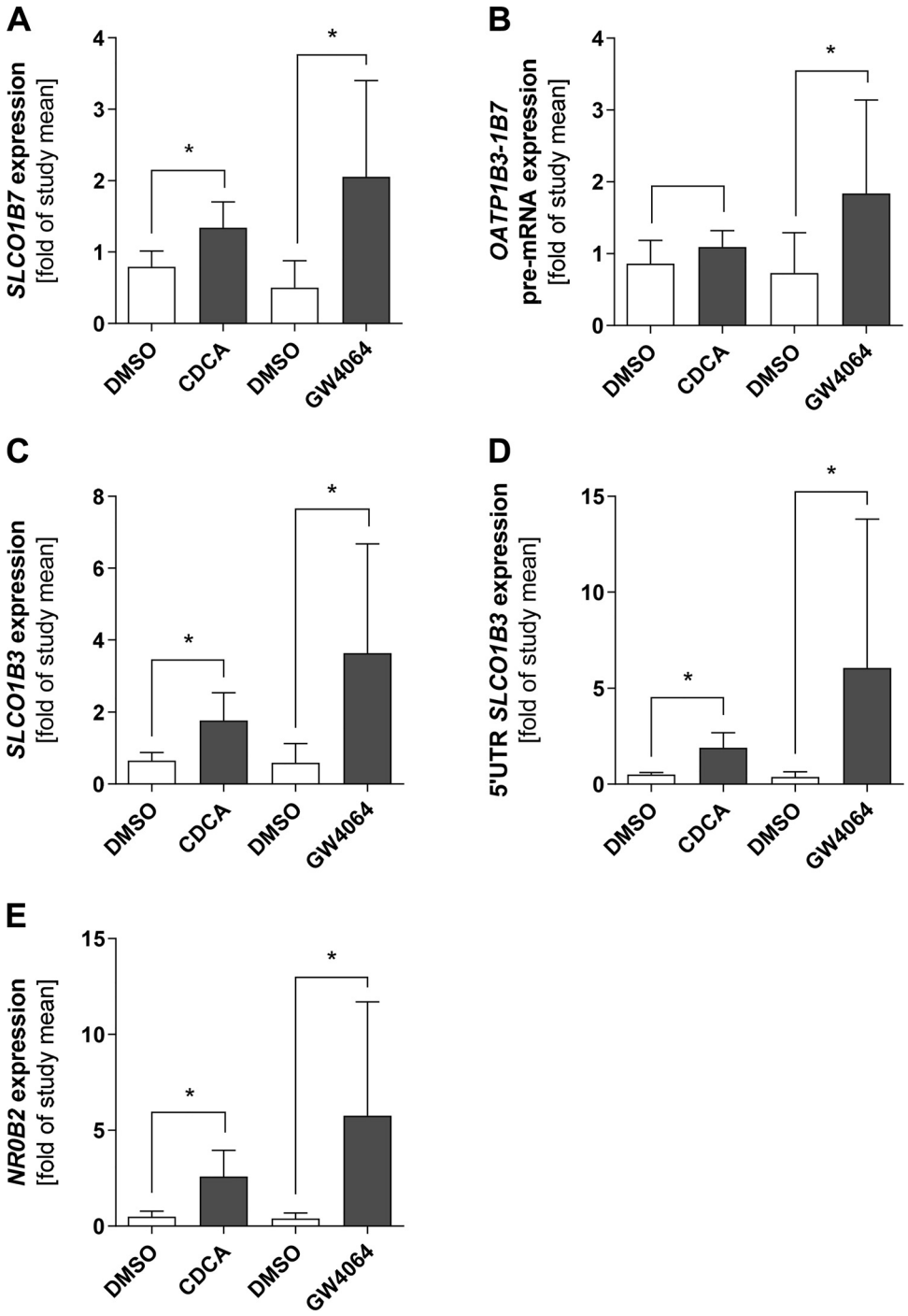

Fig. 4. Expression change in HepaRG cells when treated with farnesoid X receptor (FXR) agonists [chenodeoxycholic acid (CDCA) 100 μM and GW4064 10 μM]. Relative expression of target transcripts was normalized to the study mean (average of Δct-DMSO and Δct-treatment). Significant induction was determined with the Mann-Whitney nonparametric test ($n \leq 4$; $^*P < 0.05$). Data are presented as means ± SD. NR0B2, nuclear receptor subfamily 0 group B member 2; OATP, organic anion transporting polypeptide; SLCO, solute carrier organic anion transporter; UTR, untranslated region.

AJP-Gastrointest Liver Physiol • doi:10.1152/ajpgi.00330.2018 • www.ajpgi.org

agonists resulted in a statistically significant induction of the known FXR target genes *NR0B2* and *ABCB11*.

After treatment with 1 μM of the FXR inhibitor DY268, the expression of the target genes decreased significantly for *SLCO1B7* (control ± SD vs. DY268 ± SD; 1.57 ± 0.28 vs. 0.60 ± 0.17, $n = 7$, Mann-Whitney test, $P < 0.05$), *SLCO1B3* (control ± SD vs. DY268 ± SD; 1.36 ± 0.50 vs. 0.73 ± 0.34, $n = 7$, Mann-Whitney test, $P < 0.05$), 5′UTR *SLCO1B3* (control ± SD vs. DY268 ± SD; 1.23 ± 0.35 vs. 0.76 ± 0.28, $n = 7$, Mann-Whitney test, $P < 0.05$), *ABCB11* (control ± SD vs. DY268 ± SD; 1.73 ± 0.45 vs. 0.56 ± 0.22, $n = 7$, Mann-Whitney test, $P < 0.05$), and *NR0B2* (control ± SD vs. DY268 ± SD; 1.30 ± 0.20 vs. 0.70 ± 0.19, $n = 8$, Mann-Whitney test, $P < 0.05$) when compared with the study mean control. However, for *OATP1B3–1B7* pre-mRNA, the inhibition was not statistically significant (control ± SD vs. DY268 ± SD; 1.01 ± 0.56 vs. 1.47 ± 1.14, $n = 7$, Mann-Whitney test, $P = 0.70$).

Additionally, we tested the impact of CDCA (100 μM) and GW4064 (10 μM) on the expression of the same transcripts in the HepaRG cell line (Fig. 4). Also, in HepaRG cells, we observed the increase in transcription of *SLCO1B7*, *OATP1B3–1B7* pre-mRNA, *SLCO1B3*, 5′UTR *SLCO1B3*, and *NR0B2*. Interestingly, the effect was more pronounced in GW4064 than in CDCA-treated cells. CDCA and GW4064 had a positive effect on *SLCO1B3*, *SLCO1B7*, 5′UTR *SLCO1B3* and *NR0B2* transcription. For the *OATP1B3–1B7* pre-mRNA (Fig. 4*B*), we observed a trend for induction when treated with CDCA ($P = 0.22$), and a statistically significant increase in expression after treatment with GW4064. Statistically significant induction was confirmed using a nonparametric Mann-Whitney test ($n \leq 4$). We did not assess *ABCB11* expression in HepaRG cells, as its mRNA was not validly detectable.

Influence of FXR activators on cellular accumulation of DHEAS and E_2G in hepatoma cells. We tested whether FXR activators influence the cellular accumulation capacities of DHEAS and E_2G in Huh-7 and HepaRG cells (Fig. 5). Notably, DHEAS and E_2G are both substrates of OATP1B3–1B7 and other transporters. In Huh-7 cells (Fig. 5*A*), we observed a trend toward enhanced accumulation of DHEAS in cells treated with CDCA in comparison with control cells treated with DMSO (control vs. CDCA; 0.0208 pmol·mg^{-1}·min^{-1} vs. 0.0256 pmol·mg^{-1}·min^{-1}, $n = 5$, paired Student's t test, $P = 0.32$). However, in cells treated with GW4064, the uptake of DHEAS was significantly augmented (0.0275 pmol·mg^{-1}·min^{-1} vs. 0.0335 pmol·mg^{-1}·min^{-1}, $n = 6$, paired Student's t test, $P < 0.05$). Assessing the uptake of E_2G in Huh-7 cells (Fig. 5*C*), we observed significantly increased accumulation upon treatment with either CDCA (control vs. CDCA; 0.0138 pmol·mg^{-1}·min^{-1} vs. 0.0284 pmol·mg^{-1}·min^{-1}, $n = 5$, paired Student's t test, $P < 0.05$) or GW4064 (control vs. GW4064; 0.0131 pmol·mg^{-1}·min^{-1} vs. 0.0151 pmol·mg^{-1}·min^{-1}, $n = 6$, paired Student's t test, $P < 0.05$).

Similar results were obtained in HepaRG cells (Fig. 5*B*). Uptake of DHEAS was significantly increased in CDCA-treated cells (control vs. CDCA; 0.0107 pmol·mg^{-1}·min^{-1} vs. 0.0125 pmol·mg^{-1} min^{-1}, $n = 6$, paired Student's t test, $P < 0.05$), whereas there was a trend for increased uptake upon treatment with GW4064 (control vs. GW4064; 0.0107 pmol·mg^{-1}·min^{-1} vs. 0.0148 pmol·mg^{-1}·min^{-1}, $n = 6$, paired

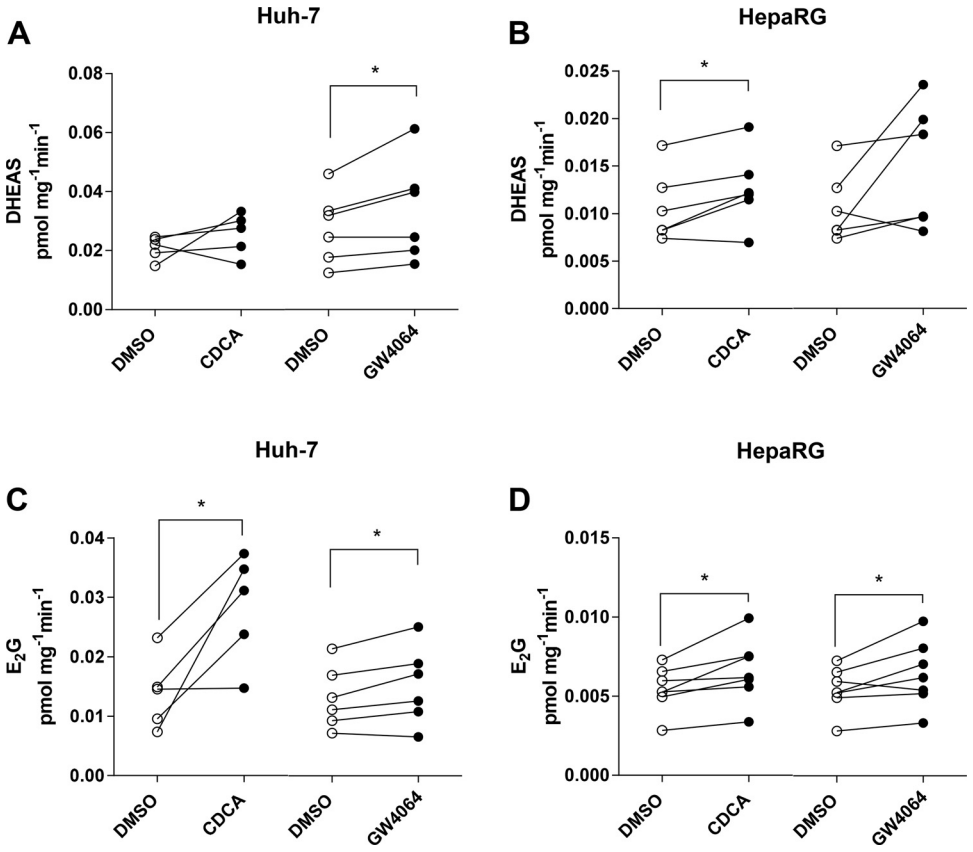

Fig. 5. Influence of chenodeoxycholic acid activation on cellular dehydroepiandrosterone sulfate (DHEAS) and estradiol 17 β-D-glucuronide uptake. Uptake of 0.1 nM DHEAS ([^{3}H]DHEAS, 100,000 disintegrations/min) (*A* and *B*) and 0.1 nM estradiol 17 β-D-glucuronide ([^{3}H]E_2G, 100,000 disintegrations/min) was assessed in Huh-7 or HepaRG cells treated with chenodeoxycholic acid (CDCA) 100 μM or GW4064 10 μM (*C* and *D*). Treatment time was 24 or 18 h for Huh-7 or HepaRG cells, respectively. Data are shown as means ± SD ($n = 5$, paired Student's t test, *$P < 0.05$).

AJP-Gastrointest Liver Physiol • doi:10.1152/ajpgi.00330.2018 • www.ajpgi.org

Student's t test, $P = 0.13$). Uptake of E_2G (Fig. 5*D*) was significant in both CDCA (control vs. CDCA; 0.0055 pmol·mg^{-1}·min^{-1} vs. 0.0066 pmol·mg^{-1}·min^{-1}, $n = 6$, paired Student's t test, $P < 0.05$) and GW4064 (control vs. GW4064; 0.0055 pmol·mg^{-1}·min^{-1} vs. 0.0065 pmol·mg^{-1}·min^{-1}, $n = 6$, paired Student's t test, $P < 0.05$) treated cells.

Bile acid interaction with OATP1B3–1B7. As mentioned before, FXR is a major regulator of bile acid homeostasis. Considering that OATP1B3–1B7 could be possibly regulated by FXR, we hypothesized that this transporter might be involved in bile acid homeostasis. Accordingly, we assayed whether bile acids interact with OATP1B3–1B7 by screening primary and secondary bile acids for their impact on OATP1B3–1B7-mediated uptake of DHEAS in transiently transfected HeLa cells. As in this assay the uptake of the tritiated DHEAS is measured, the concomitant addition of an inhibitor or substrate of OATP1B3–1B7 would result in a lowered DHEAS accumulation (see Fig. 6*A*). In the screening, all selected bile acids significantly inhibited DHEAS accumulation, as calculated by a one-sample t test in three independent experiments, each performed in triplicates (Fig. 6*A*). Subsequently, we determined the inhibitory potency assessing the IC_{50} values of these four bile acids by a log (inhibitor) versus normalized response fit with a fixed slope of -1. LCA was identified as the most potent inhibitor (IC_{50} 1.0 μM), followed by CDCA (9.0 μM) and UDCA (77.6 μM; see Fig. 6, *C–F*). However, even if 100 μM TCA significantly inhibited DHEAS accumulation, testing a concentration series of TCA did not yield a sigmoidal inhibition curve. Thus, we did not conduct an estimation of the IC_{50} value based on our data (Fig. 6*F*). Although we did not estimate the inhibitory potency, we tested whether OATP1B3–1B7 recognizes the primary bile acid TCA as a substrate. As we were able to show significantly increased accumulation in preliminary experiments (Fig. 7*A*), we determined the OATP1B3–1B7 transport kinetics for TCA. Using a concentration series of TCA ranging from 1 to 50 μM and applying a Michaelis-Menten fit for the estimation, we observed a maximal transport rate of 17.38 ± 3.20 pmol·mg^{-1}·min^{-1} ($V_{max} \pm$ SD) and an affinity of 15.99 ± 7.44 μM ($K_m \pm$ SD) (Fig. 7*B*). Furthermore, we were able to show enhanced cellular

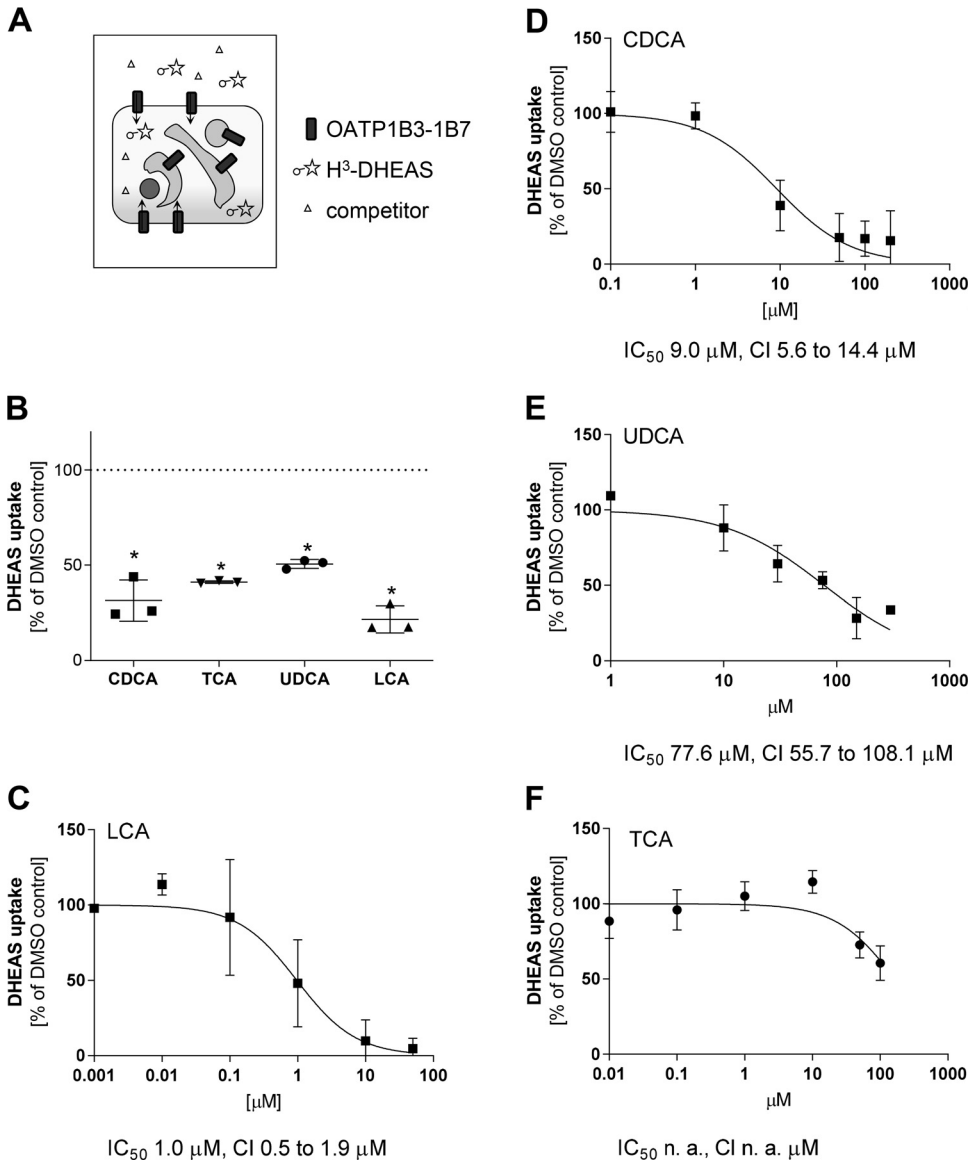

Fig. 6. Interaction of bile acids with OATP1B3–1B7 activity. *A*: substances that compete with dehydroepiandrosterone sulfate (DHEAS) uptake by OATP1B3–1B7 will lower the uptake of [^{3}H]DHEAS into the cell. *B*: impact of bile acids (100 μM) on uptake of 0.1 nM DHEAS ([^{3}H]DHEAS, 100,000 disintegrations/min) was quantified in HeLa cells heterologously expressing OATP1B3–1B7. Data are shown as means ± SD as percentage of DMSO control ($n = 3$, one-sample t test, $^*P < 0.05$). *B–D*: HeLa cells overexpressing OATP1B3–1B7 were incubated with a concentration series of each bile acid and uptake of DHEAS was quantified. IC_{50} values were estimated with a log (inhibitor) vs. normalized response fit with a fixed slope of -1 using Prism 6. Data are shown as means ± SD as percentage of DMSO control ($n \leq 3$). CDCA, chenodeoxycholic acid; CI, confidence interval; IC_{50}, half-maximal inhibitory concentration; LCA, lithocholic acid; TCA, taurocholic acid; UDCA, ursodeoxycholic acid.

AJP-Gastrointest Liver Physiol • doi:10.1152/ajpgi.00330.2018 • www.ajpgi.org

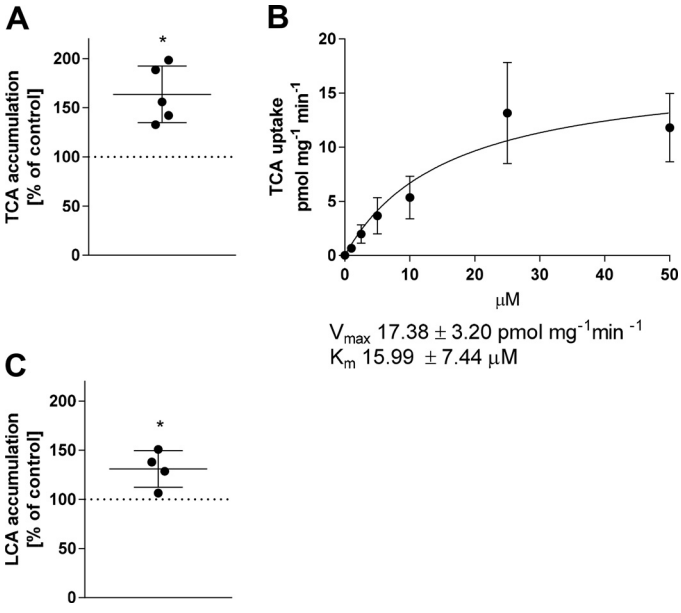

Fig. 7. Transport of taurocholic acid (TCA) and lithocholic acid (LCA). *A*: uptake of TCA (50 nM) was quantified in HeLa cells heterologously expressing OATP1B3–1B7. Data are shown as means ± SD as percentage of pEF6 control ($n = 5$, Student's t test, $^*P < 0.05$). *B*: applying the same cellular system, V_{max} and K_m of TCA transport were determined with a Michaelis-Menten fit using Prism 6. Data are shown as means ± SD ($n = 3$). *C*: intracellular accumulation of LCA (1 nM) was quantified in OATP1B3–1B7 expressing HeLa cells. Data are shown as means ± SD as percentage of pEF6 control ($n = 4$, Student's t test, $^*P < 0.05$).

accumulation of the secondary bile acid LCA (1 nM) in OATP1B3–1B7 overexpressing HeLa cells (Fig. 7*C*). Because of the extraordinarily high variability in experimental replicates, we did not perform studies on the concentration dependence to estimate parameters of the transport kinetics.

Uptake of bile acids into liver microsomes. We have previously shown that liver microsomes, which represent the enriched endoplasmic reticulum of liver tissue, express OATP1B3–1B7 (15). To test whether bile acid uptake into the SER may at least in part be attributable to OATP1B3–1B7, we investigated whether inhibition of OATP1B3–1B7 with the previously published OATP1B3–1B7 inhibitor BSP (15) would alter microsomal uptake of TCA and LCA. As shown in Fig. 8*A*, the uptake of TCA into liver microsomes was significantly reduced in the presence of BSP (uptake ± SD, 0.063 ± 0.021 pmol·mg^{-1}·min^{-1} vs. BSP treated 0.021 ± 0.005 pmol·mg^{-1}·min^{-1}, $n = 4$, Student's t test, $P < 0.05$). Similar results were obtained for LCA (Fig. 8*B*; uptake ± SD, 0.704 ± 0.377 pmol·mg^{-1}·min^{-1} vs. BSP treated 0.071 ± 0.046 pmol·mg^{-1}·min^{-1}, $n = 3$, Student's t test, $P < 0.05$).

DISCUSSION

Considering our finding that the SLCO1B3-SLCO1B7 readthrough is a splice variant of *SLCO1B3*, we hypothesized that the SLCO1B3-SLCO1B7 readthrough shares a promoter with *SLCO1B3*. This assumption is now supported by our results, showing that SLCO1B3-SLCO1B7 readthrough exhibits the same 5′UTR as *SLCO1B3*. Moreover, we demonstrated that silencing of exon 4 of *SLCO1B3* results in a decrease of *SLCO1B3*, 5′UTR *SLCO1B3*, and *SLCO1B7* transcripts. Although the decrease of 5′UTR *SLCO1B3* could also be due to increased breakdown of the *SLCO1B3* transcript, the decrease in *SLCO1B7* transcripts can only be explained by our assumption that *SLCO1B7* uses the OATP1B3 promoter for transcription. However, further experiments are necessary to ultimately prove this hypothesis.

Another way to further validate the hypothesis of SLCO1B3-SLCO1B7 readthrough being transcriptionally controlled by the *SLCO1B3* promoter is to test whether the ligand-activated nuclear receptor FXR, which has previously been shown to induce transcription of OATP1B3 in hepatocyte-like cells, also increases formation of the SLCO1B3-SLCO1B7 readthrough transcript (11). By replicating this experiment with the two FXR agonists CDCA and GW4064 in two different hepatoma-derived cell lines, we were able to confirm that treatment with FXR agonists induces *SLCO1B3* transcription and, more importantly, the transcription of SLCO1B3-SLCO1B7 readthrough mRNA (measured with the *SLCO1B7* or *OATP1B3–1B7* pre-mRNA assays). For the Huh-7 cells, we could show the statistically significant increase of *SLCO1B7* and *OATP1B3–1B7* pre-mRNA for both FXR agonists. For the HepaRG cells, we observed a statistically significant increase for *SLCO1B7* transcription when treated with both agonists. The increase in *OATP1B3–1B7* pre-mRNA transcription was, however, only statistically significant when treated with GW4064. It seems noteworthy that pre-mRNAs are not as stable as mRNAs, which increases variability (22) and might have affected our results. Given that FXR is to some extent perpetually activated by the FCS in the culturing media, we have also conducted inhibition studies with the FXR antagonist DY268 in Huh-7 cells. Importantly, we were able to report that inhibition of FXR by DY268 led to decreased transcription for all investigated targets, except for the *OATP1B3–1B7* pre-mRNA. In summary, our data support the hypothesis that OATP1B3–1B7 is regulated by FXR. However, further evidence is needed to corroborate this hypothesis.

To assess the effect of FXR stimulation on cellular function, we compared the handling of previously reported substrates of OATP1B3–1B7 after FXR activation. For this, we have subjected CDCA or GW4064-treated Huh-7 or HepaRG cells to the OATP1B substrates E_2G and DHEAS. For both cell types and both agonists, we observed significantly higher cellular accumulation of E_2G. However, when subjected to DHEAS, Huh-7 cells only demonstrated significant uptake when treated with GW4064. HepaRG cells only showed significant uptake of DHEAS when treated with CDCA.

Notably, E_2G is substrate of multiple transporters, including the uptake transporters OATP1B1 and OATP1B3 (25). However, DHEAS is preferentially transported by OATP1B1 (5). The limited effect of the FXR activation on DHEAS presumably finds its explanation in multiple factors, including the lack of affinity toward OATP1B3 and the interplay of multiple transporters (uptake and efflux) in cellular handling. Our findings show that FXR activation increased the entry or changed the cellular distribution of E_2G. As our previous findings in human liver showed that OATP1B3–1B7 was expressed in the SER (16), transport by OATP1B1 and OATP1B3 would be a prerequisite for the interaction with the intracellularly located OATP1B3–1B7. However, because of the herein described coordinated transcriptional regulation by a shared promoter, we assume that there is a functional interdependence between OATP1B3 and OATP1B3–1B7. This assumption is specula-

AJP-Gastrointest Liver Physiol • doi:10.1152/ajpgi.00330.2018 • www.ajpgi.org

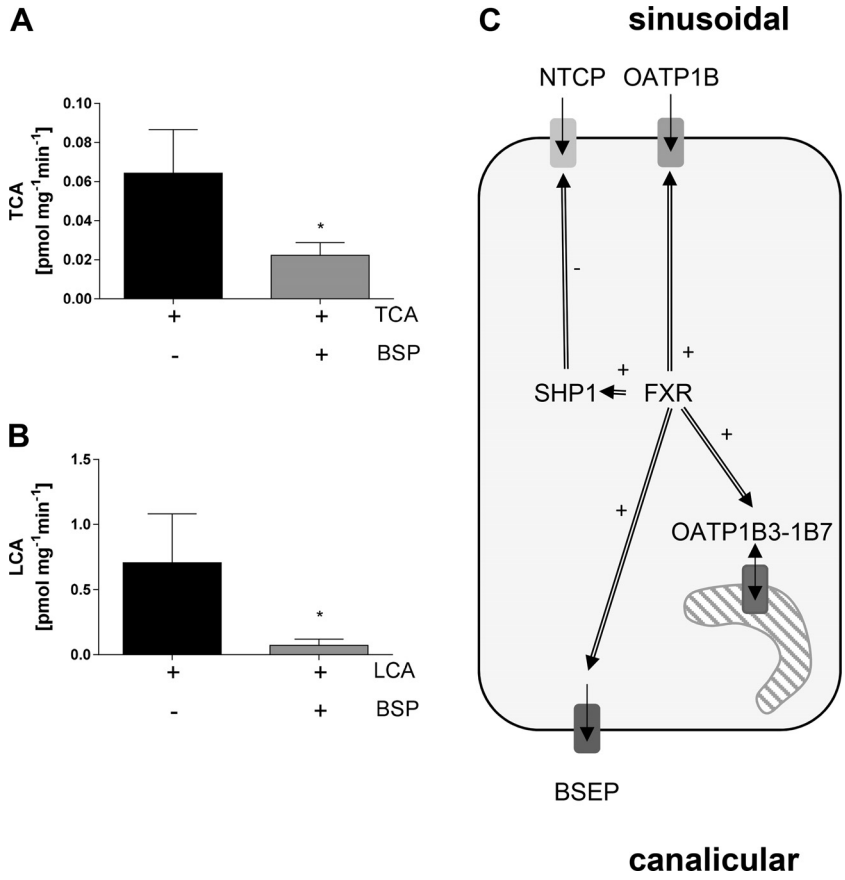

Fig. 8. Taurocholic acid (TCA) and lithocholic acid (LCA) uptake into liver microsomes. *A* and *B*: enriched liver microsomes were incubated either with TCA (0.1 nM, $n = 4$) or LCA (0.1 nM, $n = 3$) in presence or absence of bromsulphthalein (BSP; 100 μM). Data are shown as means ± SD (Student's *t* test, $*P < 0.05$). *C*: scheme of the putative function of OATP1B3–1B7 in a hepatocyte. Activated farnesoid X receptor (FXR) initiates transcription of *OATP1B3–1B7*. Increased abundance of OATP1B3–1B7 protein expression facilitates smooth endoplasmic reticulum access for bile acids that are glucuronidated by UDP-glucuronosyltransferases. Glucuronidation makes the bile acids more likely to be secreted into the bile by efflux transporters, such as bile salt export pump (BSEP). NTCP, Na^+-taurocholate cotransporting polypeptide. SHP, small heterodimer partner 1.

tive, as posttranslational modifications influence the functionality of the OATP1B transporters as well (1). However, the observed differential effect for E_2G and DHEAS supports our notion.

Bile acids exert a manifold of functions in the human organism, such as solubilizing lipids, cholesterol, and lipophilic vitamins in the small intestine. However, excessive levels of circulating bile acids are associated with toxicity because of their detergent properties (30). As mentioned before, the tuning of bile acid levels in the body is complex and involves various enzymes and transporters of whom the transcription is orchestrated by FXR (18). Accounting for the fact that FXR is a major regulator of bile acid homeostasis (18) and that our findings suggested enhanced transcription and function of OATP1B transporters upon treatment with CDCA, we tested the interaction of bile acids with OATP1B3–1B7. These experiments were performed with a heterologous expression system in which OATP1B3–1B7 is localized not only intracellularly but also at the plasma membrane (16). For our first screening, we selected two primary (CDCA and TCA) and two secondary bile acids (UDCA and LCA) and observed significant inhibition of OATP1B3–1B7-mediated DHEAS transport for all tested molecules. Evaluation of the inhibitory potency revealed LCA as the most potent modulator of DHEAS uptake, followed by CDCA, UDCA, and TCA. After having proven that bile acids do interact with OATP1B3–1B7 activity, TCA and LCA were identified to be substrates of OATP1B3–1B7. For the primary bile acid, TCA, we estimated a maximum transport rate (V_{max} ± SE) of 17.38 ± 3.28 pmol·mg^{-1}·min^{-1} and an affinity (K_m ± SE) of 15.99 ± 7.44 μM. Compared with other TCA transporters, such as NTCP (12), OST-α/OST-β (2), OATP1B1 (26), or OATP1B3 (26), OATP1B3–1B7 exhibits the lowest affinity but a very high capacity for TCA. However, even though we were able to show statistically significant uptake of LCA in OATP1B3–1B7-transfected HeLa cells, we refrained from estimating transport kinetics from the data obtained because of high experimental variability.

As OATP1B3–1B7 is mainly expressed in the SER, in which it may govern access to microsomal enzymes, we further investigated whether inhibition of OATP1B3–1B7 would have an effect on the microsomal uptake of TCA and LCA. Given that Matern et al. (17) demonstrated that bile acids are prone to glucuronidation catalyzed by UDP-glucuronosyltransferases that reside in the SER, the access of bile acids to the luminal site of the SER could be the rate-limiting step for their glucuronidation. Thus, we determined the influence of BSP, a potent inhibitor of OATP1B3–1B7, on the cellular accumulation of TCA and LCA. As the accumulation of TCA and LCA could be significantly inhibited by BSP, we hypothesize that OATP1B3–1B7 may contribute to bile acid metabolism functioning as a doorway between SER and cytosol, thereby fostering glucuronidation. In the context of glucuronidation, we recently reported that inhibition of OATP1B3–1B7 influences glucuronidation of ezetimibe, a drug substrate of OATP1B3–1B7 (15). Thus, it could be that the same mechanism plays a role in bile acid glucuronidation; however, this needs to be validated in further studies. As schematically depicted in Fig. 8*C*, we propose that OATP1B3–1B7 is a mechanism influenc-

AJP-Gastrointest Liver Physiol • doi:10.1152/ajpgi.00330.2018 • www.ajpgi.org

ing SER accumulation. Briefly, FXR activation not only leads to NTCP downregulation via SHP to protect the cells from toxic exposure but also increases expression of the uptake transporters OATP1B1 and OATP1B3 at the plasma membrane. Their increased expression ensures bile acid influx, thereby allowing continuous sensing of the levels by FXR (19). This allows contact to OATP1B3–1B7, which opens the possibility to expose bile acids to UDP-glucuronosyltransferases located in the metabolically active SER, thereby contributing to the reduction of bile acid levels and thereby the protection of the organism from their detergent properties.

ACKNOWLEDGMENTS

The herein summarized data are part of the master's thesis of A. Issa and A. Midzic and part of the PhD thesis of V. Malagnino.

GRANTS

The study was fully financed by funds of the Institute of Biopharmacy, which is mandated by the Department of Pharmaceutical Sciences of the University of Basel. This research did not receive any specific grant from funding agencies in the public, commercial, or not-for-profit sectors.

DISCLOSURES

No conflicts of interest, financial or otherwise, are declared by the authors.

AUTHOR CONTRIBUTIONS

V.M., J.H., and H.E.M.z.S. conceived and designed research; V.M., J.H., A.I., and A.M. performed experiments; V.M., J.H., and H.E.M.z.S. analyzed data; V.M., J.H., and H.E.M.z.S. interpreted results of experiments; V.M., J.H., and H.E.M.z.S. prepared figures; V.M., J.H., and H.E.M.z.S. drafted manuscript; V.M., J.H., A.I., and H.E.M.z.S. edited and revised manuscript; V.M., J.H., A.I., A.M., and H.E.M.z.S. approved final version of manuscript.

REFERENCES

1. **Alam K, Crowe A, Wang X, Zhang P, Ding K, Li L, Yue W.** Regulation of organic anion transporting polypeptides (OATP) 1B1- and OATP1B3-mediated transport: an updated review in the context of OATP-mediated drug-drug interactions. *Int J Mol Sci* 19: 855, 2018. doi:10.3390/ijms19030855.
2. **Ballatori N, Christian WV, Lee JY, Dawson PA, Soroka CJ, Boyer JL, Madejczyk MS, Li N.** OSTalpha-OSTbeta: a major basolateral bile acid and steroid transporter in human intestinal, renal, and biliary epithelia. *Hepatology* 42: 1270–1279, 2005. doi:10.1002/hep.20961.
3. **Ballatori N, Li N, Fang F, Boyer JL, Christian WV, Hammond CL.** OST alpha-OST beta: a key membrane transporter of bile acids and conjugated steroids. *Front Biosci* 14: 2829–2844, 2009. doi:10.2741/3416.
4. **Boyer JL, Trauner M, Mennone A, Soroka CJ, Cai SY, Moustafa T, Zollner G, Lee JY, Ballatori N.** Upregulation of a basolateral FXR-dependent bile acid efflux transporter OSTalpha-OSTbeta in cholestasis in humans and rodents. *Am J Physiol Gastrointest Liver Physiol* 290: G1124–G1130, 2006. doi:10.1152/ajpgi.00539.2005.
5. **Cui Y, König J, Leier I, Buchholz U, Keppler D.** Hepatic uptake of bilirubin and its conjugates by the human organic anion transporter SLC21A6. *J Biol Chem* 276: 9626–9630, 2001. doi:10.1074/jbc.M004968200.
6. **Darnell M, Ulvestad M, Ellis E, Weidolf L, Andersson TB.** In vitro evaluation of major in vivo drug metabolic pathways using primary human hepatocytes and HepaRG cells in suspension and a dynamic three-dimensional bioreactor system. *J Pharmacol Exp Ther* 343: 134–144, 2012. doi:10.1124/jpet.112.195834.
7. **Eloranta JJ, Jung D, Kullak-Ublick GA.** The human Na+-taurocholate cotransporting polypeptide gene is activated by glucocorticoid receptor and peroxisome proliferator-activated receptor-gamma coactivator-1alpha, and suppressed by bile acids via a small heterodimer partner-dependent mechanism. *Mol Endocrinol* 20: 65–79, 2006. doi:10.1210/me.2005-0159.
8. **Goodwin B, Jones SA, Price RR, Watson MA, McKee DD, Moore LB, Galardi C, Wilson JG, Lewis MC, Roth ME, Maloney PR, Willson TM, Kliewer SA.** A regulatory cascade of the nuclear receptors FXR, SHP-1, and LRH-1 represses bile acid biosynthesis. *Mol Cell* 6: 517–526, 2000. doi:10.1016/S1097-2765(00)00051-4.
9. **Hagenbuch B, Meier PJ.** Organic anion transporting polypeptides of the OATP/SLC21 family: phylogenetic classification as OATP/SLCO superfamily, new nomenclature and molecular/functional properties. *Pflugers Arch* 447: 653–665, 2004. doi:10.1007/s00424-003-1168-y.
10. **Halilbasic E, Claudel T, Trauner M.** Bile acid transporters and regulatory nuclear receptors in the liver and beyond. *J Hepatol* 58: 155–168, 2013. doi:10.1016/j.jhep.2012.08.002.
11. **Jung D, Podvinec M, Meyer UA, Mangelsdorf DJ, Fried M, Meier PJ, Kullak-Ublick GA.** Human organic anion transporting polypeptide 8 promoter is transactivated by the farnesoid X receptor/bile acid receptor. *Gastroenterology* 122: 1954–1966, 2002. doi:10.1053/gast.2002.33583.
12. **Kim RB, Leake B, Cvetkovic M, Roden MM, Nadeau J, Walubo A, Wilkinson GR.** Modulation by drugs of human hepatic sodium-dependent bile acid transporter (sodium taurocholate cotransporting polypeptide) activity. *J Pharmacol Exp Ther* 291: 1204–1209, 1999.
13. **Maeda K.** Organic anion transporting polypeptide (OATP)1B1 and OATP1B3 as important regulators of the pharmacokinetics of substrate drugs. *Biol Pharm Bull* 38: 155–168, 2015. doi:10.1248/bpb.b14-00767.
14. **Makishima M, Okamoto AY, Repa JJ, Tu H, Learned RM, Luk A, Hull MV, Lustig KD, Mangelsdorf DJ, Shan B.** Identification of a nuclear receptor for bile acids. *Science* 284: 1362–1365, 1999. doi:10.1126/science.284.5418.1362.
15. **Malagnino V, Duthaler U, Seibert I, Krähenbühl S, Meyer Zu Schwabedissen HE.** OATP1B3–1B7 (LST-3TM12) is a drug transporter that affects endoplasmic reticulum access and the metabolism of ezetimibe. *Mol Pharmacol* 96: 128–137, 2019. doi:10.1124/mol.118.114934.
16. **Malagnino V, Hussner J, Seibert I, Stolzenburg A, Sager CP, Meyer Zu Schwabedissen HE.** LST-3TM12 is a member of the OATP1B family and a functional transporter. *Biochem Pharmacol* 148: 75–87, 2018. doi:10.1016/j.bcp.2017.12.012.
17. **Matern S, Matern H, Farthmann EH, Gerok W.** Hepatic and extrahepatic glucuronidation of bile acids in man. Characterization of bile acid uridine 5′-diphosphate-glucuronosyltransferase in hepatic, renal, and intestinal microsomes. *J Clin Invest* 74: 402–410, 1984. doi:10.1172/JCI111435.
18. **Matsubara T, Li F, Gonzalez FJ.** FXR signaling in the enterohepatic system. *Mol Cell Endocrinol* 368: 17–29, 2013. doi:10.1016/j.mce.2012.05.004.
19. **Meyer zu Schwabedissen HE, Böttcher K, Chaudhry A, Kroemer HK, Schuetz EG, Kim RB.** Liver X receptor α and farnesoid X receptor are major transcriptional regulators of OATP1B1. *Hepatology* 52: 1797–1807, 2010. doi:10.1002/hep.23876.
20. **Nagai M, Furihata T, Matsumoto S, Ishii S, Motohashi S, Yoshino I, Ugajin M, Miyajima A, Matsumoto S, Chiba K.** Identification of a new organic anion transporting polypeptide 1B3 mRNA isoform primarily expressed in human cancerous tissues and cells. *Biochem Biophys Res Commun* 418: 818–823, 2012. doi:10.1016/j.bbrc.2012.01.115.
21. **Ohtsuka H, Abe T, Onogawa T, Kondo N, Sato T, Oshio H, Mizutamari H, Mikkaichi T, Oikawa M, Rikiyama T, Katayose Y, Unno M.** Farnesoid X receptor, hepatocyte nuclear factors 1alpha and 3beta are essential for transcriptional activation of the liver-specific organic anion transporter-2 gene. *J Gastroenterol* 41: 369–377, 2006. doi:10.1007/s00535-006-1784-3.
22. **Peccarelli M, Kebaara BW.** Measurement of mRNA decay rates in Saccharomyces cerevisiae using rpb1-1 strains. *J Vis Exp* 94: e52240, 2014. doi:10.3791/52240.
23. **Prestin K, Olbert M, Hussner J, Völzke H, Meyer Zu Schwabedissen HE.** Functional assessment of genetic variants located in the promoter of SHP1 (NR0B2). *Pharmacogenet Genomics* 27: 410–415, 2017. doi:10.1097/FPC.0000000000000310.
24. **Schwarz UI, Meyer zu Schwabedissen HE, Tirona RG, Suzuki A, Leake BF, Mokrab Y, Mizuguchi K, Ho RH, Kim RB.** Identification of novel functional organic anion-transporting polypeptide 1B3 polymorphisms and assessment of substrate specificity. *Pharmacogenet Genomics* 21: 103–114, 2011. doi:10.1097/FPC.0b013e328342f5b1.
25. **Stieger B, Hagenbuch B.** Organic anion-transporting polypeptides. *Curr Top Membr* 73: 205–232, 2014. doi:10.1016/B978-0-12-800223-0.00005-0.
26. **Suga T, Yamaguchi H, Sato T, Maekawa M, Goto J, Mano N.** Preference of conjugated bile acids over unconjugated bile acids as substrates for OATP1B1 and OATP1B3. *PLoS One* 12: e0169719, 2017. doi:10.1371/journal.pone.0169719.
27. **Thakkar N, Kim K, Jang ER, Han S, Kim K, Kim D, Merchant N, Lockhart AC, Lee W.** A cancer-specific variant of the SLCO1B3 gene encodes a novel human organic anion transporting polypeptide 1B3

(OATP1B3) localized mainly in the cytoplasm of colon and pancreatic cancer cells. *Mol Pharm* 10: 406–416, 2013. doi:10.1021/mp3005353.

28. **Thakkar N, Lockhart AC, Lee W.** Role of organic anion-transporting polypeptides (OATPs) in cancer therapy. *AAPS J* 17: 535–545, 2015. doi:10.1208/s12248-015-9740-x.
29. **van de Steeg E, Stránecký V, Hartmannová H, Nosková L, Hřebíček M, Wagenaar E, van Esch A, de Waart DR, Oude Elferink RP, Kenworthy KE, Sticová E, al-Edreesi M, Knisely AS, Kmoch S, Jirsa M, Schinkel AH.** Complete OATP1B1 and OATP1B3 deficiency causes human Rotor syndrome by interrupting conjugated bilirubin reuptake into the liver. *J Clin Invest* 122: 519–528, 2012. doi:10.1172/JCI59526.
30. **Wang YD, Chen WD, Moore DD, Huang W.** FXR: a metabolic regulator and cell protector. *Cell Res* 18: 1087–1095, 2008. doi:10.1038/cr.2008.289.
31. **Yu DD, Lin W, Forman BM, Chen T.** Identification of trisubstituted-pyrazol carboxamide analogs as novel and potent antagonists of farnesoid X receptor. *Bioorg Med Chem* 22: 2919–2938, 2014. doi:10.1016/j.bmc.2014.04.014.
32. **Zhang S, Pan X, Jeong H.** GW4064, an agonist of farnesoid X receptor, represses CYP3A4 expression in human hepatocytes by inducing small heterodimer partner expression. *Drug Metab Dispos* 43: 743–748, 2015. doi:10.1124/dmd.114.062836.

AJP-Gastrointest Liver Physiol • doi:10.1152/ajpgi.00330.2018 • www.ajpgi.org

3.4 Atorvastatin accumulation

Unless stated otherwise, all chemicals were purchased from Sigma Aldrich, Buchs, Switzerland.

Assessment of atorvastatin uptake was performed in heterologously transfected HeLa cells. To this end, 4 x 10^4 HeLa cells per well were seeded in 12-well plates. One day after seeding, cells were transfected with 400 ng/ well OATP1B3-1B7-pEF6 or pEF6-control using the Lipofectin® Transfection Reagent (0.5 µl/well, Thermo Fisher Scientific, Reinach, Switzerland). In this system, expression is driven by a T7 RNA-polymerase that is introduced into the cells by infection with the vTF7-3 virus (ATCC No. VR-2153) (Fuerst et al., 1986). After 16 h in culture, cells were exposed to 0.1 nM atorvastatin diluted in Hank's Balanced salt (Sigma Aldrich) supplemented with tritiated ^{3}[H]-atorvastatin (Hartmann Analytik, Braunscheig, Germany, ART 1376, specific activity 50 Ci/mmol,). Accumulation of atorvastatin after 5 min of incubation was measured with the Tri-Carb 2900TR (Toplab, Rickenbach, Switzerland). Uptake of accumulated radiolabeled atorvastatin was related to the protein content of each sample and normalized to the uptake of the control-transfected cells.

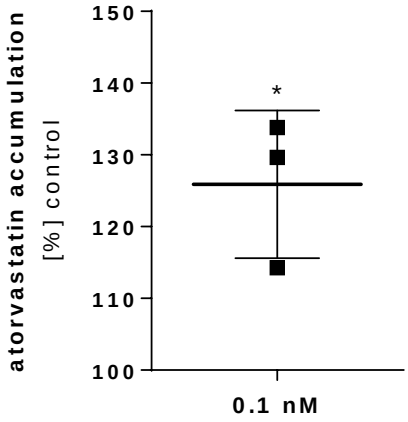

Figure 4. Cellular accumulation of atorvastatin. Atorvastatin accumaltion is significantly higher in OATP1B3-1B7 transfected cells compared to the control cells. Three independent experiments were performed in triplicate; data are presented as mean % of pEF6-control ± SD (one sample t-test,* p<0.05).

Atorvastatin is a substrate of OATP1B3-1B7. The mean accumulation ± SD of atorvastatin compared to the pEF-6 control is 125.9 ± 10.3% (see Figure 4). Three independent experiments

were performed in biological triplicates and statistically significant uptake was determined with the one sample t-test (*p<0.05).

4.0 Conclusion

The overall effectiveness of a drug is affected by its pharmacodynamic and pharmacokinetic properties (Wilson and Walker, 2010). The pharmacodynamic properties describe the drug-target relationship, whereas the pharmacokinetic properties summarize all the processes exerted on the drug during its journey through the organism until it is eventually eliminated (Herdegen et al., 2010). One mechanism that has an impact on the pharmacokinetic properties of a drug is its passage through cellular plasma membranes. This process is fueled by passive diffusion, facilitated diffusion, and active transport (Herdegen et al., 2010). The latter is executed by membrane spanning proteins, so called transporters. Of these, the families of the ABC transporters and the SLC transporters have a prominent impact on the pharmacokinetics of drugs (Liang et al., 2015).

One subfamily of the SLC transporters are OATP1B transporters, which are expressed in hepatocytes where they facilitate entry into the cytosol (Meyer zu Schwabedissen and Kim, 2009). Thereby they have an influence on the access of drugs to intracellular metabolizing enzymes, such as CYP P450s and UGTs, which are highly expressed inside hepatocytes (Drozdzik et al., 2018; Rouleau et al., 2016). Besides their impact on drug metabolism, OATP1Bs are also involved in the hepatocellular uptake of endogenous compounds such as bilirubin (Briz et al., 2003; Cui et al., 2001), coproporphyrins (Bednarczyk and Boiselle, 2016), and bile acids (Suga et al., 2017). The genes that encode OATP1B3 (*SLCO1B3*) and OATP1B1 (*SLCO1B1*) are located on chromosome 12p12 (Hagenbuch and Meier, 2003). Between these two genes lies another gene named *SLCO1B7,* which has been deemed to be a pseudogene as no function has been discovered for it (Stieger and Hagenbuch, 2014). However, two transcripts, LST-3TM12 (NCBI#, AY257470) and LST-3b (NCBI#, AY442325), that are highly similar to *SLCO1B7* were published by Mizutamari H. and Abe T. By aligning LST-3TM12 and LST-3b, it became apparent that LST-3TM12 and LST-3b have the same coding sequence. The difference between the two sequences is only that LST-3b also encompasses the

5’ and 3’ untranslated regions. Because of this, we have focused our further investigations on LST-3TM12. In a next step, we aligned the transcripts of LST-3TM12, SLCO1B3 (NCBI#, NM_019844), and the predicted exonic sequence of SLCO1B7 (NCBI#, NM_001009562) and found that the LST-3TM12 sequence appears to originate from the genes *SLCO1B3* and *SLCO1B7*, whereby the first five exons are identical to the *SLCO1B3* transcript and afterwards the sequence is identical to *SLCO1B7* from its third exon on. This brought us to the first conclusion that the gene *SLCO1B7* can be transcribed in the form of LST-3TM12. Given that, LST-3TM12 derives from *SLCO1B3* and *SLCO1B7* its translational product was named OATP1B3-1B7 and thus for the sake of simplicity we will refer to LST-3TM12 as OATP1B3-1B7 mRNA.

To get an idea of the structure of the OATP1B3-1B7 protein we predicted its 3D-model based on homology modeling with the iTASSER structure-prediction-platform (Zhang, 2008). Simultaneously, we calculated the 3D-structure of OATP1B3 and the putative OATP1B7, whereby the putative OATP1B7 sequence is derived from the predicted exonic sequence from *SLCO1B7*. The computed homology models for OATP1B3-1B7 and OATP1B3 predicted that these proteins contain twelve transmembrane domains. Which is a structural property that is conserved over all other functional SLCO-transporters (Stieger and Hagenbuch, 2014). However, OATP1B7 was predicted to have eleven transmembrane domains only, which indicated that OATP1B7 might not be functional. This finding was also confirmed by *in vitro* experiments with heterologously expressed OATP1B7 for which no transport activity could be detected in our experimental setup and for the substrates tested. OATP1B3-1B7, however, was shown to transport DHEAS, E_2G, TCA, LCA, ezetimibe, and atorvastatin.

After demonstrating that the genes *SLCO1B3* and *SLCO1B7* encode together for the functional transporter OATP1B3-1B7, it was essential to investigate in what organs of the human body this transporter is expressed. By assaying several total mRNA samples of organs by real-time

PCR, we confirmed expression of *SLCO1B7* transcripts in the liver and duodenum. Moreover, we were able to show that the OATP1B3-1B7 transcript is present in the liver by qualitative PCR. Most importantly, we also demonstrated the presence of OATP1B3-1B7 in the liver and duodenum. Thus, it can be assumed that OATP1B3-1B7 is also translated endogenously.

It is important to note that it is not possible to discriminate between OATP1B7 and OATP1B3-1B7 mRNA or protein by real-time PCR or with antibody based methods, respectively. This is due to the high similarity of the sequences. In the case of real-time PCR, we often measured the expression of OATP1B3-1B7 pre-mRNA as well, which cannot be confounded with other *SLCO1B7* transcripts (see Results section 3.3 for more details). For the sake of simplification, we addressed the mRNA and protein as OATP1B3-1B7 as it appears to be the functional transcript of *SLCO1B7*. Nevertheless, there is the possibility that OATP1B7 was also detected.

To assess the cellular localization of OATP1B3-1B7 we performed immunohistological stainings against OATP1B3-1B7 in liver slices and duodenal tissue. Strikingly, OATP1B3-1B7 is not located in the plasma membrane like OATP1B1 and OATP1B3, but in the SER. A representative overview of the differences and similarities of OATP1B3-1B7, OATP1B1 and OATP1B3 can be found in Table 1. The localization of OATP1B3-1B7 in the SER was unprecedented and motivated us to investigate what function a drug transporter could serve in the SER.

Table 1. Overview of OATP1B characteristics. Comparison of a representative selection of endogenous substrates (Bednarczyk and Boiselle, 2016; Hagenbuch and Gui, 2008), exogenous substrates (Hagenbuch and Gui, 2008; Oswald et al., 2008), tissue expression (Abe et al., 1999; Abe et al., 2001; Briz et al., 2003; Lockhart et al., 2008; Meyer zu Schwabedissen et al., 2014), and cellular localization of the OATP1Bs (Konig et al., 2000a; Konig et al., 2000b)

	OATP1B1	OATP1B3	OATP1B3-1B7
endogenous substrates	estrone-3 sulfate, estradiol β-D-glucuronide, dehydroepiandrosterone sulfate, taurocholic acid, bilirubin, leukotrienes, thyroid hormones, coproporphyrins	estrone-3 sulfate, estradiol β-D-glucuronide, bilirubin, taurocholic acid, cholecystokinin octapepetide, leukotrienes, thyroid hormones coproporphyrins	estradiol β-D-glucuronide, dehydroepiandrosterone sulfate, taurocholic acid, lithocholic acid
exogenous substrates	statins (e.g., atorvastatin), sartans, angiotensinogen converting enzyme (ACE) inhibitors, glinide, ezetimibe β-D-glucuronide	statins, sartans, angiotensinogen converting enzyme (ACE) inhibitors, glinides	ezetimibe, atorvastatin
tissue	liver	liver, placenta, colorectal tumors, pancreas	liver, small intestine
cellular localization	basolateral/sinusoidal	basolateral/sinusoidal	smooth endoplasmic reticulum

As the SER of hepatocytes and enterocytes contains an abundance of metabolizing enzymes of the cytochrome P450 and UGT families (Drozdzik et al., 2018; Rouleau et al., 2016), we hypothesized that the physiological role of OATP1B3-1B7 could be related to the high metabolic activity of these specialized SERs. More precisely, OATP1B3-1B7 could act as a gateway for exogenous and endogenous compounds to the SER lumen. This function could be essential for the metabolism of compounds that undergo glucuronidation as the active site of UGTs faces the lumen of the SER (Coleman, 2010). Hitherto, it is assumed that UGT substrates (which are often lipophilic) diffuse through the plasma membrane of the SER, reach the active site of the UGTs, become glucuronidated, and the hydrophilic metabolites are then released into the SER lumen (Coleman, 2010). In this model, it remains unknown how the glucuronidated metabolites exit the SER as their hydrophilic character does not allow them to cross the SER

membrane (Petzinger and Geyer, 2006; Yang et al., 2017). Therefore, a SER transporter with a broad substrate spectrum like OATP1B3-1B7 could provide the missing function by facilitating the entry and exit of compounds from the SER lumen. We addressed this hypothesis in the example of the OATP1B3-1B7 substrate ezetimibe, which is extensively glucuronidated in hepatocytes and enterocytes (Ghosal et al., 2004). We subjected enriched SER (known as microsomes) to a non-glucuronidated OATP1B3-1B7 inhibitor and found that the maximal glucuronidation rate of ezetimibe dropped significantly, which suggests that OATP1B3-1B7 fosters the glucuronidation of ezetimibe. Figure 5 summarizes how OATP1B3-1B7 could participate in the metabolism of a substrate drug. Firstly, the drug enters the hepatocyte by one of the many influx transporters on the sinusoidal membrane, OATP1B3-1B7 gates the entry of the drug to the SER lumen, the drug is glucuronidated, exits the SER, and is then excreted into the bile by an efflux transporter.

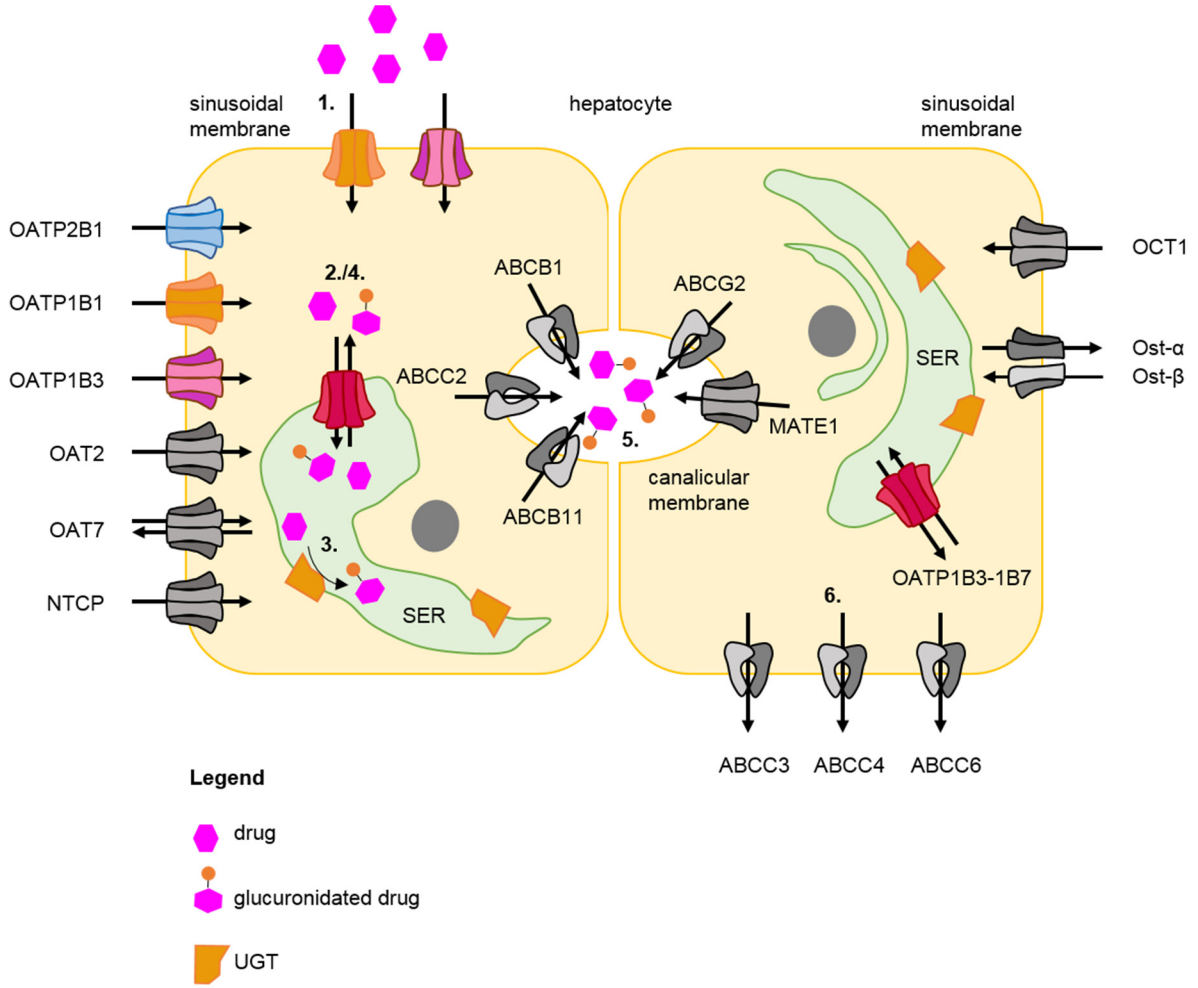

Figure 5. Putative role of OATP1B3-1B7 in drug metabolism. 1. Presumably, drug influx is executed by organic anion transporting polypeptides (OATPs). Other possible influx transporters are OAT2, OAT7, NTCP, OCT1 and OTs-α/Ost-β. 2. OATP1B3-1B7 functions as a gateway to the smooth endoplasmic reticulum (SER) lumen. 3. In the SER, drugs are glucuronidated by uridine 5'-diphospho-glucuronosyltransferases (UGTs). 4. SER exit is mediated by OATP1B3-1B7. 5. The majority of the glucuronidated drug is excreted into the canaliculi to reach the gallbladder. Excretion into the bile is executed by ABCB1, ABCG2, ABCC2, and MATE1. 6. A portion of the drug can also reenter systemic circulation by ABCC3, ABCC4, and ABCC6. Illustration adapted from Doring and Petzinger, 2014 (Doring and Petzinger, 2014).

Besides their role in drug metabolism, OATP1B1 and OATP1B3 also transport endogenous substances such as bile acids (Suga et al., 2017). These have detergent–like properties and they are secreted into the intestinal tract by the gall bladder to solubilize cholesterol and liposoluble vitamins (Moschetta, 2008). Like its subfamily members, OATP1B3-1B7 interacts with several bile acids. Of these, TCA and LCA are also substrates of OATP1B3-1B7. Similar to ezetimibe, the role of OATP1B3-1B7 in bile acid metabolism could be one of mediating access of bile acids to the SER as several bile acids are glucuronidated in order to be excreted (e.g., LCA, chenodeoxycholic acid, deoxycholic acid, and ursodeoxycholic acid) (Matern et al., 1984).

Given that excessive concentrations of bile acids in the blood are toxic, bile acid levels are tightly regulated (Chiang, 2013). One central regulator of bile acid levels is the bile acid sensor FXR (Matsubara et al., 2013). Upon binding to bile acids, the sensor dimerizes with RXR and binds to the promoter regions of the OATP1B genes, which stimulates their transcription (Jung et al., 2002; Meyer zu Schwabedissen et al., 2010). As the first five exons of the OATP1B3-1B7 mRNA originate from *SLCO1B3*, it seemed likely that the transcription of OATP1B3-1B7 mRNA is regulated by the *SLCO1B3* promoter. As the *SLCO1B3* transcription is positively activated by FXR, we evaluated whether OATP1B3-1B7 mRNA expression can be modulated by FXR activation or inhibition. To this end, we treated hepatoma cell lines with FXR agonists or antagonists and determined whether they increased or hindered OATP1B3-1B7 mRNA expression, respectively. Indeed, the result of these experiments shows that transcription of OATP1B3-1B7 mRNA can be modulated by FXR agonists or antagonists. Thus, we concluded that OATP1B3-1B7 is part of the FXR modulated gene network.

The FXR gene network is an ingenious system that modulates the expression of several proteins involved in bile acid homeostasis. Besides the OATP1B transporters, the sinusoidal bidirectional transporter Ostα/β, and the canalicular bile acid efflux transporters ABCB11 and ABCC2 are also positively controlled by FXR (see Figure 6) (Ballatori et al., 2009; Halilbasic et al., 2013). Moreover, FXR shuts down bile acid synthesis by inducing the expression of the transcription suppressor small heterodimer partner 1 (SHP1, *NR0B2*) (Zhang et al., 2015). The same pathway is used for downregulating the main hepatocellular bile acid influx transporter NTCP (*SLC10A1*) (Halilbasic et al., 2013). At first, it appears inconsequential that the major bile acid influx transporter is downregulated and the moderate OATP1Bs influx transporters are upregulated. However, it is assumed that the OATP1Bs ensure a steady and moderate influx of bile acid, which warrants continuous FXR activation without damaging the hepatocytes (Meyer zu Schwabedissen et al., 2010). To give an overview of the FXR network, Figure 6 summarizes the effect of FXR on several bile acid transporters. In this figure, we also included

the flipase ABCB4, which does not directly transport bile acids. Instead, it functions as a phospholipid phosphatidylcholine flipase that secretes phospholipids into the canaliculi which aids in solubilizing bile acids (Sundaram and Sokol, 2007).

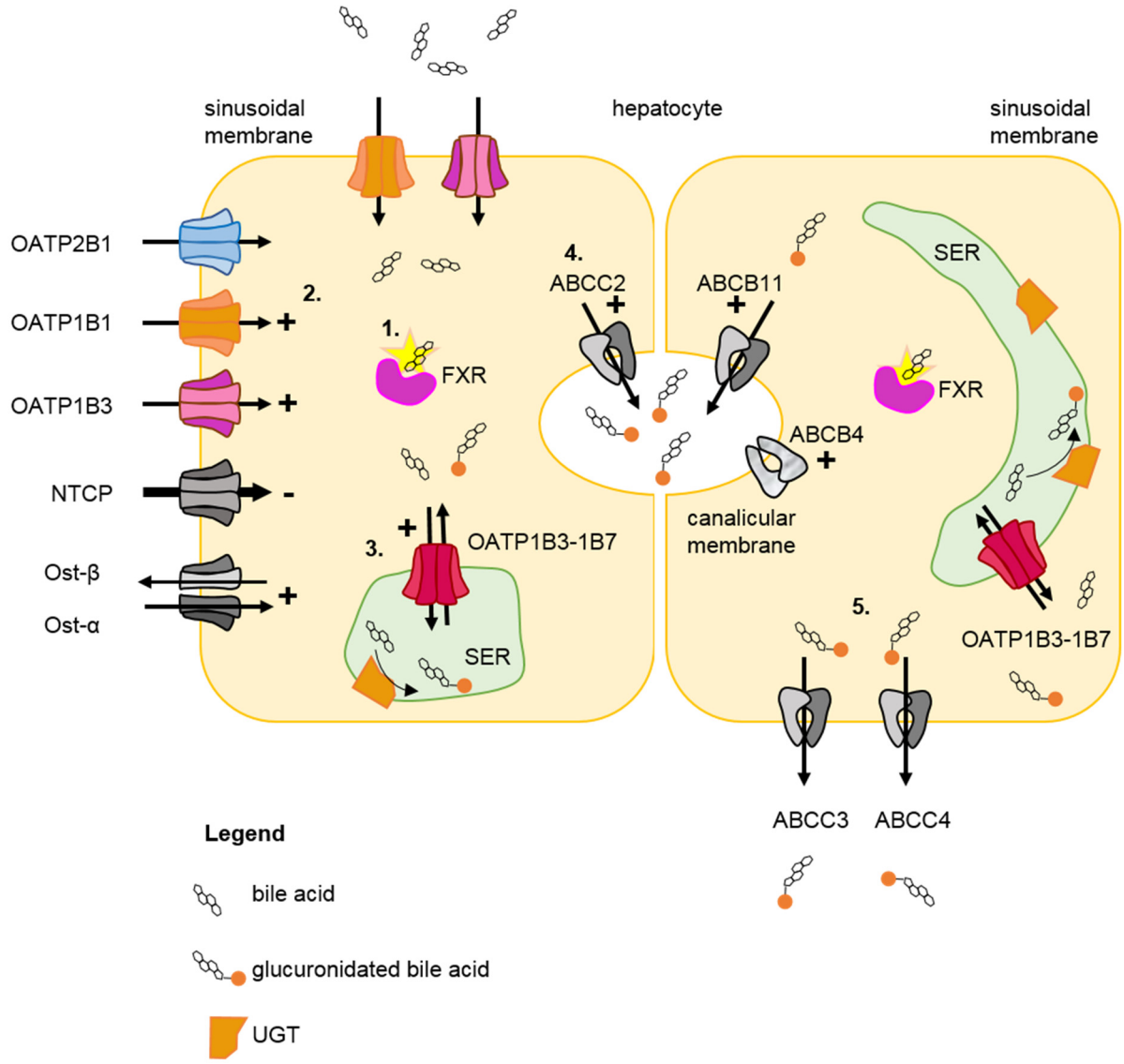

Figure 6. Effect of the farnesoid X receptor on the transcription of hepatic transporters. A "+" indicates enhancement of transcription and a "–"indicates the suppression of transcription. 1. The farnesoid X receptor (FXR) is activated by bile acids. 2. FXR induces the transcription of the bile acid influx transporters OATP2B1, OATP1B1, and OATP1B3. The transcription of the major bile acid influx transporter NTCP is indirectly suppressed by FXR. 3. OATP1B3-1B7 transcription is induced by FXR and might foster bile acid metabolism via glucuronidation. 4. The canalicular efflux transporters ABCC2 and ABCB11 are induced as well and mediate the elimination of glucuronidated bile acids. ABCB4 aids in the solubilization of the excreted bile acids. 5. A part of the glucuronidated bile acids enters systemic circulation by ABCC3 and ABCC4. Abbreviations: SER, smooth endoplasmic reticulum; UGT, uridine 5'-diphospho-glucuronosyltransferase. Illustration adapted from Doring and Petzinger, 2014 (Doring and Petzinger, 2014).

The fact that FXR regulates OATP1B3-1B7 mRNA transcription suggests that OATP1B3-1B7 expression is indeed regulated by the *SLCO1B3* promoter. We have further corroborated this

hypothesis by showing that OATP1B3-1B7 mRNA and OATP1B3 have the same 5'untranslated region and that silencing of exon 4 of OATP1B3 (which is also used in the OATP1B3-1B7 mRNA) results in diminished mRNA amounts of OATP1B3 and OATP1B3-1B7.

In order to achieve the transcription of OATP1B3-1B7 mRNA, *SLCO1B3* needs to be fully transcribed. However, instead of ending transcription at the *SLCO1B3* stop codon, transcription would continue until it reached the end of *SLCO1B7*. Thereby an alternative pre-mRNA containing the *SLCO1B3* and *SLCO1B7* sequence is created that can be spliced into the OATP1B3-1B7 mRNA (see Figure 7). By probing this pre-mRNA in real-time PCR experiments, we could show that its transcription increases when FXR is activated, which is the same effect we observed for OATP1B3 and OATP1B3-1B7 mRNA.

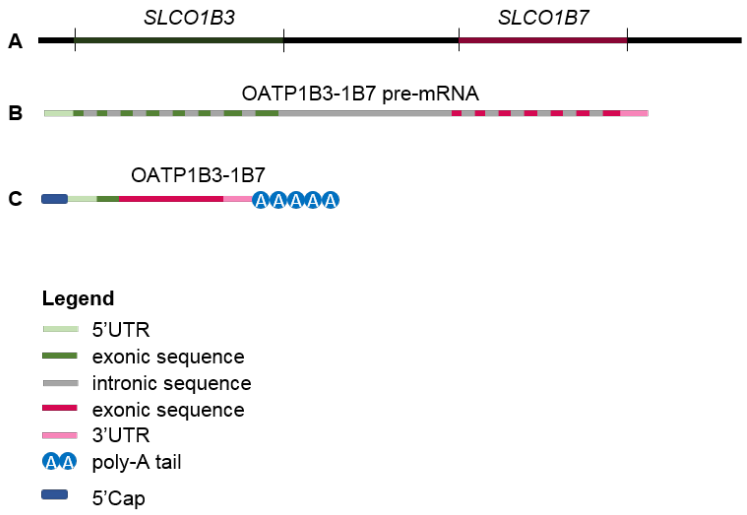

Figure 7. Origin of the OATP1B3-1B7 mRNA. A) The gene region on chromosome 12.12 encodes for *SLCO1B3* and *SLCO1B7*. B) Depiction of the OATP1B3-1B7 pre-mRNA, which is a combination of the *SLCO1B3* gene (green) and the *SLCO1B7* gene (red). C) After alternative splicing and post transcriptional processing OATP1B3-1B7 is created. Abbreviations: UTR, untranslated region.

The non-canonical splicing of a gene transcript is a process called alternative splicing (Xing and Lee, 2006). By alternative splicing, often a variant mRNA with slightly altered functions to the original is created (Stamm et al., 2005). Thereby information for various proteins with similar functions can be condensed onto a relatively short gene region or a single gene (Gilbert,

1978), which is precisely what OATP1B3-1B7 appears to be - a transporter with slightly altered functions compared to OATP1B3. On the one hand, its substrate range is similar to OATP1B3. On the other hand, the function of OATP1B3-1B7 is presumably closer to phase II metabolism than OATP1B3, as it is located in the SER where many phase II enzymes reside.

Moreover, evolution and thus adaption to new environmental challenges is fueled by alternative splicing (Black, 2003). Considering that the OATP1B transporters are involved in the metabolism of several xenobiotics (Hagenbuch and Gui, 2008), it could be speculated that they have to constantly adapt their function to new environmental challenges. Thus, alternative splicing could be one such tool with which these transporters could be adapted to varying environmental conditions.

In this PhD thesis, it was demonstrated that the transcripts OATP1B7-1B3 mRNA/LST-3TM12 and LST-3b encode for the functional transporter OATP1B3-1B7. Identified OATP1B3-1B7 substrates are DHEAS, E_2G, TCA, LCA, ezetimibe, and atorvastatin. OATP1B3-1B7 is an outstanding transporter as it is located in the SER where its function could be to facilitate access to metabolizing SER-enzymes. Moreover, the transcription of OATP1B3-1B7 mRNA is regulated by the *SLCO1B3* promoter, the consequence of which is that OATP1B3-1B7 mRNA expression can be modulated by FXR activation/inhibition.

5.0 Outlook

As mentioned before, the SNP rs4149056s in the gene region of *SLCO1B1* can be predictive for the occurrence of myopathic incidents during statin treatment (Brunham et al., 2012; Donnelly et al., 2011; Link et al., 2008; Puccetti et al., 2010; Voora et al., 2009). Importantly, this SNP codes for an impaired function OATP1B1 variant, which mechanistically explains why the adverse event during statin treatment occur (Tirona et al., 2001). It would thus be interesting to know if the genes encoding for OATP1B3-1B7 contain SNPs that alter the function of OATP1B3-1B7 and if these lead to physiological consequences.

Indeed, during our research on OATP1B3-1B7, Meyer zu Schwabedissen *et al.* identified several SNPs that encoded for OATP1B3-1B7 variants with attenuated transport function. Namely the variants containing the SNPs rs1546308, rs11045681, and rs188817665 had significantly lower transport function compared to wild type OATP1B3-1B7 (submitted manuscript). Interestingly, the rs1546308 was already associated with adverse events during clozapine treatment by Legge *et al*. (Legge et al., 2016). As clozapine is highly metabolized and also glucuronidated (Schaber et al., 2001) the most obvious connection between a non-functional OATP1B3-1B7 and adverse events caused by clozapine could be explained by the fact that clozapine elimination is hindered due to delayed metabolism by glucuronidation. However, evidence suggests that the incidence of neutropenia during clozapine treatment is not correlated with the plasma levels of clozapine but with the plasma levels of its metabolite N-desmethylclozapine (also known as norclozapine) (Legare et al., 2013). This is in accordance with our findings, which showed that there is only a small interaction between clozapine and OATP1B3-1B7 transport function (see section 3.2 for more details). Desmethylclozapine however, can either be directly eliminated by the kidney or subjected to phase II metabolism. One of the possible phase II reactions involves the glucuronidation of desmethylclozapine (Schaber et al., 2001). Thus, we speculate that OATP1B3-1B7 might foster the glucuronidation of desmethylclozapine by mediating SER access. This assumption would need to be functionally verified by assessing whether desmethylclozapine is an OATP1B3-1B7 substrate. Moreover, it would need to be assessed whether OATP1B3-1B7 inhibition attenuates the glucuronidation rate of desmethylclozapine. Eventually a patient based study could investigate whether the metabolism of clozapine in carriers of the rs1546308 is attenuated compared to carriers of the wild type OATP1B3-1B7.

In general, the discovery of the non-functional polymorphisms offers a means to investigate the physiological relevance of OATP1B3-1B7. As OATP1B3-1B7 exhibits transport affinities towards DHEAS, E_2G and bile acids, it would be interesting to investigate whether carriers of

non-functional OATP1B3-1B7 polymorphisms exhibit altered serum/plasma concentrations of these substances. As OATP1B3-1B7 also transports ezetimibe and atorvastatin, it is apparent that it would be of major interest to determine the pharmacokinetics in carriers of a non-functional polymorphism.

Given that OATP1B3-1B7 interacts with marketed drugs, an *in vitro* model that allows for the prediction of drug interaction is needed. As OATP1B3-1B7 is deemed to mediate access to the UGTs, an ideal *in vitro* model would express OATP1B3-1B7 and functional UGTs. These two criteria are fulfilled by the HepaRG cell line (Darnell et al., 2012). The impact of OATP1B3-1B7 on glucuronidation could be estimated by the creation of an OATP1B3-1B7 knock out cell-line. The UGT-activity of the knock out cell-line could be compared to the wild type and eventually the generated data could be used to create an interaction prediction system.

The more we understand about the pharmacokinetic processes that affect a drug, the better we can predict and eventually avoid adverse events. There is still very little knowledge on how drugs reach intracellular drug targets or their respective metabolizing enzymes. In the case of SER access, there are only a couple of reviews suggesting that intracellular drug transport is necessary for drug metabolism, (Csala et al., 2007; Petzinger and Geyer, 2006). The reason for this lack of research could be due to the fact that conducting robust experiments investigating intracellular drug transport is quite difficult or indirect (an issue we have experienced ourselves). Nevertheless, it seems very unlikely that drugs just diffuse to their metabolizing enzymes or to their excretion transporters. Therefore, it seems essential that more research should focus on intracellular drug transport.

6.0 Bibliography

Abe T, Kakyo M, Tokui T, Nakagomi R, Nishio T, Nakai D, Nomura H, Unno M, Suzuki M, Naitoh T, Matsuno S and Yawo H (1999) Identification of a novel gene family encoding human liver-specific organic anion transporter LST-1. *J Biol Chem* **274**(24): 17159-17163.

Abe T, Unno M, Onogawa T, Tokui T, Kondo TN, Nakagomi R, Adachi H, Fujiwara K, Okabe M, Suzuki T, Nunoki K, Sato E, Kakyo M, Nishio T, Sugita J, Asano N, Tanemoto M, Seki M, Date F, Ono K, Kondo Y, Shiiba K, Suzuki M, Ohtani H, Shimosegawa T, Iinuma K, Nagura H, Ito S and Matsuno S (2001) LST-2, a human liver-specific organic anion transporter, determines methotrexate sensitivity in gastrointestinal cancers. *Gastroenterology* **120**(7): 1689-1699.

Ballatori N, Li N, Fang F, Boyer JL, Christian WV and Hammond CL (2009) OST alpha-OST beta: a key membrane transporter of bile acids and conjugated steroids. *Front Biosci (Landmark Ed)* **14**: 2829-2844.

Bednarczyk D and Boiselle C (2016) Organic anion transporting polypeptide (OATP)-mediated transport of coproporphyrins I and III. *Xenobiotica* **46**(5): 457-466.

Bielinski SJ, Chai HS, Pathak J, Talwalkar JA, Limburg PJ, Gullerud RE, Sicotte H, Klee EW, Ross JL, Kocher JP, Kullo IJ, Heit JA, Petersen GM, de Andrade M and Chute CG (2011) Mayo Genome Consortia: a genotype-phenotype resource for genome-wide association studies with an application to the analysis of circulating bilirubin levels. *Mayo Clin Proc* **86**(7): 606-614.

Black DL (2003) Mechanisms of alternative pre-messenger RNA splicing. *Annu Rev Biochem* **72**: 291-336.

Boyd AE, 3rd, Aguilar-Bryan L and Nelson DA (1990) Molecular mechanisms of action of glyburide on the beta cell. *The American journal of medicine* **89**(2a): 3S-10S; discussion 51S-53S.

Briz O, Serrano MA, MacIas RI, Gonzalez-Gallego J and Marin JJ (2003) Role of organic anion-transporting polypeptides, OATP-A, OATP-C and OATP-8, in the human placenta-maternal liver tandem excretory pathway for foetal bilirubin. *Biochem J* **371**(Pt 3): 897-905.

Brunham LR, Lansberg PJ, Zhang L, Miao F, Carter C, Hovingh GK, Visscher H, Jukema JW, Stalenhoef AF, Ross CJ, Carleton BC, Kastelein JJ and Hayden MR (2012) Differential effect of the rs4149056 variant in SLCO1B1 on myopathy associated with simvastatin and atorvastatin. *The pharmacogenomics journal* **12**(3): 233-237.

Bryan J and Aguilar-Bryan L (1999) Sulfonylurea receptors: ABC transporters that regulate ATP-sensitive K(+) channels. *Biochim Biophys Acta* **1461**(2): 285-303.

Chiang JY (2013) Bile acid metabolism and signaling. *Compr Physiol* **3**(3): 1191-1212.

Coleman MD (2010) Glucuronidation, in *Human Drug Metabolism* John Wiley & Sons Ltd, Chichester.

Csala M, Marcolongo P, Lizak B, Senesi S, Margittai E, Fulceri R, Magyar JE, Benedetti A and Banhegyi G (2007) Transport and transporters in the endoplasmic reticulum. *Biochim Biophys Acta* **1768**(6): 1325-1341.

Csanaky IL, Lu H, Zhang Y, Ogura K, Choudhuri S and Klaassen CD (2011) Organic anion-transporting polypeptide 1b2 (Oatp1b2) is important for the hepatic uptake of unconjugated bile acids: Studies in Oatp1b2-null mice. *Hepatology* **53**(1): 272-281.

Cui Y, Konig J, Leier I, Buchholz U and Keppler D (2001) Hepatic uptake of bilirubin and its conjugates by the human organic anion transporter SLC21A6. *J Biol Chem* **276**(13): 9626-9630.

Darnell M, Ulvestad M, Ellis E, Weidolf L and Andersson TB (2012) In vitro evaluation of major in vivo drug metabolic pathways using primary human hepatocytes and HepaRG cells in suspension and a dynamic three-dimensional bioreactor system. *The Journal of pharmacology and experimental therapeutics* **343**(1): 134-144.

de Graaf W, Hausler S, Heger M, van Ginhoven TM, van Cappellen G, Bennink RJ, Kullak-Ublick GA, Hesselmann R, van Gulik TM and Stieger B (2011) Transporters involved in the hepatic uptake of (99m)Tc-mebrofenin and indocyanine green. *Journal of hepatology* **54**(4): 738-745.

Donnelly LA, Doney AS, Tavendale R, Lang CC, Pearson ER, Colhoun HM, McCarthy MI, Hattersley AT, Morris AD and Palmer CN (2011) Common nonsynonymous substitutions in SLCO1B1 predispose to statin intolerance in routinely treated individuals with type 2 diabetes: a go-DARTS study. *Clin Pharmacol Ther* **89**(2): 210-216.

Doring B and Petzinger E (2014) Phase 0 and phase III transport in various organs: combined concept of phases in xenobiotic transport and metabolism. *Drug metabolism reviews* **46**(3): 261-282.

Drozdzik M, Busch D, Lapczuk J, Muller J, Ostrowski M, Kurzawski M and Oswald S (2018) Protein Abundance of Clinically Relevant Drug-Metabolizing Enzymes in the Human Liver and Intestine: A Comparative Analysis in Paired Tissue Specimens. *Clin Pharmacol Ther* **104**(3): 515-524.

Fuerst TR, Niles EG, Studier FW and Moss B (1986) Eukaryotic transient-expression system based on recombinant vaccinia virus that synthesizes bacteriophage T7 RNA polymerase. *Proc Natl Acad Sci U S A* **83**(21): 8122-8126.

Ghosal A, Hapangama N, Yuan Y, Achanfuo-Yeboah J, Iannucci R, Chowdhury S, Alton K, Patrick JE and Zbaida S (2004) Identification of human UDP-glucuronosyltransferase enzyme(s) responsible for the glucuronidation of ezetimibe (Zetia). *Drug Metab Dispos* **32**(3): 314-320.

Ghose AK, Viswanadhan VN and Wendoloski JJ (1999) A knowledge-based approach in designing combinatorial or medicinal chemistry libraries for drug discovery. 1. A qualitative and quantitative characterization of known drug databases. *J Comb Chem* **1**(1): 55-68.

Giacomini KM, Huang SM, Tweedie DJ, Benet LZ, Brouwer KL, Chu X, Dahlin A, Evers R, Fischer V, Hillgren KM, Hoffmaster KA, Ishikawa T, Keppler D, Kim RB, Lee CA, Niemi M, Polli JW, Sugiyama Y, Swaan PW, Ware JA, Wright SH, Yee SW, Zamek-Gliszczynski MJ and Zhang L (2010) Membrane transporters in drug development. *Nat Rev Drug Discov* **9**(3): 215-236.

Gilbert W (1978) Why genes in pieces? *Nature* **271**(5645): 501.

Hagenbuch B and Gui C (2008) Xenobiotic transporters of the human organic anion transporting polypeptides (OATP) family. *Xenobiotica* **38**(7-8): 778-801.

Hagenbuch B and Meier PJ (2003) The superfamily of organic anion transporting polypeptides. *Biochim Biophys Acta* **1609**(1): 1-18.

Hagenbuch B and Meier PJ (2004) Organic anion transporting polypeptides of the OATP/ SLC21 family: phylogenetic classification as OATP/ SLCO superfamily, new nomenclature and molecular/functional properties. *Pflugers Arch* **447**(5): 653-665.

Hagenbuch B and Stieger B (2013) The SLCO (former SLC21) superfamily of transporters. *Mol Aspects Med* **34**(2-3): 396-412.

Halilbasic E, Claudel T and Trauner M (2013) Bile acid transporters and regulatory nuclear receptors in the liver and beyond. *Journal of hepatology* **58**(1): 155-168.

Hartkoorn RC, Kwan WS, Shallcross V, Chaikan A, Liptrott N, Egan D, Sora ES, James CE, Gibbons S, Bray PG, Back DJ, Khoo SH and Owen A (2010) HIV protease inhibitors are substrates for OATP1A2, OATP1B1 and OATP1B3 and lopinavir plasma

concentrations are influenced by SLCO1B1 polymorphisms. *Pharmacogenet Genomics* **20**(2): 112-120.
Herdegen T, Böhm R, Cimin-Bredée N, Culman J, Gohlke P, Ley L, Luippold G, Ufer M and Wätzig V (2010) Allgemeine Pharmakologie, in *Kurzlehrbuch Pharmakologie und Toxikologie* pp 3-33, Georg Thieme Verlag, Stuttgart.
Hsiang B, Zhu Y, Wang Z, Wu Y, Sasseville V, Yang WP and Kirchgessner TG (1999) A novel human hepatic organic anion transporting polypeptide (OATP2). Identification of a liver-specific human organic anion transporting polypeptide and identification of rat and human hydroxymethylglutaryl-CoA reductase inhibitor transporters. *J Biol Chem* **274**(52): 37161-37168.
Johnson AD, Kavousi M, Smith AV, Chen MH, Dehghan A, Aspelund T, Lin JP, van Duijn CM, Harris TB, Cupples LA, Uitterlinden AG, Launer L, Hofman A, Rivadeneira F, Stricker B, Yang Q, O'Donnell CJ, Gudnason V and Witteman JC (2009) Genome-wide association meta-analysis for total serum bilirubin levels. *Hum Mol Genet* **18**(14): 2700-2710.
Joy TR and Hegele RA (2009) Narrative review: statin-related myopathy. *Annals of internal medicine* **150**(12): 858-868.
Jung D, Podvinec M, Meyer UA, Mangelsdorf DJ, Fried M, Meier PJ and Kullak-Ublick GA (2002) Human organic anion transporting polypeptide 8 promoter is transactivated by the farnesoid X receptor/bile acid receptor. *Gastroenterology* **122**(7): 1954-1966.
Kalliokoski A, Neuvonen M, Neuvonen PJ and Niemi M (2008) The effect of SLCO1B1 polymorphism on repaglinide pharmacokinetics persists over a wide dose range. *Br J Clin Pharmacol* **66**(6): 818-825.
Kalliokoski A and Niemi M (2009) Impact of OATP transporters on pharmacokinetics. *Br J Pharmacol* **158**(3): 693-705.
Kang TW, Kim HJ, Ju H, Kim JH, Jeon YJ, Lee HC, Kim KK, Kim JW, Lee S, Kim JY, Kim SY and Kim YS (2010) Genome-wide association of serum bilirubin levels in Korean population. *Hum Mol Genet* **19**(18): 3672-3678.
Konig J, Cui Y, Nies AT and Keppler D (2000a) Localization and genomic organization of a new hepatocellular organic anion transporting polypeptide. *J Biol Chem* **275**(30): 23161-23168.
Konig J, Cui Y, Nies AT and Keppler D (2000b) A novel human organic anion transporting polypeptide localized to the basolateral hepatocyte membrane. *Am J Physiol Gastrointest Liver Physiol* **278**(1): G156-164.
Kullak-Ublick GA, Ismair MG, Stieger B, Landmann L, Huber R, Pizzagalli F, Fattinger K, Meier PJ and Hagenbuch B (2001) Organic anion-transporting polypeptide B (OATP-B) and its functional comparison with three other OATPs of human liver. *Gastroenterology* **120**(2): 525-533.
Kunze A, Huwyler J, Camenisch G and Poller B (2014) Prediction of organic anion-transporting polypeptide 1B1- and 1B3-mediated hepatic uptake of statins based on transporter protein expression and activity data. *Drug Metab Dispos* **42**(9): 1514-1521.
Langguth P, Fricker G and Wunderli-Allenspach H (2004a) Einführung, in *Biopharmazie* pp 3-4, WILEY-VCH Verlag GmBH & Co., Weinheim.
Langguth P, Fricker G and Wunderli-Allenspach H (2004b) Grundlagen der Pharmakokineitk, in *Biopharmazie* pp 79-159, WILEY-VCH Verlag GmBH & Co., Weinheim.
Langguth P, Fricker G and Wunderli-Allenspach H (2004c) Physiologische Grundlagen-Biologische Membranen und Barrieren, in *Biopharmazie* pp 7-49, WILEY-VCH Verlag GmBH & Co., Weinheim.
Legare N, Gregoire CA, De Benedictis L and Dumais A (2013) Increasing the clozapine: norclozapine ratio with co-administration of fluvoxamine to enhance efficacy and minimize side effects of clozapine therapy. *Medical hypotheses* **80**(6): 689-691.

Legge SE, Hamshere ML, Ripke S, Pardinas AF, Goldstein JI, Rees E, Richards AL, Leonenko G, Jorskog LF, Chambert KD, Collier DA, Genovese G, Giegling I, Holmans P, Jonasdottir A, Kirov G, McCarroll SA, MacCabe JH, Mantripragada K, Moran JL, Neale BM, Stefansson H, Rujescu D, Daly MJ, Sullivan PF, Owen MJ, O'Donovan MC and Walters JT (2016) Genome-wide common and rare variant analysis provides novel insights into clozapine-associated neutropenia. *Mol Psychiatry*.

Leuthold S, Hagenbuch B, Mohebbi N, Wagner CA, Meier PJ and Stieger B (2009) Mechanisms of pH-gradient driven transport mediated by organic anion polypeptide transporters. *American journal of physiology Cell physiology* **296**(3): C570-582.

Liang Y, Li S and Chen L (2015) The physiological role of drug transporters. *Protein Cell* **6**(5): 334-350.

Link E, Parish S, Armitage J, Bowman L, Heath S, Matsuda F, Gut I, Lathrop M and Collins R (2008) SLCO1B1 variants and statin-induced myopathy--a genomewide study. *N Engl J Med* **359**(8): 789-799.

Lipinski CA, Lombardo F, Dominy BW and Feeney PJ (2001) Experimental and computational approaches to estimate solubility and permeability in drug discovery and development settings. *Adv Drug Deliv Rev* **46**(1-3): 3-26.

Lockhart AC, Harris E, Lafleur BJ, Merchant NB, Washington MK, Resnick MB, Yeatman TJ and Lee W (2008) Organic anion transporting polypeptide 1B3 (OATP1B3) is overexpressed in colorectal tumors and is a predictor of clinical outcome. *Clin Exp Gastroenterol* **1**: 1-7.

Maeda K (2015) Organic anion transporting polypeptide (OATP)1B1 and OATP1B3 as important regulators of the pharmacokinetics of substrate drugs. *Biol Pharm Bull* **38**(2): 155-168.

Mahagita C, Grassl SM, Piyachaturawat P and Ballatori N (2007) Human organic anion transporter 1B1 and 1B3 function as bidirectional carriers and do not mediate GSH-bile acid cotransport. *Am J Physiol Gastrointest Liver Physiol* **293**(1): G271-278.

Makishima M, Okamoto AY, Repa JJ, Tu H, Learned RM, Luk A, Hull MV, Lustig KD, Mangelsdorf DJ and Shan B (1999) Identification of a nuclear receptor for bile acids. *Science* **284**(5418): 1362-1365.

Matern S, Matern H, Farthmann EH and Gerok W (1984) Hepatic and extrahepatic glucuronidation of bile acids in man. Characterization of bile acid uridine 5'-diphosphate-glucuronosyltransferase in hepatic, renal, and intestinal microsomes. *J Clin Invest* **74**(2): 402-410.

Matsubara T, Li F and Gonzalez FJ (2013) FXR signaling in the enterohepatic system. *Mol Cell Endocrinol* **368**(1-2): 17-29.

Meier-Abt F, Mokrab Y and Mizuguchi K (2005) Organic anion transporting polypeptides of the OATP/SLCO superfamily: identification of new members in nonmammalian species, comparative modeling and a potential transport mode. *The Journal of membrane biology* **208**(3): 213-227.

Meyer zu Schwabedissen HE, Albers M, Baumeister SE, Rimmbach C, Nauck M, Wallaschofski H, Siegmund W, Volzke H and Kroemer HK (2015) Function-impairing polymorphisms of the hepatic uptake transporter SLCO1B1 modify the therapeutic efficacy of statins in a population-based cohort. *Pharmacogenet Genomics* **25**(1): 8-18.

Meyer zu Schwabedissen HE, Boettcher K, Steiner T, Schwarz UI, Keiser M, Kroemer HK and Siegmund W (2014) OATP1B3 is expressed in pancreatic beta-islet cells and enhances the insulinotropic effect of the sulfonylurea derivative glibenclamide. *Diabetes* **63**(2): 775-784.

Meyer zu Schwabedissen HE, Bottcher K, Chaudhry A, Kroemer HK, Schuetz EG and Kim RB (2010) Liver X receptor alpha and farnesoid X receptor are major transcriptional regulators of OATP1B1. *Hepatology* **52**(5): 1797-1807.

Meyer zu Schwabedissen HE and Kim RB (2009) Hepatic OATP1B transporters and nuclear receptors PXR and CAR: interplay, regulation of drug disposition genes, and single nucleotide polymorphisms. *Mol Pharm* **6**(6): 1644-1661.

Miura M, Kagaya H, Satoh S, Inoue K, Saito M, Habuchi T and Suzuki T (2008) Influence of drug transporters and UGT polymorphisms on pharmacokinetics of phenolic glucuronide metabolite of mycophenolic acid in Japanese renal transplant recipients. *Ther Drug Monit* **30**(5): 559-564.

Moschetta A (2008) Welcoming Foxa2 in the bile acid entourage. *Cell Metab* **8**(4): 276-278.

Oswald S, Konig J, Lutjohann D, Giessmann T, Kroemer HK, Rimmbach C, Rosskopf D, Fromm MF and Siegmund W (2008) Disposition of ezetimibe is influenced by polymorphisms of the hepatic uptake carrier OATP1B1. *Pharmacogenet Genomics* **18**(7): 559-568.

Petzinger E and Geyer J (2006) Drug transporters in pharmacokinetics. *Naunyn-Schmiedeberg's Archives of Pharmacology* **372**(6): 465-475.

Picard N, Yee SW, Woillard JB, Lebranchu Y, Le Meur Y, Giacomini KM and Marquet P (2010) The role of organic anion-transporting polypeptides and their common genetic variants in mycophenolic acid pharmacokinetics. *Clin Pharmacol Ther* **87**(1): 100-108.

Puccetti L, Ciani F and Auteri A (2010) Genetic involvement in statins induced myopathy. Preliminary data from an observational case-control study. *Atherosclerosis* **211**(1): 28-29.

Roitelman J, Olender EH, Bar-Nun S, Dunn WA, Jr. and Simoni RD (1992) Immunological evidence for eight spans in the membrane domain of 3-hydroxy-3-methylglutaryl coenzyme A reductase: implications for enzyme degradation in the endoplasmic reticulum. *The Journal of cell biology* **117**(5): 959-973.

Rouleau M, Tourancheau A, Girard-Bock C, Villeneuve L, Vaucher J, Duperre AM, Audet-Delage Y, Gilbert I, Popa I, Droit A and Guillemette C (2016) Divergent Expression and Metabolic Functions of Human Glucuronosyltransferases through Alternative Splicing. *Cell Rep* **17**(1): 114-124.

Sandritter TL, McLaughlin M, Artman M and Lowry J (2017) The Interplay between Pharmacokinetics and Pharmacodynamics. *Pediatrics in Review* **38**(5): 195-206.

Sanna S, Busonero F, Maschio A, McArdle PF, Usala G, Dei M, Lai S, Mulas A, Piras MG, Perseu L, Masala M, Marongiu M, Crisponi L, Naitza S, Galanello R, Abecasis GR, Shuldiner AR, Schlessinger D, Cao A and Uda M (2009) Common variants in the SLCO1B3 locus are associated with bilirubin levels and unconjugated hyperbilirubinemia. *Hum Mol Genet* **18**(14): 2711-2718.

Schaber G, Wiatr G, Wachsmuth H, Dachtler M, Albert K, Gaertner I and Breyer-Pfaff U (2001) Isolation and identification of clozapine metabolites in patient urine. *Drug Metab Dispos* **29**(6): 923-931.

Schwarz UI, Meyer zu Schwabedissen HE, Tirona RG, Suzuki A, Leake BF, Mokrab Y, Mizuguchi K, Ho RH and Kim RB (2011) Identification of novel functional organic anion-transporting polypeptide 1B3 polymorphisms and assessment of substrate specificity. *Pharmacogenet Genomics* **21**(3): 103-114.

Schweizer U, Johannes J, Bayer D and Braun D (2014) Structure and function of thyroid hormone plasma membrane transporters. *European thyroid journal* **3**(3): 143-153.

Shitara Y (2011) Clinical importance of OATP1B1 and OATP1B3 in drug-drug interactions. *Drug Metab Pharmacokinet* **26**(3): 220-227.

Stamm S, Ben-Ari S, Rafalska I, Tang Y, Zhang Z, Toiber D, Thanaraj TA and Soreq H (2005) Function of alternative splicing. *Gene* **344**: 1-20.

Steiner C, Othman A, Saely CH, Rein P, Drexel H, von Eckardstein A and Rentsch KM (2011) Bile acid metabolites in serum: intraindividual variation and associations with coronary heart disease, metabolic syndrome and diabetes mellitus. *PLoS One* **6**(11): e25006.

Stewart A (2013) SLCO1B1 Polymorphisms and Statin-Induced Myopathy. *PLoS Curr* **5**.

Stieger B and Hagenbuch B (2014) Organic anion-transporting polypeptides. *Curr Top Membr* **73**: 205-232.

Suga T, Yamaguchi H, Sato T, Maekawa M, Goto J and Mano N (2017) Preference of Conjugated Bile Acids over Unconjugated Bile Acids as Substrates for OATP1B1 and OATP1B3. *PLoS One* **12**(1): e0169719.

Sundaram SS and Sokol RJ (2007) The Multiple Facets of ABCB4 (MDR3) Deficiency. *Curr Treat Options Gastroenterol* **10**(6): 495-503.

Thummel KE (2007) Gut instincts: CYP3A4 and intestinal drug metabolism. *J Clin Invest* **117**(11): 3173-3176.

Tirona RG, Leake BF, Merino G and Kim RB (2001) Polymorphisms in OATP-C: identification of multiple allelic variants associated with altered transport activity among European- and African-Americans. *J Biol Chem* **276**(38): 35669-35675.

van de Steeg E, Stranecky V, Hartmannova H, Noskova L, Hrebicek M, Wagenaar E, van Esch A, de Waart DR, Oude Elferink RP, Kenworthy KE, Sticova E, al-Edreesi M, Knisely AS, Kmoch S, Jirsa M and Schinkel AH (2012) Complete OATP1B1 and OATP1B3 deficiency causes human Rotor syndrome by interrupting conjugated bilirubin reuptake into the liver. *J Clin Invest* **122**(2): 519-528.

van der Deure WM, Friesema EC, de Jong FJ, de Rijke YB, de Jong FH, Uitterlinden AG, Breteler MM, Peeters RP and Visser TJ (2008) Organic anion transporter 1B1: an important factor in hepatic thyroid hormone and estrogen transport and metabolism. *Endocrinology* **149**(9): 4695-4701.

Voora D, Shah SH, Spasojevic I, Ali S, Reed CR, Salisbury BA and Ginsburg GS (2009) The SLCO1B1*5 genetic variant is associated with statin-induced side effects. *Journal of the American College of Cardiology* **54**(17): 1609-1616.

Wang H, Yan Z, Dong M, Zhu X, Wang H and Wang Z (2012) Alteration in placental expression of bile acids transporters OATP1A2, OATP1B1, OATP1B3 in intrahepatic cholestasis of pregnancy. *Arch Gynecol Obstet* **285**(6): 1535-1540.

Watchko JF and Tiribelli C (2013) Bilirubin-induced neurologic damage--mechanisms and management approaches. *N Engl J Med* **369**(21): 2021-2030.

Werner U, Werner D, Heinbuchner S, Graf B, Ince H, Kische S, Thurmann P, Konig J, Fromm MF and Zolk O (2010) Gender is an important determinant of the disposition of the loop diuretic torasemide. *Journal of clinical pharmacology* **50**(2): 160-168.

Wilson K and Walker J (2010) Drug discovery and development, in *Principles and Techniques of Biochemistry and Molecular Biology*, Cambridge University Press, Cambridge.

Xiang X, Han Y, Neuvonen M, Pasanen MK, Kalliokoski A, Backman JT, Laitila J, Neuvonen PJ and Niemi M (2009) Effect of SLCO1B1 polymorphism on the plasma concentrations of bile acids and bile acid synthesis marker in humans. *Pharmacogenet Genomics* **19**(6): 447-457.

Xing Y and Lee C (2006) Alternative splicing and RNA selection pressure--evolutionary consequences for eukaryotic genomes. *Nat Rev Genet* **7**(7): 499-509.

Yan Z, Li E, He L, Wang J, Zhu X, Wang H and Wang Z (2015) Role of OATP1B3 in the transport of bile acids assessed using first-trimester trophoblasts. *J Obstet Gynaecol Res* **41**(3): 392-401.

Yang G, Ge S, Singh R, Basu S, Shatzer K, Zen M, Liu J, Tu Y, Zhang C, Wei J, Shi J, Zhu L, Liu Z, Wang Y, Gao S and Hu M (2017) Glucuronidation: driving factors and their impact on glucuronide disposition. *Drug metabolism reviews* **49**(2): 105-138.

Zaher H, Meyer zu Schwabedissen HE, Tirona RG, Cox ML, Obert LA, Agrawal N, Palandra J, Stock JL, Kim RB and Ware JA (2008) Targeted disruption of murine organic anion-transporting polypeptide 1b2 (Oatp1b2/Slco1b2) significantly alters disposition of prototypical drug substrates pravastatin and rifampin. *Mol Pharmacol* **74**(2): 320-329.

Zhang S, Pan X and Jeong H (2015) GW4064, an agonist of farnesoid X receptor, represses CYP3A4 expression in human hepatocytes by inducing small heterodimer partner expression. *Drug Metab Dispos* **43**(5): 743-748.

Zhang W, He YJ, Han CT, Liu ZQ, Li Q, Fan L, Tan ZR, Zhang WX, Yu BN, Wang D, Hu DL and Zhou HH (2006) Effect of SLCO1B1 genetic polymorphism on the pharmacokinetics of nateglinide. *Br J Clin Pharmacol* **62**(5): 567-572.

Zhang Y (2008) I-TASSER server for protein 3D structure prediction. *BMC Bioinformatics* **9**: 40.